THE TIDAL PRISM, VIABLE EELGRASS HABITAT, AND THE EFFECTS OF SEA LEVEL RISE IN MORRO BAY

A Thesis

presented to

the Faculty of California Polytechnic State University,

San Luis Obispo

In Partial Fulfillment

of the Requirements for the Degree

Master of Science in Civil and Environmental Engineering

by

Kaden Caliendo

December 2023

COMMITTEE MEMBERSHIP

TITLE:	The Tidal Prism, Viable Eelgrass Habitat, and the Effects of Sea Level Rise in Morro Bay
AUTHOR:	Kaden Alexander Caliendo
DATE SUBMITTED:	December 2023
COMMITTEE CHAIR:	Stefan Talke, Ph.D. Associate Professor of Civil Engineering
COMMITTEE MEMBER:	Rebekah Oulton, Ph.D. Graduate Coordinator Associate Professor of Environmental Engineering Associate Chair
COMMITTEE MEMBER:	Ryan Walter, Ph.D. Associate Professor of Physics

ABSTRACT

The Tidal Prism, Viable Eelgrass Habitat, and the Effects of Sea Level Rise in Morro Bay

Kaden Alexander Caliendo

The tidal prism, or the volume of water exchanged from the sea to an estuary from mean low to mean high tide, influences system hydrodynamics and ecological functioning. Since 1884, the tidal prism in Morro Bay, California has been estimated to be decreasing over time due to sedimentation from upstream practices. What is the current tidal prism in Morro Bay and how will that change with sea level rise? How will eelgrass respond to rising sea levels?

For this study, inexpensive tidal gauges were deployed at four locations in Morro Bay from March to August 2023 to measure spatially varying tidal elevations and datums within the bay. I utilized a Digital Elevation Model (DEM) and tidal information to determine volumes of water in Morro Bay. Estimated sea level rise scenarios were utilized to project the 2022 tidal prism into the years 2050 and 2100. Additionally, I estimated the 2019 and 2022 viable eelgrass habitat area using the vertical growth range. I estimated the future potential viable habitat area in the years 2050 and 2100 using estimated sea level rise scenarios. Future projections were made assuming no change in bathymetry over time.

Different instruments used to obtain water levels yielded up to ~4 percent differences in the tidal prism estimate. Measurement uncertainty in the monthly tidal datums produced ~3 percent uncertainty within the tidal prism estimate. Compared to the tidal prism in August 2019, the August 2022 tidal prism was lower by ~2 percent. Compared to the tidal prism in August 2019, the August 2023 tidal prism estimated from two nearly co-located tidal instruments at the mouth of Morro Bay were higher by ~5 and ~7 percent, respectively. Spatially varying tidal datums in Morro Bay were found to affect the tidal prism by up to ~3 percent, compared to tidal prism estimates using only a tidal datum near the estuary mouth. However, the effect of spatially varying tidal datums on the tidal prism is the same order of magnitude as measurement uncertainty and is thus not statistically significant. As sea levels rise, the tidal prism is projected to increase by ~40 percent by 2100 from 2022 under the most extreme scenario, H++. Initially, as sea levels rise, the potential viable eelgrass habitat area will increase from the area in 2022 (1108 acres (4.47E+06 m^2)). After sea levels rise to 1.5 m above 2000 levels, the potential viable eelgrass area will have reached a maximum area of 1938 acres (7.82E+06 m^2). However, under SLR scenario H++, potential viable habitat area is predicted to decrease by up to 59% by 2100 from 2022.

Keywords: Tidal Prism, Eelgrass Habitat, Sea Level Rise, Tidal Datums, Bathymetry

ACKNOWLEDGMENTS

I would like to thank the following people for their encouragement, time, and support:

My Cal Poly Advisors: Dr. Talke, Dr. Oulton, Dr. Walter

Postdoctoral Research Fellow: Serena Lee

Cal Poly Peer and Instrument Inventor: Alex Dunn

MatFlood Developer: Alejandra Enriquez

Surveyors: Rudy Schalk and his Advanced Surveying Class

Other Cal Poly Peers: Drake Abrahamson, August Northrup, Luke Wierl, Danica Wong

I am extremely grateful for the financial support. This thesis research was entirely funded by: The Baker/Koob Endowment Award, The Morro Bay National Estuary Program, The Santa Rosa Creek Foundation

This project would not be possible without the approval for installation from the following entities:

John and Carol Ann, Morro Bay Bayfront Marina, United States Coast Guard, The County of San Luis Obispo, Morro Bay Harbor Department, and Morro Bay State Park

TABLE OF CONTENTS

Content Page

LIST OF TABLES

LIST OF FIGURES

Figure Page

Chapter 1: INTRODUCTION

1.1 Problem Statement

Estuarine habitats support the marine ecosystem by creating critical spawning and nursing habitat (Gerdes et al., 1974). The plethora of marine biological resources available off California's coastline makes it the largest ocean economy in the nation, standing at $44 Billion per year. Coastal counties hold over 75% of the jobs in the state of California (Griggs & Lester, 2017).

Anthropogenic modification and degradation of the natural environment threaten estuaries around the world. A large threat to estuaries is increased sedimentation due to coastal land development and loss of upstream riparian habitat. Siltation in estuaries can result in a decrease in water depth and area, resulting in a loss of biodiversity, as seen in the late 1990's in the Chilika lagoon in eastern India (Authority, 1996; Ghosh et al., 2006; Panda et al., 2013; Samal, 2011). Additionally, sea level rise (SLR) is predicted to occur along California's coastlines (Griggs et al., 2017). Because of existing infrastructure, many estuarine habitats have little space to shift landward, and potentially get squeezed out with rises in sea levels (Pontee et al., 2022).

Morro Bay is an estuary on the Central Coast of California that supports a healthy and biodiverse ecosystem that sets the foundation for coastal tourism and commercial fishing (Jacob & Cravo, 2019). With important ecological, economical, and recreational resources at stake, it is essential to monitor the health of Morro Bay Estuary and plan for future climate scenarios (Gerdes et al., 1974). A metric to monitor estuarine health is through the tidal prism, or the volume of water exchanged from the sea to an estuary from mean low to mean high tide (Marani et al., 2003; Petti et al., 2021). The tidal prism is potentially influenced by artificial opening of tidal channels and changes in morphology over time, as seen in the western portion of the Rio Formosa lagoon in Portugal (Jacob & Cravo, 2019). Additionally, a study conducted on the Chilika lagoon suggests that geomorphological changes, primarily at the tidal inlet, can greatly influence the tidal exchange, salinity and oxygenation values, and sedimentation patterns (Panda et al., 2013; Petti et al., 2019). Morro Bay has undergone many anthropogenic changes, such as dredging of the navigational channels and the artificial closure of the north inlet (Haltiner, 1998). In 1998, the Central Coast Regional Water Quality Control Board identified Morro Bay as at risk for accelerated sedimentation and siltation (Central Coast Regional Water Quality Control Board, 2002). Since then, more efforts have been made to track the trajectory of the tidal prism in Morro Bay. Most recently, in August of 2019, Tetra Tech estimated that the tidal prism in Morro Bay had increased in volume, in contradiction to previous estimates that the tidal prism was decreasing due to sediment deposition from upstream practices (Tetra Tech, 2020). What is the current trajectory of the tidal prism and what does this mean for the future of biological resources in Morro Bay?

1.2 Significance

The ratio of the volume of the tidal prism relative to the volume of the entire estuary is used to determine flushing characteristics, tide current speeds, sediment transport and bed scouring characteristics (Haltiner, 1998). Thus, an estuary's tidal prism can influence an estuary's health through coastal erosion patterns, and contaminant transport (Tetra Tech, 2020). The tidal exchange can greatly influence the transport of nutrients, contaminants, and sediments between the land, estuary and sea (Jacob & Cravo, 2019; Sassi et al., 2015). The California Water Board currently sets the minimum required tidal prism in Morro Bay at

4,200 acre-feet, or 5.18E+06 cubic meters (m^3), to handle Total Maximum Daily Loads in Los Osos and Chorro Creeks (Central Coast Regional Water Quality Control Board, 2002).

The environmental conditions of Morro Bay are supportive of rich biodiversity. Morro Bay is included in the Pacific Flyway, a major migratory path for many endangered bird species, such as the Black Brant (Gerdes et al., 1974). Eelgrass (Zostera marina) in Morro Bay provides nursing grounds for fish and invertebrate species which support the plethora of birds and marine mammals in the area (**Figure 1**) (Gerdes et al., 1974). Estuarine regions are important for ecology, economy, and coastal tourism (Jacob & Cravo, 2019). Changes in sea levels may threaten the ecological health of Morro Bay by altering the available habitat (Pontee et al., 2022). Loss of eelgrass habitat can significantly impact biodiversity and overall ecological health (Short et al., 2011). The United States Geological Survey (USGS) predicts that most of the high marsh in Morro Bay will be lost to mudflats between 144 and 166 cm rise in sea level, causing major changes and disruptions to existing ecosystems (Freeman & Chase M, 2016).

*Figure 1: An Eelgrass bed in Morro Bay. Photo provided by the Morro Bay National Estuary Program (*Birds and Morro Bay*, n.d.)*.

1.3 Objectives

Historical records indicated that the tidal prism in Morro Bay was shrinking, yet a recent study by Tetra Tech in August of 2019 indicated that it has grown (Tetra Tech, 2020). In this thesis, possible reasons for the decrease in the tidal prism are explored. The current tidal prism is assessed, and implications of sea level rise on the tidal prism are explored. Similarly, the long-term variation in potential eelgrass habitat area is assessed. More specifically, this study aims to:

1. Evaluate the mean high and low tides in various locations of Morro Bay using student-made ultrasonic tidal instruments for 2022 and 2023
2. Calculate the 2022 and 2023 tidal prism in Morro Bay
3. Estimate the tidal prism in the years 2050 and 2100 based on official California Sea Level Rise Scenarios for San Francisco (Griggs et al., 2017) (assuming no change in bathymetry)

4. Determine the viable available eelgrass habitat area in the years 2019 and 2022 in Morro Bay
5. Estimate the potential viable eelgrass habitat area in the years 2050 and 2100 based on official California Sea Level Rise Scenarios for San Francisco (Griggs et al., 2017) (assuming no change in bathymetry)

Chapter 2: LITERATURE REVIEW

2.1 Tides, Tidal Datums, and the Tidal Prism

The tidal prism, or the volume of water exchanged with the ocean during a typical tidal cycle, is crucially dependent on tidal datums established by typical tides (Tetra Tech, 1999). Therefore, the next section discusses tidal theory and how tidal datums are determined.

2.1.1 Tides

The Sun and Moon produce varying gravitational forces on water particles in Earth's Oceans. Under their influence, water particles are drawn along the axis between Earth and said celestial body, creating tidal bulges around Earth's surface (**Figure 2**Error! Reference source not found.). The mass and distance between celestial bodies greatly influence gravitational forcing and therefore water levels. Earth's Moon has the largest effect on tides (Pugh, 1987). The magnitude of the tidal elevations in a region can directly influence the tidal prism volume (Marani et al., 2003).

A location on Earth is aligned with the Earth-Moon axis twice in a Lunar day, and therefore experiences two tidal bulges per Lunar day (Tyler, 2021). This results in a semidiurnal, or twice a day, timescale variation in gravitational forcing and therefore water levels. However, the declination angle of the Sun and Moon relative to the Earth's equator influences the magnitude of the gravitational forcing and therefore the magnitude of tides on a diurnal, once a day scale (**Figure 2**) (Pugh, 1987). This can introduce diurnal inequality into the semidiurnal tides, resulting in uneven high and low tides. Mixed tides occur when this diurnal inequality results in unequal highs and lows and diurnal tides occur when there is only one high and one low per day (Kvale, 2006). An example time series depicting diurnal, semidiurnal, and mixed tides can be seen in **Figure 3**. Tides in Morro Bay are mixed, semidiurnal tides, with two unequal daily highs and two unequal daily lows (Tetra Tech, 1999).

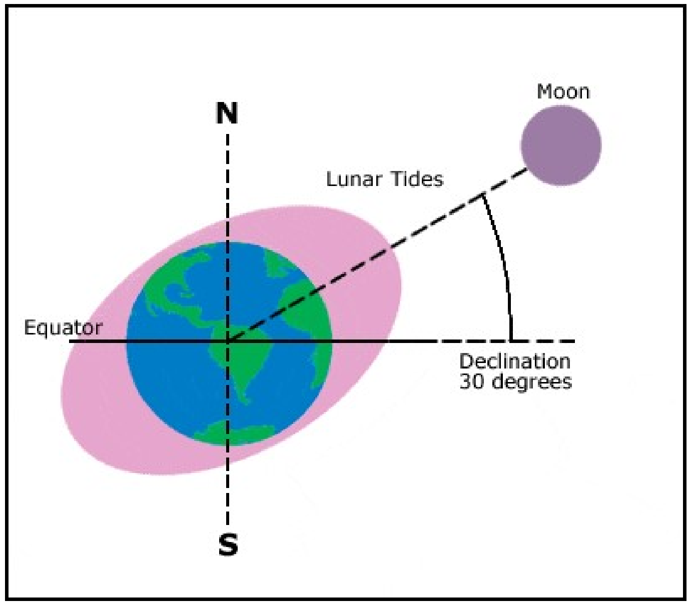

Figure 2: Depiction of Tidal Bulge due to the Moon at a Declination Angle (Gravitational Forces *, n.d.)*

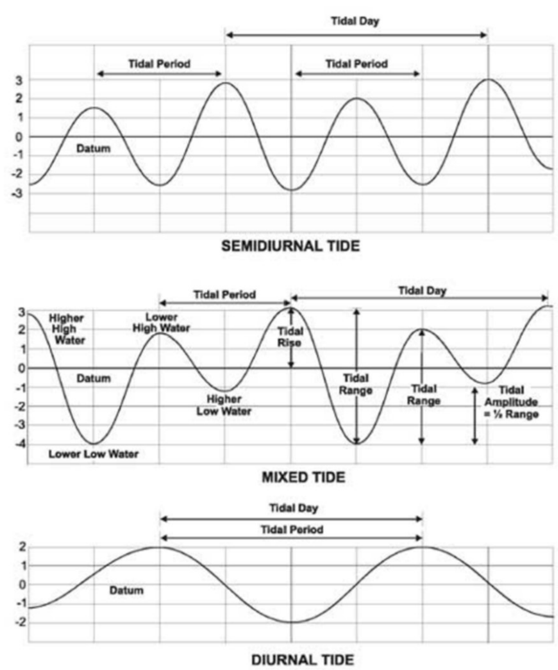

Figure 3: Example Timeseries of Semidiurnal, Mixed, and Diurnal Tides (Basic Concepts in Physical Oceanography: Tides*, n.d.)*

Harmonic tidal constituents are mathematical constants used to describe the effect that the cyclical motion of the Moon or Sun has on Earth's tides. The harmonic tidal constituents can be used to make tidal predictions by superimposing the constituent curves (**Figure 4**) (Schureman, 2001).

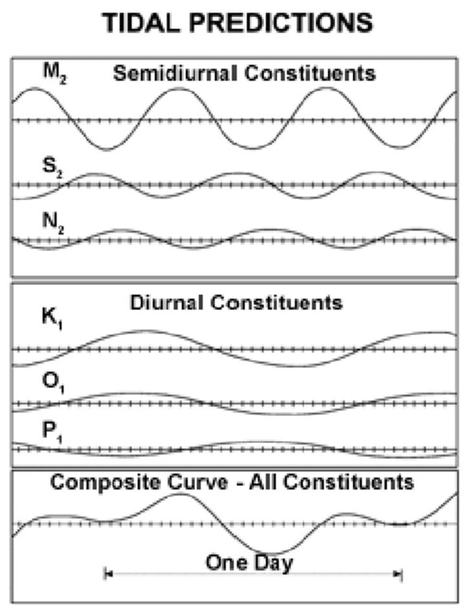

Figure 4: Visual Representation of Tidal Constituents and the Composite Curve Representing the Tide Prediction (Basic Concepts in Physical Oceanography: Tides*, n.d.)*

The rotation of Earth with respect to a celestial body is represented by the principle semidiurnal constituent and occurs every orbital period. For example, The Earth completes a full rotation relative to the moon in 24 hours and 50 minutes, or one Lunar day, and has an orbital period of 12 hours and 25 minutes, or half the Lunar day (Kvale, 2006). The M2 constituent, or the principle lunar semidiurnal constituent, represents the rotation of Earth with respect to the Moon. S2 is the principle solar semidiurnal constituent and has a solar day of 24 hours and an orbital period of 12 hours. The effect of the declination angle of the Moon is expressed as the diurnal constituent. For example, the O1 constituent, or the lunar diurnal constituent, represents the effect of the Moon's declination on tides on Earth. P1 is the solar diurnal constituent and K1 is the lunisolar diurnal constituent. The Moon also contributes a larger lunar elliptic semidiurnal constituent, N2. The N2 constituent accounts for the effect of variation in the Moon's orbital speed with changing elliptical orbits (Pugh, 1987). The plane of this ecliptic orbit of the Moon rotates over an 18.613-year cycle referred to as the "nodal cycle" (Yasuda, 2018).

Extreme variations in tides can be attributed to spring and neap tides (**Figure 5**). Spring and Neap tides occur on a roughly 14.76-day cycle based on the varying superposition of the Earth, Moon and Sun. When the Sun and Moon are aligned, or in syzygy, the gravitational forcing is maximized, and spring tides occur. When the Sun and Moon are at a right angle, the gravitational force is lower, and neap tides occur (Kvale, 2006). Neap tides have smaller tidal ranges while spring tides have relatively large tidal ranges (Parker et al., 2007). The spring and neap cycle is reproduced by considering the M2 and S2 tidal constituent together (Pugh, 1987).

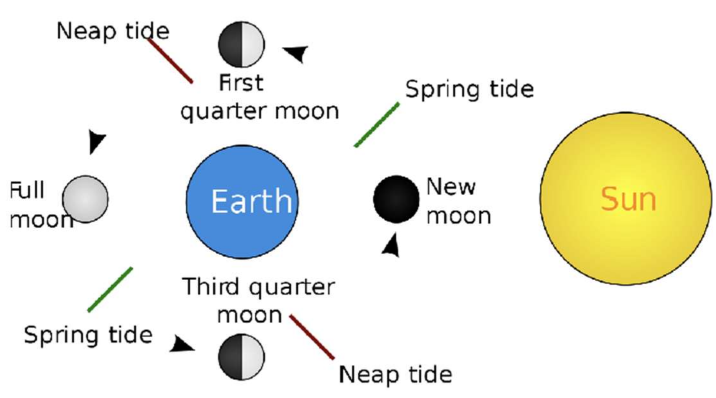

Figure 5: Mechanics of a Spring/Neap Tide Cycle (What Is the Tide?*, n.d.)*

2.1.2 Tidal Datums

A tidal datum is a vertical reference plane constructed from tidal data over a 19 year span of time, known as an epoch. NOAA currently uses the National Tidal Datum Epoch from 1983 to 2001 (*Tides and Currents Glossary*, n.d.). Datums as established by NOAA in Port San Luis using the National Tidal Datum Epoch can be seen in **Figure 6**. Predicted and measured water levels are commonly referenced to accepted tidal datums, such as mean sea level (MSL) or mean lower low water (MLLW). MSL is a tidal datum representing the arithmetic mean of hourly tidal heights observed over the National Tidal Datum Epoch in a particular region. MLLW is a tidal datum representing the average of the daily lowest water heights observed over the National Tidal Datum Epoch in a particular region. Mean low water (MLW) is a tidal datum representing the average of all the low water heights observed over the National Tidal Datum Epoch in a particular region. Other tidal datums used are mean higher high water (MHHW), mean high water (MHW), the greater tidal range (GT), the mean tidal range (MN), the diurnal low water inequality (DLQ), and the diurnal high-water inequality (DHQ) (**Figure 6**) (Parker et al., 2007).

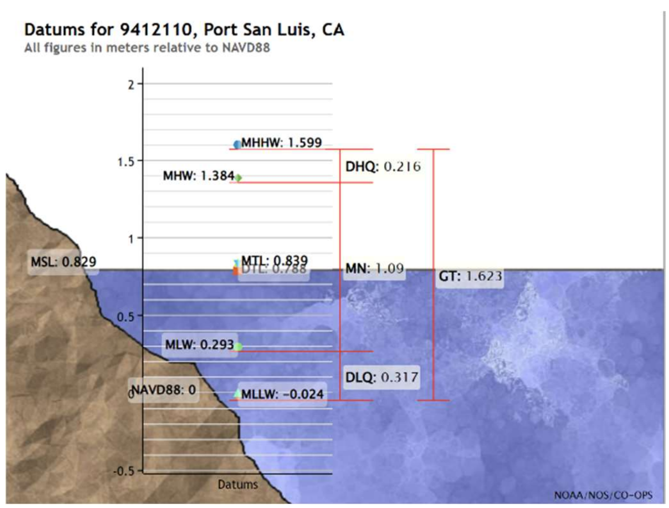

Figure 6: Tidal Datums for NOAA Port San Luis relative to NAVD88 in meters (About Tidal Datums, *n.d.)*

Tidal datums are often related to fixed geodetic reference datums. Geodetic reference datums are often held fixed to an equipotential surface. An example of an equipotential surface is the geoid, or the theoretical surface of the ocean, extending through continents, under the influence of gravity and in the absence of forces such as wind and tides (U.S. Coast and Geodetic Survey, 2001). Currently, the most common geodetic datum that is used in the United States and that is accepted by the National Spatial Reference System (NSRS) is the North American Vertical Datum of 1988 (NAVD88) (Office of Science Quality and Integrity, 2019). This datum utilized one tidal gauge in Canada to estimate the MSL over the span of 19 years and relies on a leveling network on the North American Continent (U.S. Coast and Geodetic Survey, 2001). NGVD 29 was the historical fixed geodetic reference datum used in the United States and was based on MSL from 26 tide gauges and leveling across benchmarks (U.S. Coast and Geodetic Survey, 2001).

Converting between geodetic and tidal datums is typically defined locally due to differences in tides between locations (*About Tidal Datums*, n.d.). For example, the difference between NAVD88 and MLLW in Port San Luis, California reported by NOAA is -0.024 meters (m) in **Figure 6** (*Datums - NOAA Tides & Currents*, 2023).

Figure 6 and **Figure 7** bring the concept of tidal datums and fixed geodetic reference datums together. **Figure 6** depicts the tidal datums as relative to NAVD88. **Figure 7** depicts roughly two days of verified NOAA water levels, relative to NAVD88, from Port San Luis with the mean tidal datums overlayed. Also depicted is the composite tidal curve prediction determined by NOAA using the sum of the tidal constituents described in **Section 2.1.1** (*NOAA Tides & Currents*, n.d.).

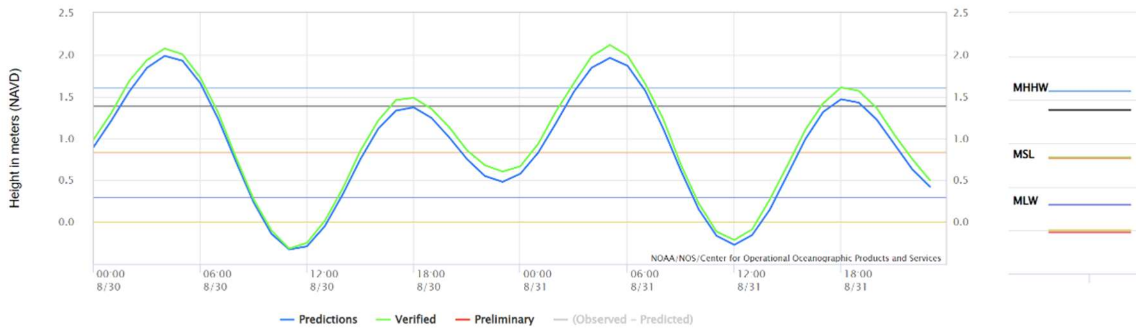

Figure 7: Verified and Predicted Tidal Timeseries Relative to NAVD88 with Tidal Datums Overlayed (NOAA Port San Luis Data Inventory Page*, n.d.)*

2.1.3 The Tidal Prism

The tidal prism is defined by the average volume of water that fills an estuary from mean low to mean high tide (Marani et al., 2003; Petti et al., 2021; Tetra Tech, 2020). From a quantitative standpoint, the tidal prism can be estimated using experimentally determined mean high and mean low water levels, and a bathymetric model. The tidal prism volume is defined as follows (**Eq. 1**):

$$P = V_{MHW} - V_{MLW} \quad \textbf{(1)}$$

where P is the tidal prism volume (acre-feet or m^3) and V is the volume of water in Morro Bay at a given monthly mean high or mean low tidal datum (acre-feet or m^3).

It should be noted that the volume of water exchanged can vary greatly with tidal phase, and that the tidal prism describes the average volume exchanged (Tetra Tech, 2020).For example, a transition from MHHW to MLLW exchanges a larger volume than a transition from MHW to MLW.

2.2 Projected Sea Level Rise Estimates

The California Ocean Protection Council Science Advisory Team has defined sea level rise (SLR) scenarios to guide California State Agencies, such as the California Coastal Commission, in planning future projects (Griggs et al., 2017). The SLR scenarios consider both global and local SLR. Contributors to global SLR include thermal expansion of seawater and volume inputs of fresh water from melting land ice. Contributors to local SLR include vertical land motion, changes in the geoid height and changes in water levels relative to the geoid due to shifting gravitational potential on Earth's Surface as land ice melts (Griggs et al., 2017). The future SLR scenarios can vary based on expected different future anthropogenic emission scenarios defined by the Intergovernmental Panel on Climate Change (IPCC). Each of these potential scenarios are known as a Representative Concentration Pathway (RCP) and are distinguished by their associated radiative forcing. The associated radiative forcing is the average heat trapping capacity of the earth's atmosphere, measured in watts/square meter. The IPCC adopted four main RPC scenarios ranging in severity of future SLR. RCP-2.6 assumes a strict effort to reduce greenhouse gas emissions by 70% by 2050 and by 100% by 2080. RCP-8.5 assumes no change in anthropogenic actions towards reducing global greenhouse gas emissions. The H++ scenario is based on a rapid loss in Antarctic land ice mass. The baseline for the SLR projections is the average sea level for 1991-2009 and is also referred to as the MSL in the year 2000, or the Y2K. The median SLR predictions in San Francisco in the years 2050 and 2100 as estimated by Griggs are depicted in **Table 1** (Griggs et al., 2017).

Table 1: Predictions for Median Sea Level Rise in San Francisco from Griggs (Griggs et al., 2017)

Scenario	feet (above Y2K MSL)	m (above Y2K MSL)
2050	0.9	0.274
2100 RCP-2.6	1.6	0.488
2100 RCP-4.5	1.9	0.579
2100 RCP-8.5	2.6	0.792

2100 H++	10	3.048

2.3 Morro Bay Estuary

Morro Bay lies roughly 160 km South of Monterey Bay within Estero Bay off the coast of Central California (**Figure 8**). The bay is 4 miles (6.44 km) long by 1.75 miles (2.80 km) wide, and typically encompasses over 2000 acres (8.09E+06 m^2) of open water at high tide, and just over 600 acres (2.43E+06 m^2) at low tide (Gerdes et al., 1974; Haltiner, 1998).

Figure 8: Morro Bay can be seen 160 km south of Monterey Bay (Central Coast California Map, *n.d.)*

Morro Bay was created 10 to 15 thousand years ago, when sea levels rose due to glacial melt and submerged the confluence of Los Osos and Chorro creeks. In 1998, the watershed for Los Osos and Chorro creeks encompassed 186 square kilometers. Since the rate of Spanish settlement increased in the early 19th century, Morro Bay has been subject to increased sedimentation due to upstream urbanization and agricultural practices, with accretion of up to +0.5 m measured in the high marsh (Haltiner, 1998).

2.4 Historical Tidal Prism Estimates in Morro Bay

The tidal prism from 1884 to 1998 was estimated by Haltiner, Josselyn, and Tetra Tech (Haltiner, 1998; Josselyn et al., 1989; Tetra Tech, 1999)(**Figure 9** and **Table 2)**. These estimates of the tidal prism in Morro Bay show a 20-30% decrease between 1884 and 1998 (Tetra Tech, 1999). Haltiner attributed this reduction in the tidal prism to the +0.50 m accretion of sediment in the high marsh of Morro Bay (Haltiner, 1998).

Available reports regarding more recent tidal prism estimates were conducted by Tetra Tech in 1998 and 2019 (Tetra Tech, 1999, 2020). In 2019, Tetra Tech amended the 1998 tidal prism estimate from 4700 AF to 6280 AF by adjusting the originally used tidal range of +1.0 to +4.0 feet (ft) MLLW (+0.304 to +1.219 m MLLW) to +1.0 to +4.8 ft MLLW (+0.304 to +1.463 m MLLW) due to comments by David Jay regarding available tidal data for the time period. Surprisingly, with these changes, the tidal prism estimate determined by Tetra Tech for 1998 and 2019 did not follow the historical downward trend.

I directly plotted the tidal prism estimates from Figure 17 in Haltiner (Haltiner, 1998). I plotted the tidal prism estimates from Figure 11 in Haltiner that were adjusted by Tetra Tech in 1998 to account for an underestimation in historical estimates in deep water depths (Tetra Tech, 1999). I also plotted the tidal prism estimated as estimated by Tetra Tech in 1998 using the areal imagery from Table 3 in Josselyn, Martindale and Callaway (Josselyn et al., 1989; Tetra Tech, 1999). Variations in tidal datum analysis, bathymetric surveying and calculation methodology can cause discrepancy in the tidal prism estimate (**Figure 9**)(**Table 2**). When comparing estimates between studies and years, this must be taken into consideration.

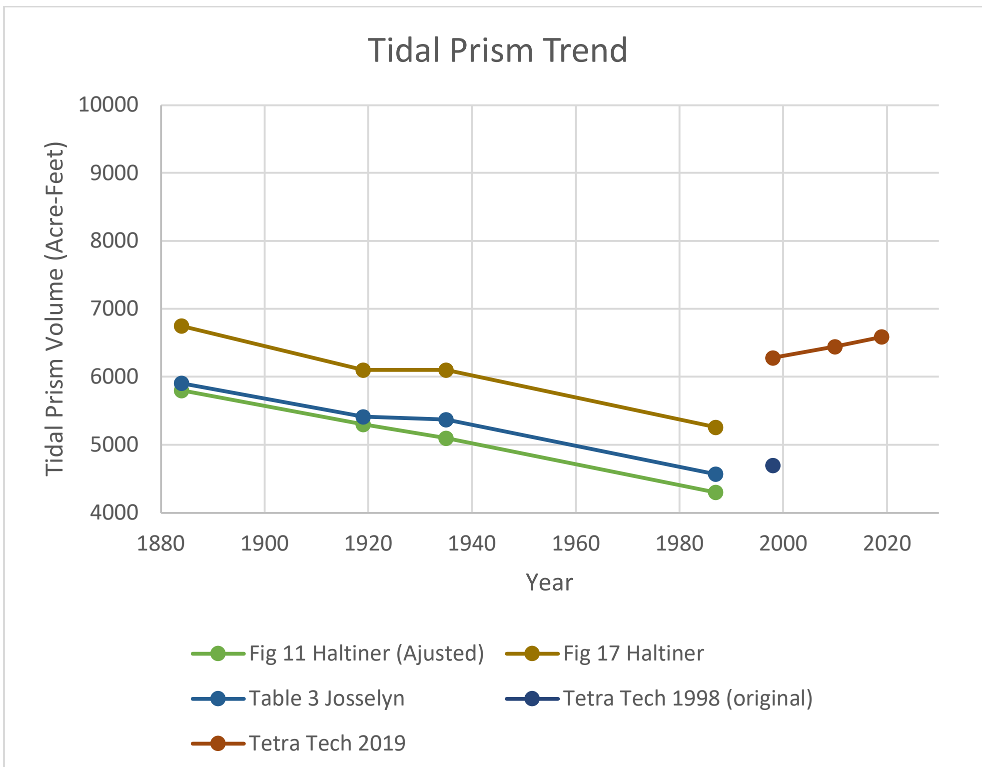

Figure 9: Estimates of the mean tidal prism in Morro Bay between 1884 and 2019

Table 2: Estimates of the mean tidal Prism in Morro Bay between 1884 and 2019.

Data Source	2019 Acre-Feet (m^3)	2010 Acre-Feet (m^3)	1998 Acre-Feet (m^3)	1987 Acre-Feet (m^3)	1935 Acre-Feet (m^3)	1919 Acre-Feet (m^3)	1884 Acre-Feet (m^3)
Fig. 17 Haltiner	-	-	-	5260 (6.49E+06)	6100 (7.52E+06)	6750 (8.33E+06)	6750 (8.33E+06)
Fig. 11 Haltiner	-	-	-	4300 (5.30E+06)	5100 (6.29E+06)	5300 (6.54E+06)	5800 (7.15E+06)
Table 3 Josselyn	-	-	-	4569 (5.64E+06)	5372 6.63E+06)	5415 (6.68E+06)	5906 (7.28E+06)
Tetra Tech 1998	-	-	4700 (5.80E+06)	-	-	-	-
Tetra Tech 2019	6589.4 (8.13E+06)	6651.5 (8.20E+06)	6280 (7.75E+06)	-	-	-	-

2.4.1 Historical Mean Tides in Morro Bay

Various methodologies and instruments have been used to gather historical tidal datums for Morro Bay (**Table 3**). To determine the tidal prism, an accurate estimation for MHW and MLW (relative to a geodetic reference datum such as NAVD88) must be used, as different tidal datums can lead to discrepancies in the tidal prism estimation. When comparing the tidal monitoring between years, a few differences arise. A notable difference between studies is that the tidal data from each monitoring period were taken during different times of the year. Tidal elevation data taken from a small time period may not be representative of monthly and yearly averages due to sea level variability over time. Additionally, the instrumentation used to conduct tidal monitoring has changed and can influence the overall accuracy of the measurement. Differences in surveying, tidal monitoring and calculations can all lead to discrepancies. Finally, the datums that tidal elevations are referenced to influence overall accuracy. For example, MLLW was historically used and was determined for a relatively short period of time during the hydrographic survey. MLLW can also vary between the years of measurement (Haltiner, 1998). In the table below, I adjusted any tidal elevations relative to NGVD29 to NAVD88 by adding 2.79 ft (0.850 meters) based on vertical control points from the National Geodetic Survey points along Morro Bay (NOAA, n.d.).

Table 3: Historical MHW and MLW when calculating the tidal prism in Morro Bay. "Measured" refers to tides that were observed in the field for a period of time. "Assumed" refers to a tidal range that was assumed for the tidal prism calculation when tidal surveys were unavailable for given years with bathymetric models.

Year	Assumed or Measured	Dates of Measurement	MLW (m NAVD88)	MTL (m NAVD88)	MHW (m NAVD88)
1884[1]	**Assumed**	-	0.424	0.914	1.338
1919[2]	**Measured**	-	0.362	0.849	1.338
1919[1]	**Assumed**	-	0.424	0.914	1.338
1935[1]	**Assumed**	-	0.424	0.914	1.338
1987[3]	**Assumed**	-	0.299	0.756	1.213
1988[4]	**Measured**	-	0.302	0.851	1.402
1998[5]	**Assumed**	-	0.338	0.795	1.252
1998[6]	**Measured**	March 9th -April 10th	0.338	0.917	1.500
1998[7]	**Measured**	March 9th -April 10th	0.260	0.840	1.42
2010[8]	**Assumed**	-	0.260	0.840	1.42
2010[9]	**Assumed**	-	0.275	0.835	1.395
2019[10]	**Measured**	August 1st -30th	0.275	0.835	1.395

1) Originally tides datums used by Haltiner for the tidal prism relative to the 1919 MLLW. I adjusted values to NAVD29 by subtracting 2.40 feet (0.731 m). Adjustment made based on measured 1919 tidal data from the US Coast and Geodetic Survey specified MLLW to be -2.40 ft (-0.731 meters) NGVD29 (Haltiner, 1998).

2) Originally measured tidal datums in 1919 relative to NGVD29 (Tetra Tech, 1999).

3) Originally tidal datums used by Haltiner for the tidal prism relative to the 1988 MLLW (Haltiner, 1998). I adjusted valued to NGVD29 by subtracting 2.81 feet (-0.856 m). Adjustment made based on measured 1988 tidal data form the US Coast and Geodetic Survey specified MLLW to be -2.81 ft (-0.856 meters) NGVD29 (Haltiner, 1998).

4) Measured tidal data in 1988 by the National Ocean Survey, originally relative to NGVD29 (Haltiner, 1998).

5) Original 1998 tidal range used for tidal prism calculation by Tetra Tech in 1998. For this period, Tetra Tech specified MLLW to be 2.68 feet (0.817 meters) below NGVD29 (Tetra Tech, 1999). Therefore, I adjusted the assumed tidal datums from MLLW to NGVD29 by subtracting 2.68 feet (0.817 m).

6) The measured 1998 tidal datums as reported by Tetra Tech in 1998, however not utilized for the tidal prism calculation (Tetra Tech, 1999). For this period, Tetra Tech specified MLLW to be 2.68 feet (0.817 meters) below NGVD29 (Tetra Tech, 1999). Therefore, I adjusted the assumed tidal datums from MLLW to NGVD29 by subtracting 2.68 feet (0.817 m).
7) The updated tidal range used for the accepted 1998 tidal prism calculation by Tetra Tech in 2019. Comments made by David Jay to reflect measured tidal data in 1998 by the National Ocean Survey. Tetra Tech converted the tidal datums to NAVD88 using the 2019 MLLW value offset of -0.045 meters (Tetra Tech, 2020). The datum conversion made by Tetra tech in 2019 may not be reflective of 1998 tidal conditions.
8) No tidal data existed for the 2010 estimate, therefore Tetra Tech used 1998 tidal datums (Tetra Tech, 2020). Tetra Tech converted the tidal datums to NAVD88 using the 2019 MLLW value offset of -0.045 meters (Tetra Tech, 2020). The datum conversion is not reflective of 1998 tidal conditions.
9) No tidal data existed for the 2010 estimate, therefore Tetra Tech used 2019 tidal datums (Tetra Tech, 2020).
10) The tidal datum as determined by Tetra Tech in 2019 relative to NAVD88 (Tetra Tech, 2020).

The tidal prism estimates for 1884, 1919, 1935 and 1987 determined by Haltiner, Josselyn, and Tetra Tech assuming a tidal range of +1.0 to +4.0 ft MLLW (+0.304 to +1.219 m MLLW) (Haltiner, 1998; Josselyn et al., 1989; Tetra Tech, 1999). The 1919 tidal data relative to NGVD29 from the US Coast and Geodetic Survey were utilized for the datum conversions and for guidelines in creating the assumption surrounding the tidal range used to calculate the mean tidal prism (Tetra Tech, 1999). It should be noted that despite the 1919 experimental tide measurements showing a tidal range from +0.8 ft MLLW to +4.0 ft MLLW (+0.243 to +1.219 m MLLW), the tidal range used to calculate the tidal prism was +1.0 ft MLLW to +4.0 ft MLLW (+0.304 to +1.219 m MLLW).

The 1987 tidal survey was conducted by Phillips Williams and Associates during a 30-hour period from August 6th to August 7th (Haltiner, 1998). A continuous water level monitor at the Coast Guard Pier recorded tidal elevations every 15 seconds and was placed in a stilling basin to remove high frequency fluctuations. The other four locations had a tide staff gauge installed and were surveyed into benchmark “Rod 22” (**Figure 10**). However, a conversion to NGVD29 was not available. Instead, MHW and MLW were estimated and corrected based on historical observed events and measured tide staff values. Because of the lack of surveying data, the previously used tidal range of +1.0 to +4.0 ft MLLW (+0.304 to +1.219 m MLLW) was assumed to calculate the tidal prism in 1987 (Haltiner, 1998).

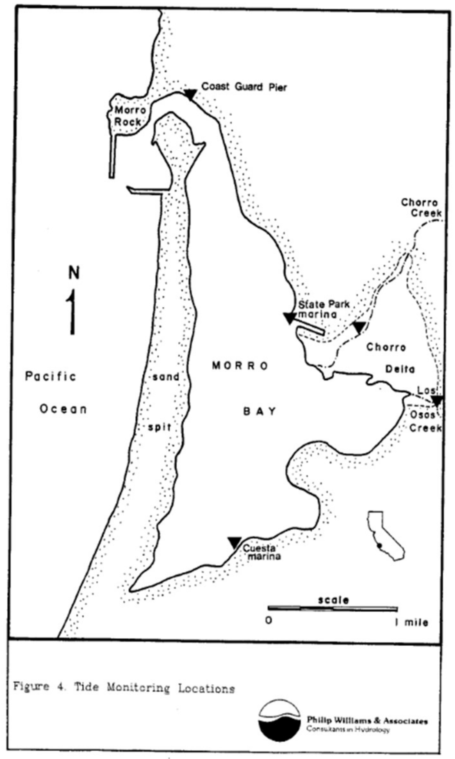

Figure 10: Water Level Gauge Locations for the 1987 tidal survey as stated by Haltiner in 1988 (Haltiner, 1998)

In 1998, Tetra Tech utilized two hydrostatic pressure gauges to determine the tidal elevations in Morro Bay from March 9th to April 10th (**Figure 11**) (Tetra Tech, 1999). The gauges were set to switch on every 10 minutes and record the average of 60 readings sampled every one-half second. Despite the tidal monitoring, the original 1998 tidal prism estimate also assumed a tidal range of +1.0 to +4.0 ft MLLW (+0.304 to +1.219 m MLLW). In 2019, Tetra Tech amended the original tidal range to +1.0 to +4.8 ft MLLW (+0.304 to +1.463 m MLLW) due to comments by David Jay. The tidal range was updated to reflect the experimentally determined tidal datums presented in Table 1-1 of the Tetra Tech 1998 study, rather than using the assumed values of +1.0 to +4.0 ft MLLW (+0.304 to +1.219 m MLLW) (Tetra Tech, 1999). It should be noted that this is the first year in which the tidal prism was calculated using a tidal range above +4.0 ft MLLW (+1.219 m).

In August of 2019, Tetra Tech conducted a tidal survey utilizing two "temporary tidal gauges" for 30 days (**Figure 11**) (Tetra Tech, 2020). The 2019 study used the averages between the two gauge locations to determine the mean tidal datums.

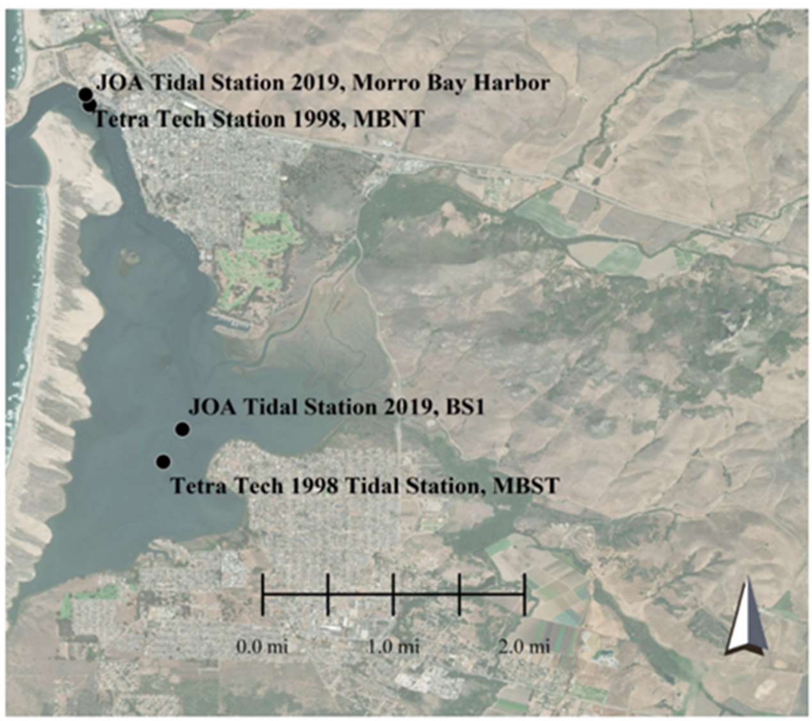

Figure 11: Gauge locations for the 1998 and 2019 tidal surveys conducted by Tetra Tech (Tetra Tech, 2020)

2.4.2 Historical Bathymetric Surveys

Various methodologies and instruments have been used to generate bathymetric maps of Morro Bay during different time periods (**Table 4**). It is important to acknowledge the factors that produce inconsistencies when comparing elevation data. Variation in reference datums, spatial resolutions, equipment, methodology and the associated accuracy can all influence bathymetric data, and in turn, the tidal prism estimate.

A large challenge that Haltiner addressed in 1998 was the conversion of all bathymetric maps to a fixed datum. Historically, bathymetric maps have been based on MLLW, a tidal datum, from a short period of tidal monitoring. Haltiner assumed that MLLW was 2.4 ft (0.731 m) below NGVD29 for the 1884, 1919 and 1935 tidal prism analysis based on available data from 1919 tidal conditions. Haltiner used data from the National Ocean Survey in 1988 to determine that MLLW was 2.81 ft (0.856 m) below NGVD29 for bathymetry model created in 1987. Additionally, to compare to a common datum, the elevations in the 1884, 1919 and 1935 bathymetric maps were adjusted by 0.41 ft (0.125 m) to reflect tidal conditions in 1998 (Haltiner, 1998). It is known that MLLW in 1998 was 2.68 ft (0.817 meters) below NGVD29 (Tetra Tech, 1999).

Haltiner also made the point that bathymetric maps from 1884, 1919 and 1935 had scarce elevation data +2.0 ft MLLW (+0.609 m MLLW), and virtually no data above the +4.0 ft MLLW (+1.219 m MLLW) line. For this reason, it was assumed that the +4.0 ft MLLW (+1.219 m MLLW) mark would be used to approximate average upper limit of tidal action. It should be noted that 1919 tidal data from the US Coast and Geodetic Survey does reflect that MHW is +4.0 ft MLLW (+1.219 m MLLW), but data from the National Ocean Survey in 1988 indicates that MHW is +4.62 ft above MLLW (+1.408 m MLLW) (Haltiner, 1998). This shift in the tidal range could be due to deepening of the harbor entrance and subtidal channels through dredging operations dating back to 1949 (US ARMY COE, 1974). Pareja-Roman et al. showed that deepening of the harbor entrance in

Jamaica Bay, New York reduced tidal dampening and increased tidal reflection, resulting in an amplification of the tidal range (Pareja-Roman et al., 2023).

Table 4: The information regarding the historical bathymetric maps used to calculate the tidal prism in Morro Bay.

Year	Source	Scale	Datum
1884	US Coast and Geodetic Survey	1:10,000	MLLW
1919	US Coast and Geodetic Survey	1:5,000	MLLW
1935	US Coast and Geodetic Survey	1:5,000	MLLW
1987	Phillips Williams and Associates	1:5,000	MLLW
1998	Tetra Tech	-	MLLW
2010	NOAA	-	NAVD88
2019	NOAA	-	NAVD88

The technology and methodology for collecting bathymetry has varied, and with that, so has its accuracy. Below is a more detailed overview of methodology in past surveys to create bathymetric maps that have been used to calculate the tidal prism.

Historical bathymetric maps from 1884, 1919, and 1935 can be found in Haltiner (Haltiner, 1998). Haltiner created contour lines relative to MLLW by interpolating to known elevation points of geographically significant surroundings in Morro Bay (Haltiner, 1998). Haltiner converted all the maps to a fixed datum, NGVD29.

The 1987 survey conducted by Haltiner utilized a precision-depth fathometer with a hull-mounted transducer during September to determine water depths in Morro Bay. The fathometer was determined to be accurate to +/- 0.5 percent. A computer navigation system paired with four transponders was used to spatially locate the boat while recording individual depth readings. This allowed surveyors to maintain measurements along the predetermined track lines across the bay. The accuracy of this positioning system was determined to be +/- 2 ft (0.610 m). Boat motion could have added $1/10^{th}$ of a foot (0.031 m) of error to the depth readings, but it was relatively calm during the survey. A computer was used to reduce the data by post-plot track line maps. This generated a plot of water depth along the track lines of measurement which was then used to hand develop contour lines at one foot depth intervals. After Haltiner interpolated depth measurements from a partial bathymetric data for 1987, he verified the points with the full 1979 bathymetry data (Haltiner, 1998).

The 1998 bathymetric survey conducted by Tetra Tech from March 11^{th}-16^{th} utilized a digital fathometer. Measurements occurred every 30 ft (9.144 m) along predetermined survey lines 500 ft (152.4 m) apart, resulting in 4,500 total measurements. Differential GPS was used to fix the positions of each measurement while monitoring. This was combined with GPS high tide line markings taken every 30 seconds by a surveyor walking around the bay, or on a kayak with the instrument antenna attached to a 10 ft (3.048 m) pole. According to Tetra Tech, this method most likely underestimated the tidal prism because the coarse resolution excluded the deeper side channels of the bay while marking the high tide line. Vertical accuracy due to instrument accuracy, boat movement, and tidal corrections was estimated to be 0.50 ft (0.152 m). The horizontal accuracy of the high tide line ranges from 6 to 15 ft (1.829 to 4.572 m) depending on the steepness of the beach slope. Steeper slopes allowed for better accuracy at identifying the high tide line, whereas beaches with low slopes were more difficult to define (Tetra Tech, 1999).

For the 2010 tidal prism estimate by Tetra Tech, topobathy LiDAR from 2009 to 2011 was merged with 2013 acoustic sonar. Data gaps in the LiDAR survey in the deeper channels were infilled with the acoustic sonar data from 2013. These data gaps were in regions below MLLW, thus not affecting the tidal prism. Vertical accuracy was shown to be 5 to 15 centimeters (cm) for topographic LiDAR, and 15 to 30 cm for bathymetric sonar data (Tetra Tech, 2020).

For the 2019 tidal prism estimate, Quantum Spatial acquired airborne LiDAR on May 22, and acoustic sonar data was acquired from June 17th - June 19th. These two data sets were merged, providing a complete Digital Elevation Model (DEM). Data gaps below the MLLW line in flat areas were linearly interpolated. A polygon tool in Google Earth was used to eliminate data outside of Morro Bay on the DEM. Vertical accuracy was shown to be 5 to 15 cm for topographic LiDAR, and 15 to 30 cm for bathymetric sonar data (Tetra Tech, 2020).

2.4.3 Calculation Methods

The method in which the tidal prism volume was calculated differs between studies and is described below. With different methods of calculating the tidal prism, there can be expected deviation between calculated values.

For the tidal prism estimates for 1884, 1919, 1935, and 1987, Haltiner used hand planimetering between elevation contour lines to determine volumes of water (Haltiner, 1998). This is a conventional method historically used to calculate volumes between contour lines before widespread computer program usage.

Tetra Tech analyzed the bathymetric model for 1998 using conventional contouring, arial photos, and Geographic Information System (GIS) tools. For 1998, depth contours were plotted separately and added to GIS. The volume of water between contour lines was then determined by multiplying the difference in depth by the average of the areas of the two contours. This method can drastically overestimate or underestimate the tidal prism by assuming averages (Tetra Tech, 1999).

The adjusted 1998, 2010 and 2019 tidal prism calculations were estimated by Tetra Tech in 2019 using Global Mapper Version 20 by Blue Marble Geographics, a GIS software tool. The "Calculate Cut and Fill Volume" tool was used to determine the volume between given tidal levels (Tetra Tech, 2020).

2.4.4 Spatially Varying Water Levels in Morro Bay

On March 30th, 1998, Tetra Tech observed differences in the magnitudes of high tides between tidal stations at the Coast Guard North T-Pier and in Baywood Los Osos (**Figure 12**). Tetra Tech identified that the maximum elevation at high tides in Baywood Los Osos were roughly +0.5 ft (0.152 m) above the Coast Guard North T-Pier, while differences at low tide were very small (Tetra Tech, 1999). However, in the tidal prism estimate, they assumed a unform water level by averaging the water levels between the two stations.

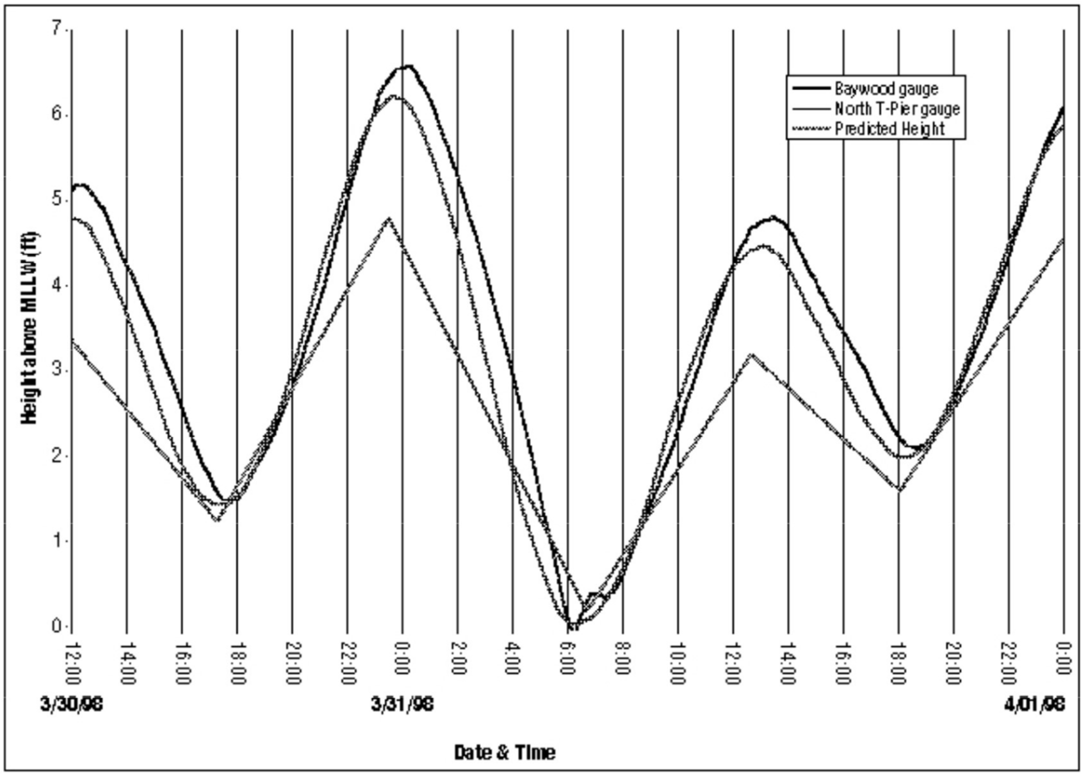

Figure 12: A 36-hour tidal timeseries from March 30th, 1998 depicting elevation differences at maximum tides from Tetra Tech (Tetra Tech, 1999).

Spatial variation in water levels can influence the tidal prism volume. Until now, the estimates for the tidal prism volume in Morro Bay have used a singular tidal monitoring station or the average between two stations. Accounting for this spatial difference by linearly interpolating between tidal monitoring stations may influence the estimations of the volume of water entering Morro Bay over a tidal cycle. Therefore, an assessment to determine the spatial variation of water levels within Morro Bay is needed.

2.5 Eelgrass (Zostera marina)

Intertidal habitats such as intertidal mudflats, low marsh and high marsh are distinct vegetation habitat zones that are strongly influenced by tidal elevations. The USGS utilized a 10-year span from 2004 to 2013 of NOAA data to define habitat zonation in various estuaries along the West Coast, including Morro Bay (Freeman & Chase M, 2016).

They modeled local and regional differences in tidal marsh vulnerability to SLR. With SLR, the high marsh habitat in Morro Bay is predicted to be lost and is expected to transition to intertidal mudflats.

Eelgrass (Zostera marina) plays an vital role in estuaries along the west coast of North America and is considered an ecosystem engineer because it creates habitat for other organisms (S. H. Munsch et al., 2023). Eelgrass in Morro Bay creates necessary breeding grounds for fish, Dungeness crab, and clams which are all essential food sources for California Sea Otters and waterfowl (Chestnut, 1999). Eelgrass is limited in its lower band of growth by the light compensation point, or the water depth at which the eelgrass cannot receive sufficient sunlight for growth in turbid estuarine water. The upper limit is limited by desiccation and grazing when exposed to at low tide (Chestnut, 1999). According to a report conducted by Tetra Tech for the Morro Bay National Estuary Program (MBNEP), eelgrass has a lower growth limit of -6 ft MLLW and an upper limit of +1.5 ft MLLW (-1.822 to +0.457 m MLLW) (Tetra Tech, 2021). The MBNEP considers zones within this viable habitat range to be future expansion zones for targeting restoration efforts. These bands of growth were determined by analyzing historical eelgrass density at various depths in Morro Bay during 2007, 2009, 2010 and 2019. Based on historical eelgrass coverage from 2007 to 2019, Tetra Tech generated histograms depicting the distribution of eelgrass density as a percentage as it varies with depth. Any depths at which there was more than five percent coverage were deemed within the typical viable eelgrass growth range for Morro Bay. Historical eelgrass extents have been overlayed onto viable eelgrass habitat and overrepresent the actual coverage (**Figure 13)** (Tetra Tech, 2021). Additional historical records dating back to 1960 indicate that eelgrass acreage in Morro Bay has ranged from merely 9 acres (3.64E+04 m^2) in 2017, to as much as 435 acres (1.76E+06 m^2) in 1994 (Bay, 2021).

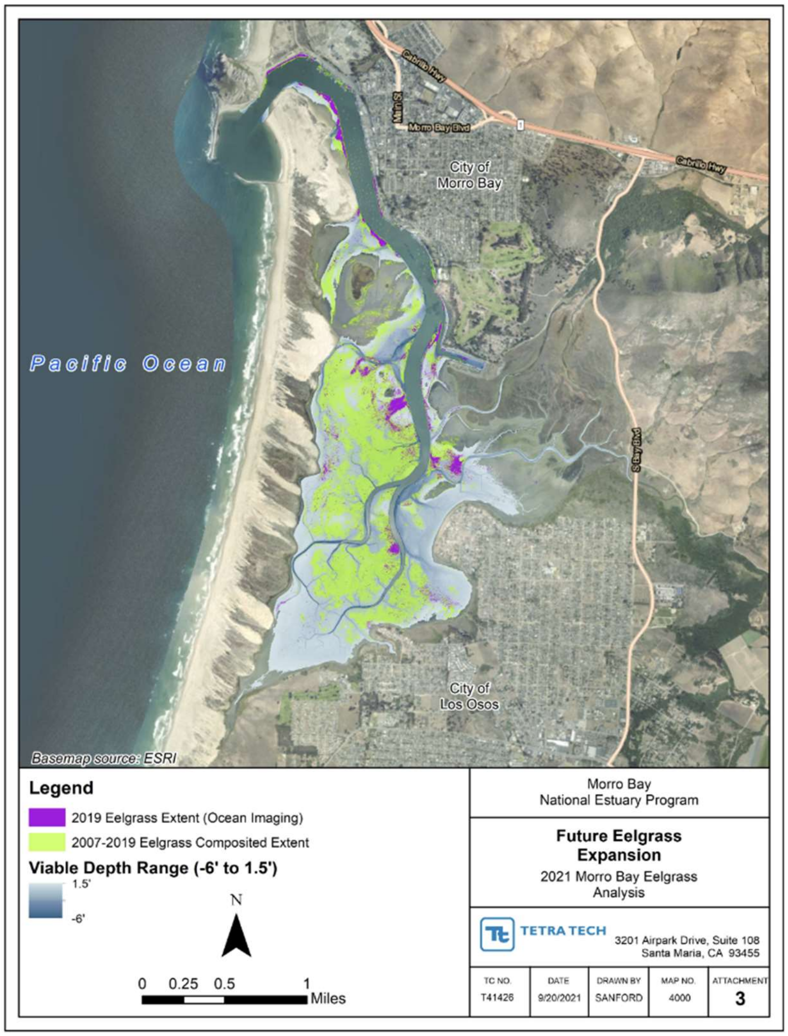

Figure 13: Identified 2007-2019 Composite Eelgrass Extent in Morro Bay Overlayed onto Viable Habitat Area from Tetra Tech in 2021 (Tetra Tech, 2021)

A widespread collapse of eelgrass in Morro Bay after 2010 is thought to have caused large amounts of erosion in Morro Bay (**Figure 14**). Some locations in Morro Bay experienced up to a +0.50 m increase in depth, with an average of +0.10 m of depth increase in the entire bay (**Figure 15**).

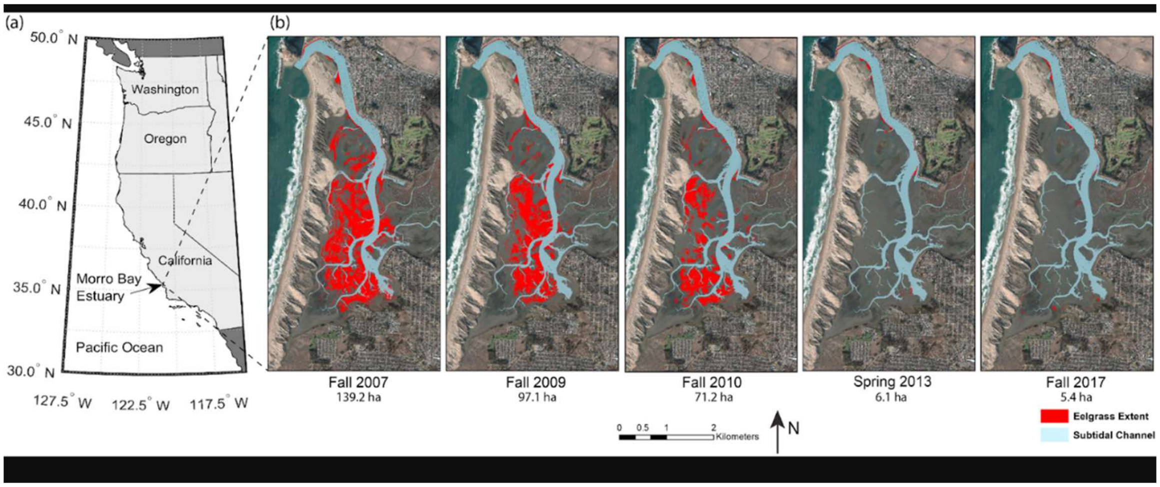

Figure 14: Eelgrass area plotted over satellite imagery from 2007 to 2017. Figure from (Walter et al., 2020)

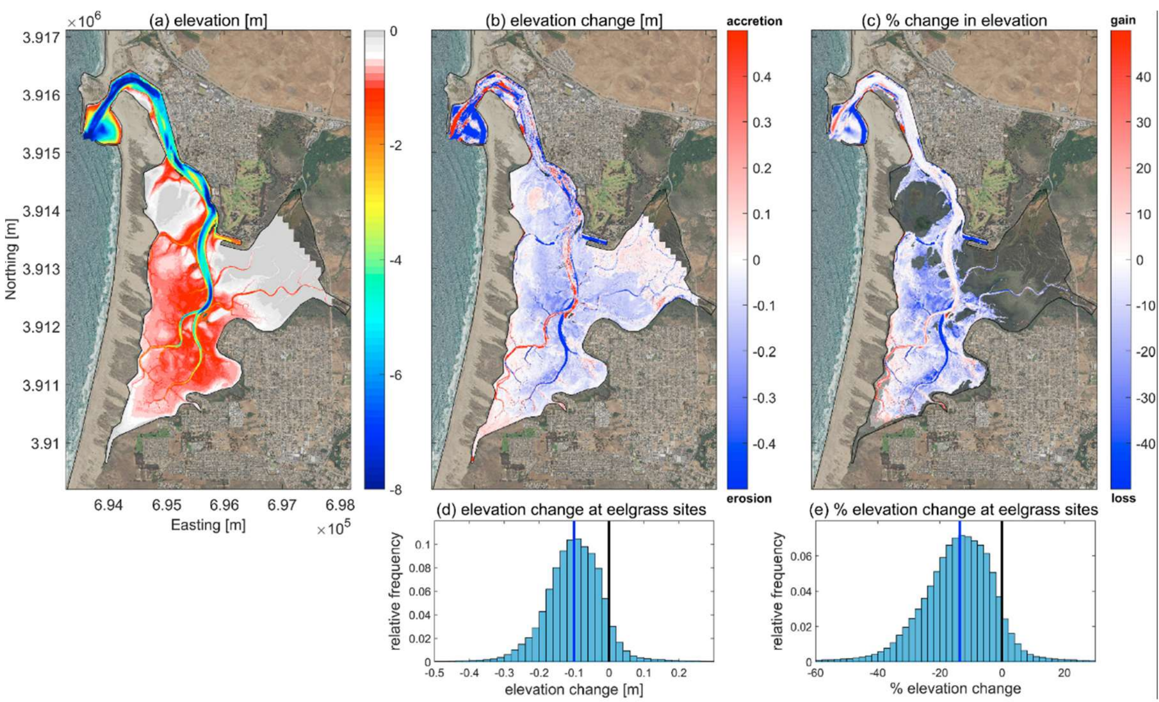

Figure 15: Elevation changes between 2010 and 2019. Figure from (Walter et al., 2020)

Eelgrass can dampen wave energy, slow near-bed velocities, and increase drag on the flow. Eelgrass also promotes sediment deposition and accretion over time, combatting erosion. When this habitat is lost, bottom shear stress on the bed is increased, sediment becomes suspended, and is lost via erosion (Walter et al., 2020). Additionally, it is proven that eelgrass loss negatively impacts biodiversity and ecological health inside an estuary (Short et al., 2011). Following the large spread eelgrass decline in Morro Bay after 2010, it has been observed that bay pipefish and invertebrate populations declined, while flatfish and staghorn sculpin populations increased (O'Leary et al., 2021). Eelgrass exposed to great stressors, such as anthropogenic modification of estuaries and drought, can result in larger changes over time (S. Munsch et al., 2023). Changes in vegetation coverage can directly influence sedimentation and erosion patterns, and thus the tidal prism (by changing the bathymetry) (Panda et al., 2013). Using the viable vertical growth range of eelgrass in Morro Bay determined by the Tetra Tech in 2021, the current viable eelgrass habitat area can be estimated and projected into the future.

2.6 Moving Forward

This study aims to determine the current tidal prism in Morro Bay and project it to the years 2050 and 2100 using the SLR scenarios for San Francisco (Griggs et al., 2017). The tidal prism was calculated using experimental tidal data obtained using student-built ultrasonic gauges. The water level data from these instruments were verified with measurements from commercial style gauges and tide staffs. The tidal prism was calculated using the tidal datum from one or multiple water level measurements. Reasons for shifts in the tidal prism such as varying sea levels and bathymetry was explored to search for a potential explanation. Additionally, a model was created to predict current and future potential viable eelgrass habitat area.

Chapter 3: MATERIALS & METHODS

This section details the methodology used to evaluate the monthly mean tidal datums, the tidal prism, and the viable eelgrass habitat area in Morro Bay.

3.1 Student-Built Ultrasonic Tidal Gauges

The primary instrumentation to evaluate tides used for this project were student-built ultrasonic tidal gauges described in Dunn (Dunn, 2023). Over the course of this project, I assembled, deployed, surveyed, and maintained four Cal Poly instruments in Morro Bay. Additionally, I utilized a commercial Stilltek gauge and the NOAA Port San Luis gauge to estimate tidal datums, discussed later in **Section 3.2**.

3.1.1 Instrumentation Parts and Mechanism

The components needed to build the instruments cost around $300 each and must be hand assembled. This gauge was protected inside a watertight encasement (**Figure 16**). As needed, components were soldered onto a custom Arduino Printed Circuit Board. The instrument was powered by a Voltaic Systems 2-Watt solar panel (**Figure 16**), with Adafruit LiPo (Lithium Ion) battery storage. An Adafruit Solar Charger and Solar Adaptor were both needed for the connection. To preserve battery life, I utilized a duty cycle where the instrument measured at 6 Hz for 5 minutes and was in sleep mode for 10 minutes. A Maxbotix Ultrasonic Sensor **(Figure 16)** with a range of 0.5 m to 10 m was used to record distance measurements. An Adafruit GPS Clock was used for timing. An onboard Adafruit Temperature and Humidity sensor probe (**Figure 16**) was also included. An external temperature and humidity gauge was deployed near the tidal instrument in the shade (**Figure 17**). An Adafruit micro-storage device breakout directed all data to a micro-storage device card with all the output data: timestamp, distance, temperature, humidity. More information regarding instrument design and components can be found in Dunn (Dunn, 2023).

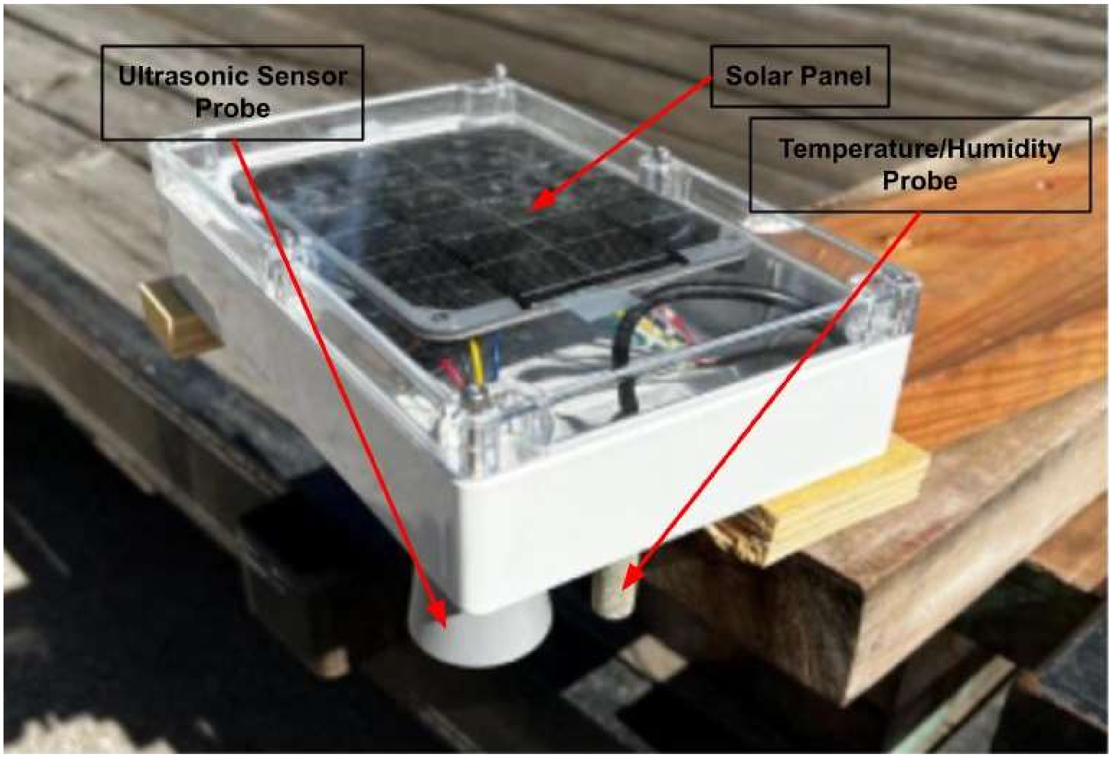

Figure 16: Cal Poly Ultrasonic Tidal Gauge

Figure 17: Cal Poly External Temperature and Humidity Gauge

To obtain water level measurements, the gauge records the total time it takes for the ultrasonic signal to travel from the ultrasonic probe to rebound off the water's surface and return to the ultrasonic probe. This time is translated into an original distance measurement based on an estimate of the speed of sound in the Maxbotix sensor probe, using the air temperature at the transducer (not disclosed from the instrument). The data from the Cal Poly external temperature and humidity probe is then used to correct the original distance measurement to account for the speed of sound varying with changing air densities.

3.1.2 Location Selection in Morro Bay

Many factors were considered in the placement of Cal Poly gauges in Morro Bay. The gauges must be mounted to a stable and stationary location, be completely level, unobstructed below, in adequate sunlight for solar recharging and accessible for data retrieval. Additionally, the instrument must be placed at a location above the water such that it is never less than 0.5 m or more than 10 m above the water, at any given tidal stage. It was also desired that each gauge be placed in different locations around Morro Bay to observe potential spatial differences in water levels, and the implications on the tidal prism volume. For this reason, locations in both the tidal flats and in the sub-tidal channels were desirable. Lastly, any locations that were in the way of potential boat traffic were not desirable due to the possibility of damaging the instruments and interfering with the data collection.

Due to these constraints, limited locations were available for gauge deployment around Morro Bay. I used Google Earth, a geospatial rendering platform used to visualize the Earth, to identify potential locations such as stationary (non-floating) piers and vertical dock pylons near floating piers. I then contacted the responsible organizations to obtain permission to deploy the instruments. Organizations contacted included the Morro Bay State Park, County of SLO, and the City of Morro Bay. Permission to deploy at the Coast Guard North T-Pier was previously obtained. The Cal Poly Coast Guard gauge, the commercial Stilltek gauge, and the Coast Guard Tide Staff are located at the Coast Guard North T-Pier in Morro Bay (**Figure 18**). I installed three additional Cal Poly gauges at the Morro Bay Bayfront Marina, the Morro Bay State Park Marina, and a private pier in Los Osos (**Figure 19**). I installed an additional tide staff at the Morro Bay State Park Marina. Additionally, NOAA maintains a Meteorological (MET) station at the Coast Guard North T-Pier that will later be used to compare ambient air temperatures.

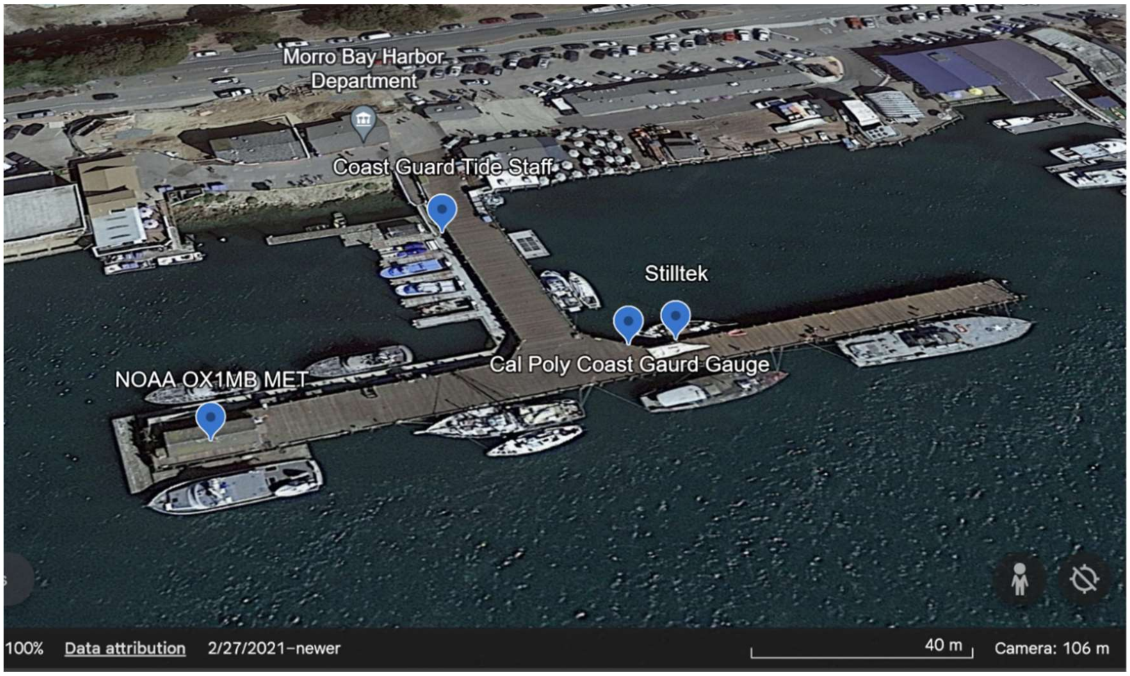

Figure 18: Instrument Locations at the Morro Bay Coast Guard North T-Pier

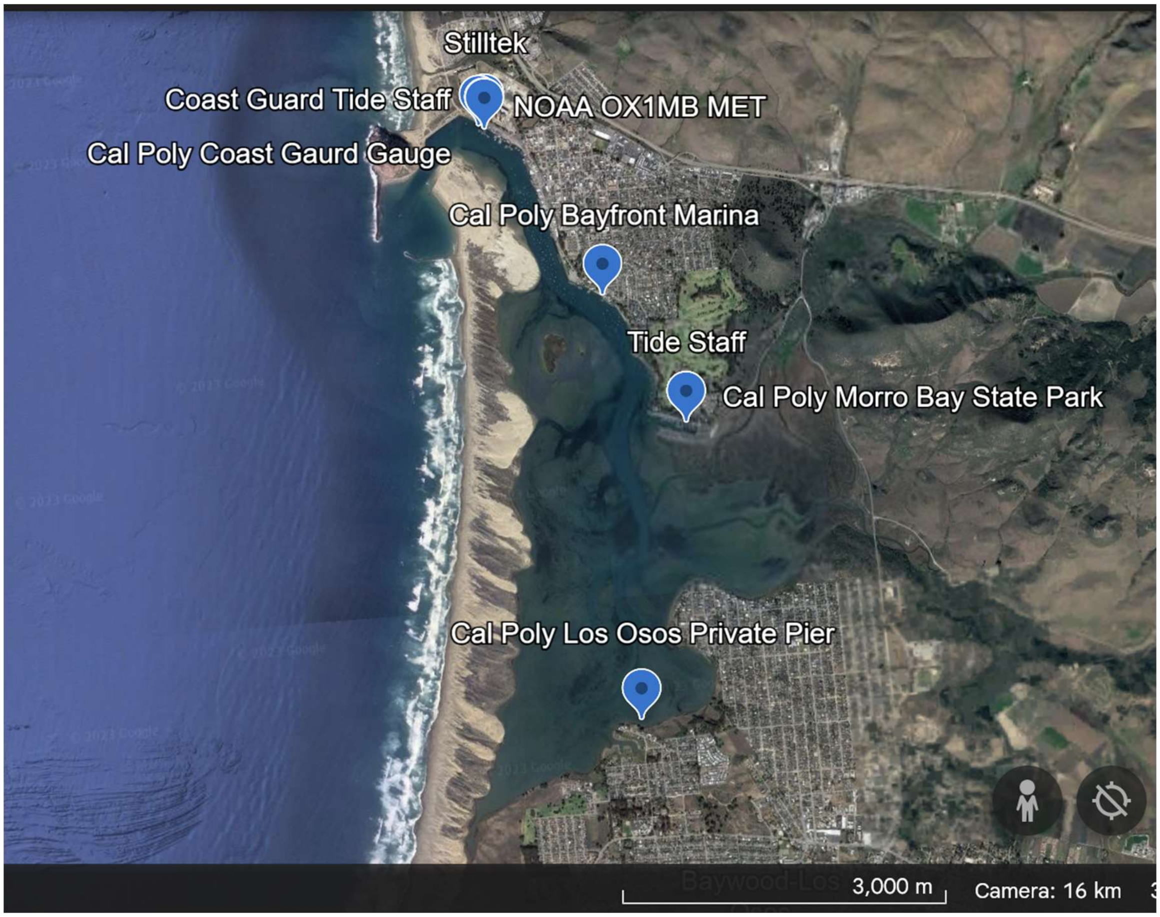

Figure 19: All Instrument Locations in Morro Bay

3.1.3 Gauge Installation

I used a basic wooden cantilever to deploy the Cal Poly gauge at the Coast Guard North T-Pier (**Figure 20**), Bayfront Marina (**Figure 21**), and a private residential pier in Los Osos (**Figure 22**). I screwed the cantilevered instrument directly into the wooden pier, ensuring no obstructions below.

Figure 20: Cantilever Instrument Mount at the Coast Guard North T-Pier

Figure 21: Cantilever Instrument Mount at the Morro Bay Bayfront Marina

Figure 22: Cantilever Instrument Mount at the Private Pier in Los Osos

Due to the limited structures available at the Morro Bay State Park Marina, pylons for floating docks were also used as a mounting structure. Hose clamps were used to secure a wooden L-shaped platform for the Cal Poly gauge, as in Morro Bay State Park Marina (**Figure 23**). I installed the gauge at a high tide at the highest point possible on the pylon to ensure measurement of all tidal stages and to avoid immersion. Because of this, any data retrieval or maintenance occurred at high tide. More information regarding installation of specific instruments is available in **Appendix A**.

Figure 23: Hose Clamps to secure L-Shaped Platform on Pylon at Morro Bay State Park Marina

Additionally, two tide staffs were used to verify water level data from the Cal Poly gauges. I cleaned and maintained an existing tide staff installed by Dunn on a pylon at the Coast Guard North T-Pier (**Figure 24**) (Dunn, 2023). I installed an additional tide staff on a pylon directly under the Cal Poly gauge at the Morro Bay State Park Marina (**Figure 25**).

Figure 24: Tide Staff at the Coast Guard North T-Pier (Before Cleaning)

Figure 25: Tide Staff at the Morro Bay State Park Marina

3.1.4 Gauge Maintenance and Data Retrieval

I visited the gauges monthly to collect data and conduct any necessary maintenance. I checked the instrument for broken parts, dirty solar panels, and accumulation of debris and biofouling near the sensor probe. Then, I opened the gauge case, and removed the battery and storage device (SD) card. I uploaded raw data to a personal laptop and replaced the SD card after clearing the data. Then, I swapped in a freshly charged battery. To ensure functionality, I checked indicator lights before sealing the instrument casing up. More information regarding necessary maintenance of specific instruments is available in **Appendix A**.

3.1.5 Surveying

The corrected distance measurements obtained from the Cal Poly gauges are relative to the zero point of the sensor probe, not a fixed datum. To tie the water level gauges into a fixed datum, specifically NAVD88, surveying was conducted by Cal Poly Lecturer Rudy Schalk and his Advanced Surveying Class. Over the course of three separate field surveys, his class utilized three separate surveying methods, Leveling, Static Global Navigation Satellite System (Static GNSS), and Total Station to obtain elevations in meters relative to NAVD88. The Total Station used was a Trimble s7 with a TSC3 data collector and Topcon prisms. The static GNSS instrument used was a Trimble R8s GNSS. The leveling instrument used was a Topcon DL-500. When available, known National Geodetic Survey benchmarks were used to backsight, but, when necessary, back sighting was done on points set during a Static GNSS survey.

When leveling and Static GNSS were conducted, there was an offset between the elevation of the survey and the elevation of the zero point of the instrument probe. For each instrument, I corrected the survey elevation to be relative to the zero of the sensor probe based on instrument geometry.

3.2 Monthly Mean Tidal Datums in Morro Bay

I estimated the monthly mean tidal datums (MHW/MLW) in Morro Bay from multiple sources of data. More information about the methodology used to determine monthly MHW/MLW is described below.

3.2.1 Tidal Datums from NOAA Port San Luis

NOAA measures water levels using an Aquatrek ultrasonic gauge deployed in a stilling well at the Port San Luis Pier, Station #94212110 (*NOAA Port San Luis Data Inventory Page*, n.d.) (see **Figure 26** for location). The NOAA Port San Luis station is the closest NOAA tidal station to Morro Bay. Additionally, the NOAA Port San Luis gauge was shown by Dunn to closely follow tidal amplitudes of the Stilltek gauge in Morro Bay, but with a 49-minute time lag (Dunn, 2023). For this thesis, I obtained monthly averaged water level data referenced to NAVD88 and in SI units from January 2022 to August 2023.

Figure 26: NOAA Port San Luis Instrument Location

3.2.2 Tidal Datums from Stilltek

In August 2021, Dunn (2023) installed an ultrasonic Stilltek commercial tide gauge at the Coast Guard North T-Pier (**Figure 18**Error! Reference source not found.). The gauge is mounted facing downwards and measures the air temperature and the median distance to the water over the course of a minute. Every 15 minutes, an internal measurement is made, while every 30 minutes, a measurement is relayed by satellite to an online datalink (*IGuage Data Link*, n.d.). In January of 2023, a storm likely damaged the gauge and it needed to be replaced. The gauge was not deployed again until May 9th, 2023. When designing the Cal Poly gauges, Dunn emphasized the influence that air temperatures have on the speed of sound, and therefore the distance measurements while using ultrasonic gauges (Dunn, 2023). For example, in lab conditions with a stationary gauge at a constant distance above the ground, the corrected distance measurement from a Cal Poly gauge differed by up to 50 mm from the constant distance. In the results, I explore the influence that gauge uncertainty has on the tidal prism estimate.

To determine the high and low waters, I analyzed the time series of Stilltek water levels in MATLAB after correcting to NAVD88. I obtained data maxima and minima by estimating the first and second derivatives. I culled the data to ensure that there were only two highs and two lows per day, with only one lower low and one higher high. I manually checked all extrema data, and any errors were removed. An example of high and low water from the Stilltek gauge can be seen in **Figure 27**. To reduce the effect of bias due to missing data, I filled data gaps from the Stilltek gauge with available data from the Cal Poly Coast Guard gauge (discussed below). Finally, I determined the monthly mean high and low tidal datums for each instrument.

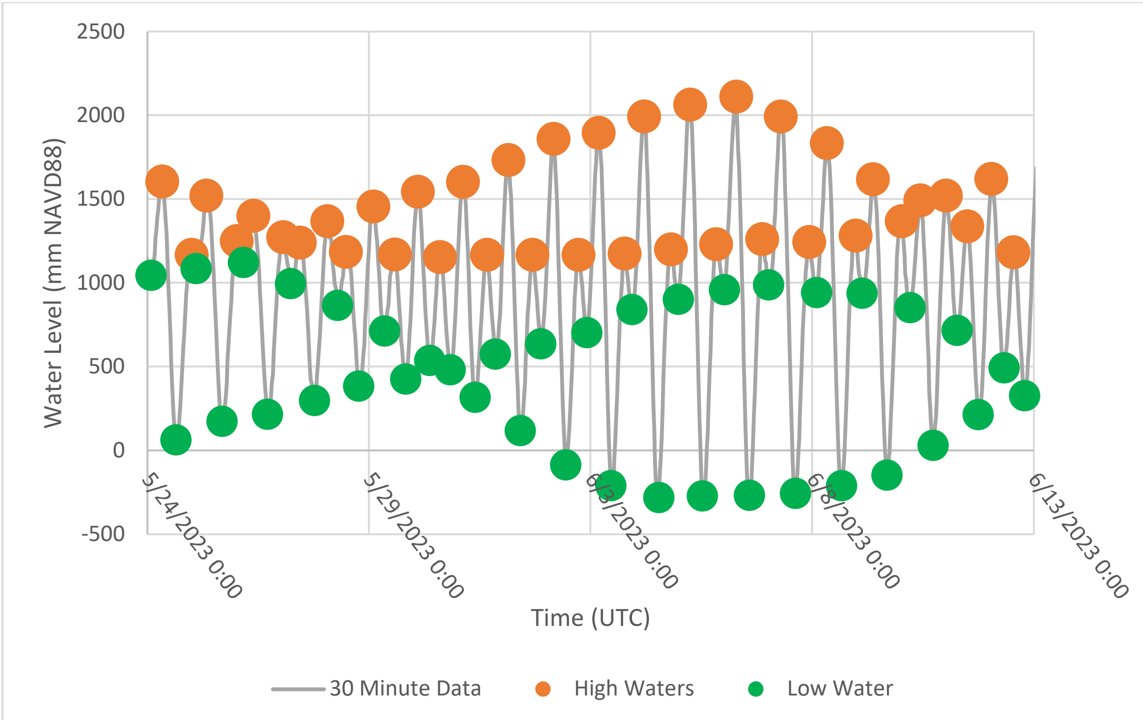

Figure 27: The Identified High and Low Waters Overlayed onto the 30-minute data from Stilltek

3.2.3 Tidal Datums from Student-Built Cal Poly Instruments

I installed multiple student-built tide gauges around Morro Bay to explore the possibility of spatially varying tidal datums (**Figure 19**). **Section 3.1** describes more specific details about the setup and installation process for the Cal Poly instruments.

I first preprocessed raw distance data collected from the Cal Poly gauges as described by Dunn (Dunn, 2023). I corrected the raw distance estimates **(Figure 28),** using the external temperature and humidity measurements **(Figure 29),** into corrected distances **(Figure 30)** to account for the speed of sound (Cramer, n.d.; Dunn, 2023; Wong, 1990). Afterwards, I processed the data into 5-minute averages using a separate script developed in Dunn (Dunn, 2023).

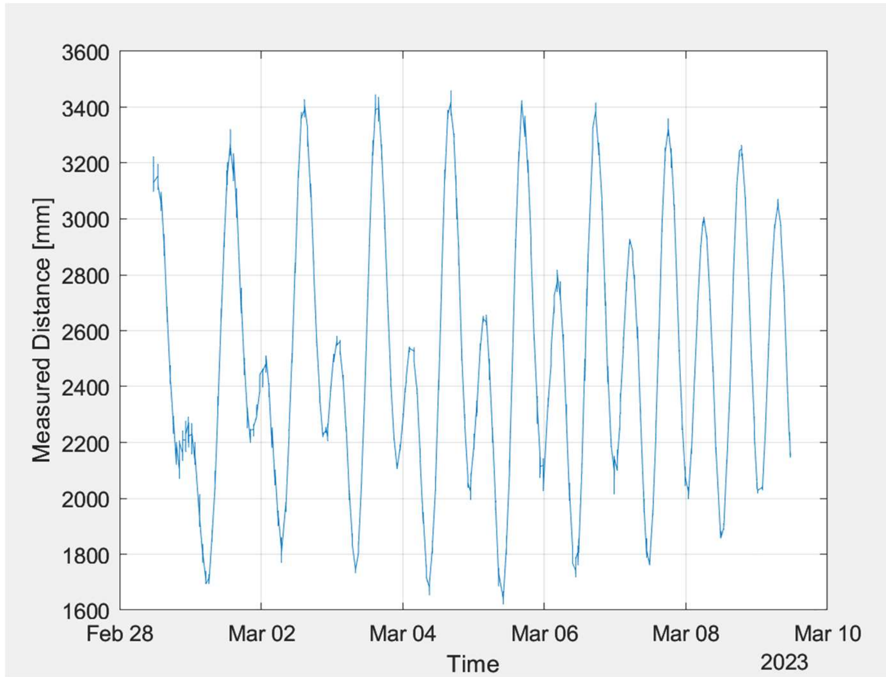

Figure 28: Example of the Raw Distance Data Collected from a Cal Poly Gauge at the Coast Guard North T-Pier in Morro Bay

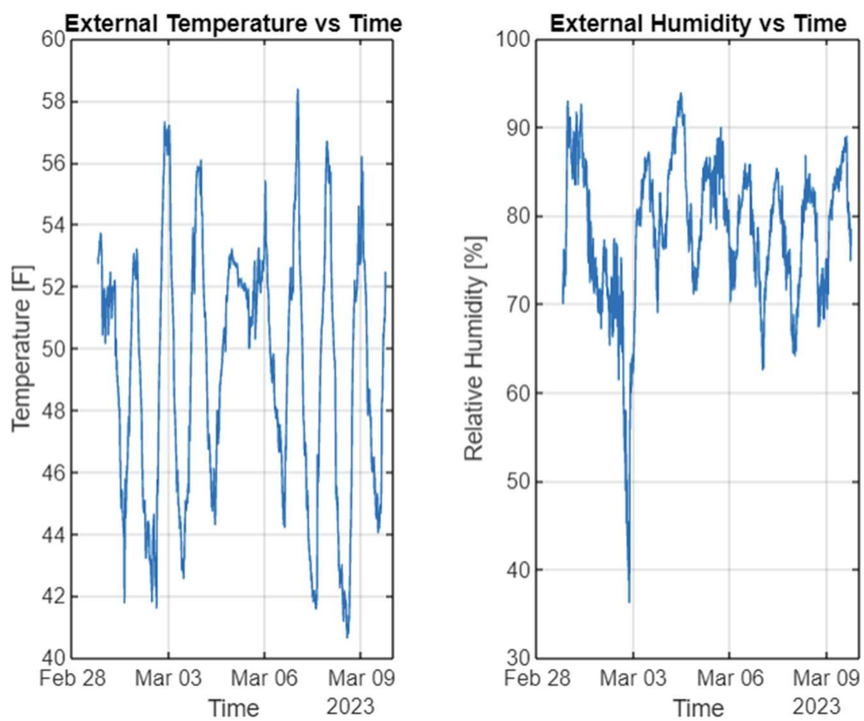

Figure 29: Raw Temperature and Humidity Data from an External Cal Poly Temperature and Humidity Gauge at the Coast Guard North T-Pier in Morro Bay

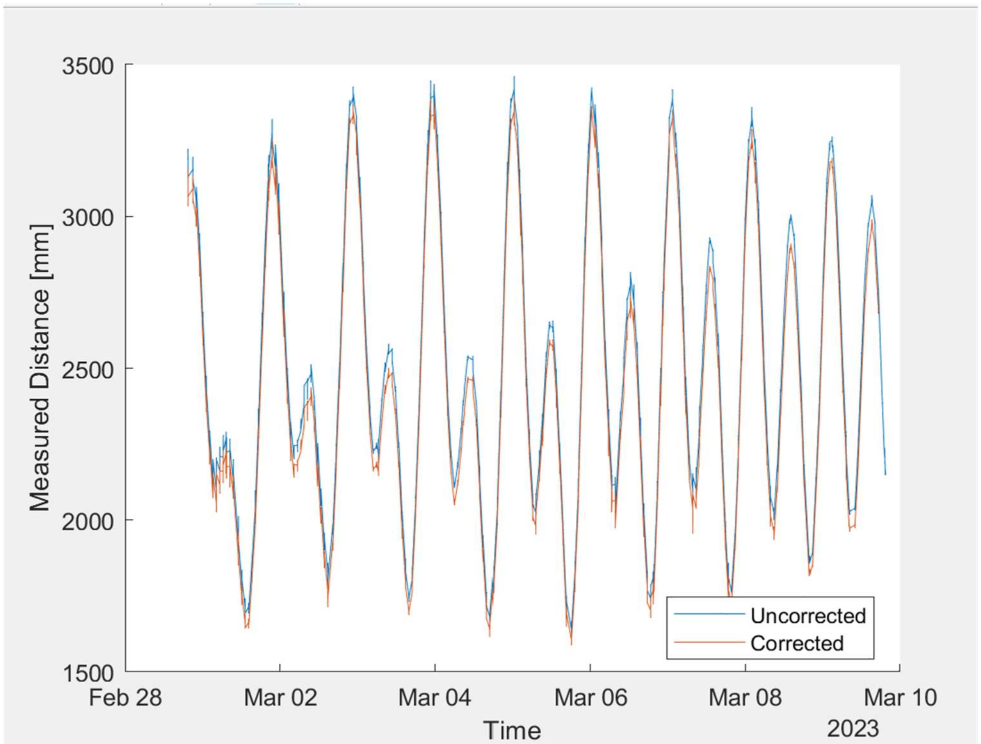

Figure 30: Corrected Distance vs Uncorrected Distance for a Cal Poly Gauge at the Coast Guard North T-Pier in Morro Bay

I corrected distance measurements to be relative to NAVD88 based on the surveying results of this study. To determine the daily high and low waters, I conducted the same process for the Stilltek gauge, described in **Section 3.2.2**, using 5-minute averages from the Cal Poly gauges (example in **Figure 31**). To reduce the effect of bias due to missing data, I filled data gaps from the Cal Poly Coast Guard gauge with available data from the NOAA Port San Luis gauge. I infilled missing data from the other Cal Poly gauges with the Cal Poly Coast Guard gauge data. Finally, I determined the monthly mean high and mean low tidal datums for each instrument.

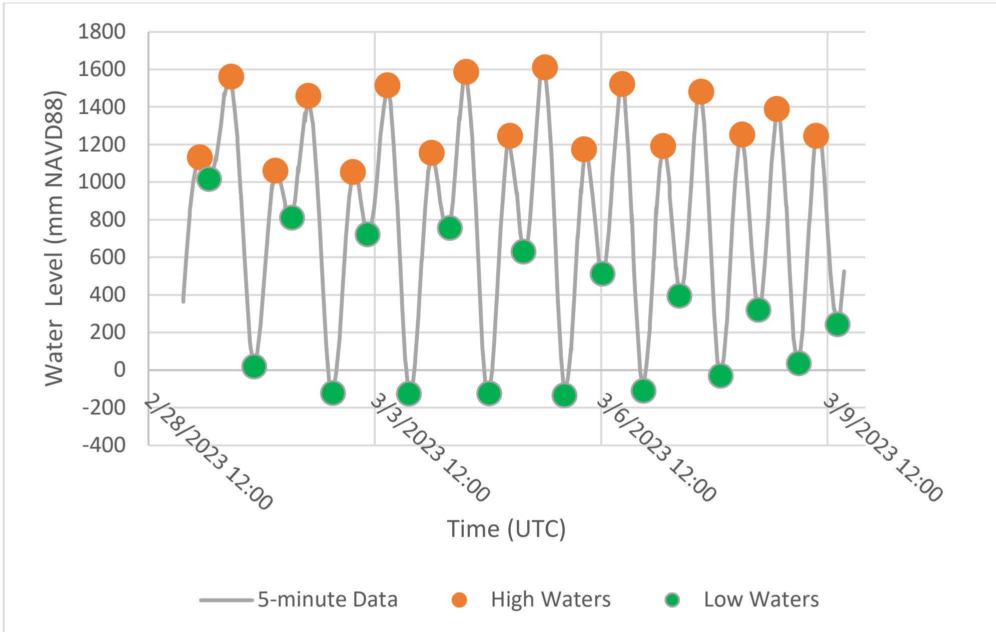

Figure 31: The Identified High and Low Waters Overlayed onto the 5-minute data for a Cal Poly Gauge at the Coast Guard North T-Pier

3.2.4 RMSE and Precision

I estimated the root mean squared error (RMSE) between available tide gauges at the Morro Bay Coast Guard North T-Pier. I estimated the 95 percent confidence precision error for the monthly mean tidal datums by utilizing the RMSE as a conservative order of magnitude estimation for observed standard deviation, or sigma (σ), between the Stilltek gauge and Cal Poly Coast Guard gauge. The precision error is defined as (**Eq. 2**):

$$E = \frac{t * \sigma}{\sqrt{N}} \qquad \textbf{(2)}$$

where E represents the 95 percent confidence interval precision error (mm), t* represents the test statistic at the 95% confidence interval, σ (sigma) represents the standard deviation (mm), and N represents the degrees of freedom, or the sample size minus one.

3.2.5 Bias

I compared the identified high and low waters from the Stilltek gauge and the Cal Poly Coast Guard gauge to observe potential differences between the two instruments. Reasons for possible uncertainty and bias are explored later in this thesis.

3.2.6 Temperature Comparison

I compared available air temperature data between the Stilltek gauge and the Cal Poly Coast Guard external temperature and humidity sensor. Both the Stilltek and Cal Poly gauge utilize atmospheric air temperatures to determine the speed of sound and correct the measured distance. Discrepancies between the two air temperature data sources would lead to discrepancies in the corrected distance measurements. Additionally, I compared available air temperature data from the NOAA OX1MB MET station at the Coast Guard North T-Pier to the Cal Poly Coast Guard gauge.

3.3 Volume from MatFlood

MatFlood is a MATLAB code that identifies inundation using a Digital Elevation Model (DEM) and gauge locations with specified water levels (Enriquez et al., 2023). The code allows either a constant (uniform) water level based on a singular gauge, or a spatially interpolated water level based on multiple gauge locations with unique water levels specified. The code assumes that only regions that are hydraulically connected will be inundated. For this thesis, I adapted and expanded MatFlood to determine surface area and volume of water estimates (discussed below).

3.3.1 Bathymetry from NOAA

I used the NOAA Digital Access Data Viewer to obtain a GeoTiff file containing the bathymetry for 2019 and 2022 (**Figure 32**) (*NOAA Data Access Viewer*, n.d.). The elevation data is given in meters relative to the NAVD88 vertical datum, and the coordinates are given in latitude and longitude in the North American Datum of 1983, or the NAD83 horizontal datum. NOAA estimated the vertical accuracy of unvegetated regions at the 95% confidence level as 0.052 m using 21 ground control points with an RMSE of 0.026 m. No control points within vegetated regions were utilized by NOAA. NOAA in 2019 utilized sonar at high tide and LiDAR at low tide to obtain a complete elevation dataset with plenty of overlap (**Figure 33**). For the 2022 dataset, only LiDAR was conducted, leaving the deeper channels unmapped (**Figure 34**). For this reason, I used the 2019 bathymetry to infill missing data from the 2022 bathymetry.

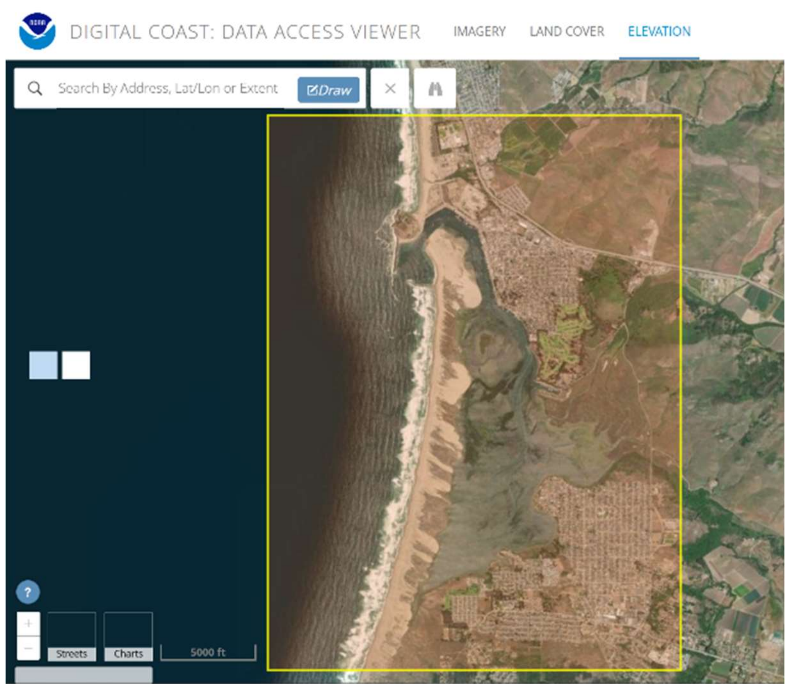

Figure 32: Control Area for the Morro Bay Bathymetry from NOAA (*NOAA Data Access Viewer*, n.d.)

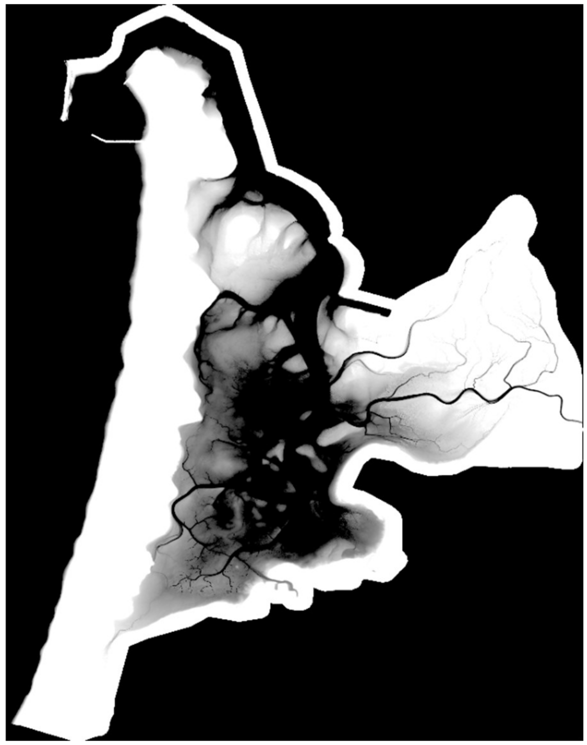

Figure 33: GeoTiff for 2019 (Full DEM)

Figure 34: GeoTiff for 2022 (Partial DEM Missing the Deeper Channels)

I used Geospatial Information Systems (GIS) to merge the 2019 and 2022 GeoTiff files. I added each of the files to the GIS map as data. Then, I used the "Mosaic to New Raster" tool to merge the bathymetry models. During this step, I infilled missing data from the 2022 DEM with values from the 2019 DEM. I used Google Earth to create a bounding polygon similar to the bounding polygon used by Tetra Tech in 2019, to allow the exclusion of volumes of water that are outside the bay (Tetra Tech, 2020). I uploaded this polygon into GIS and used the "Clip Raster" tool to omit any data outside the polygon. The result is a clipped 2019 GeoTiff file **(Figure 35)** and a clipped 2019/2022 merged GeoTiff file (**Figure 36**) using the same bounding polygon.

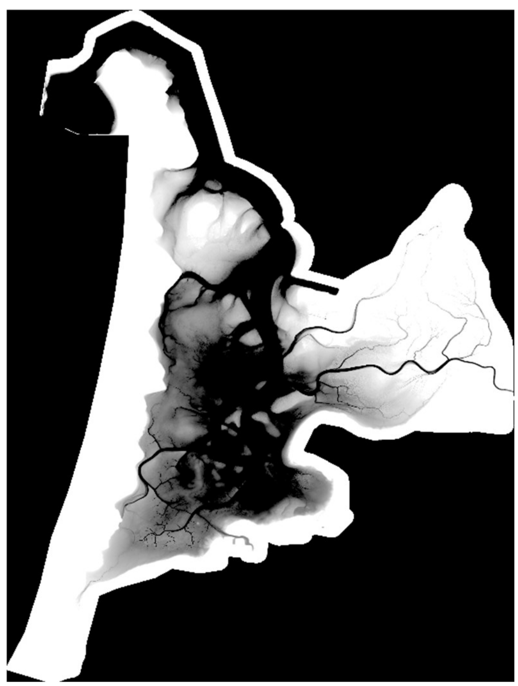

Figure 35: 2019 Bathymetry with Bounding Polygon

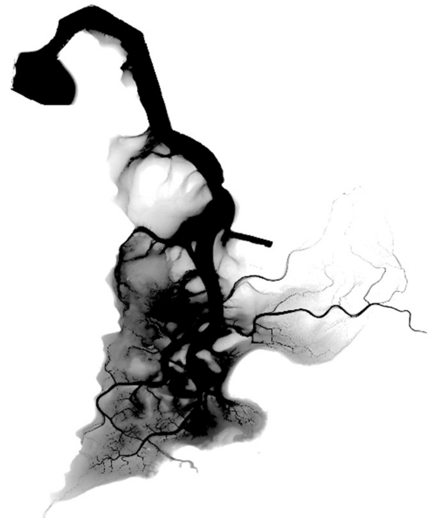

Figure 36: 2019/2022 Bathymetry Merge with Bounding Polygon

Then, in MATLAB, I used a code associated with MatFlood to extract pixel information from the GeoTiff file and convert the data into MATLAB compatible matrices of latitude, longitude, and elevation (Enriquez et al., 2023). I adapted this code for this thesis to allow the calculation of surface areas of water by converting the latitude and longitude into UTM coordinates. I used the MATLAB command "mstruct" in the 10S zone for San Luis Obispo, California. I used the "gradient" function to determine the spacing between the individual pixels in both horizontal UTM coordinate's (X and Y) matrices. I defined an individual surface area for each pixel. The UTM coordinates and the grid resolution will later be needed in the tidal prism calculation.

3.3.2 Adjusting MatFlood to Calculate Volume

I adapted MatFlood to output overall water depth, surface area of water and volume of water instead of depth of inundation (example **Figure 37)**.

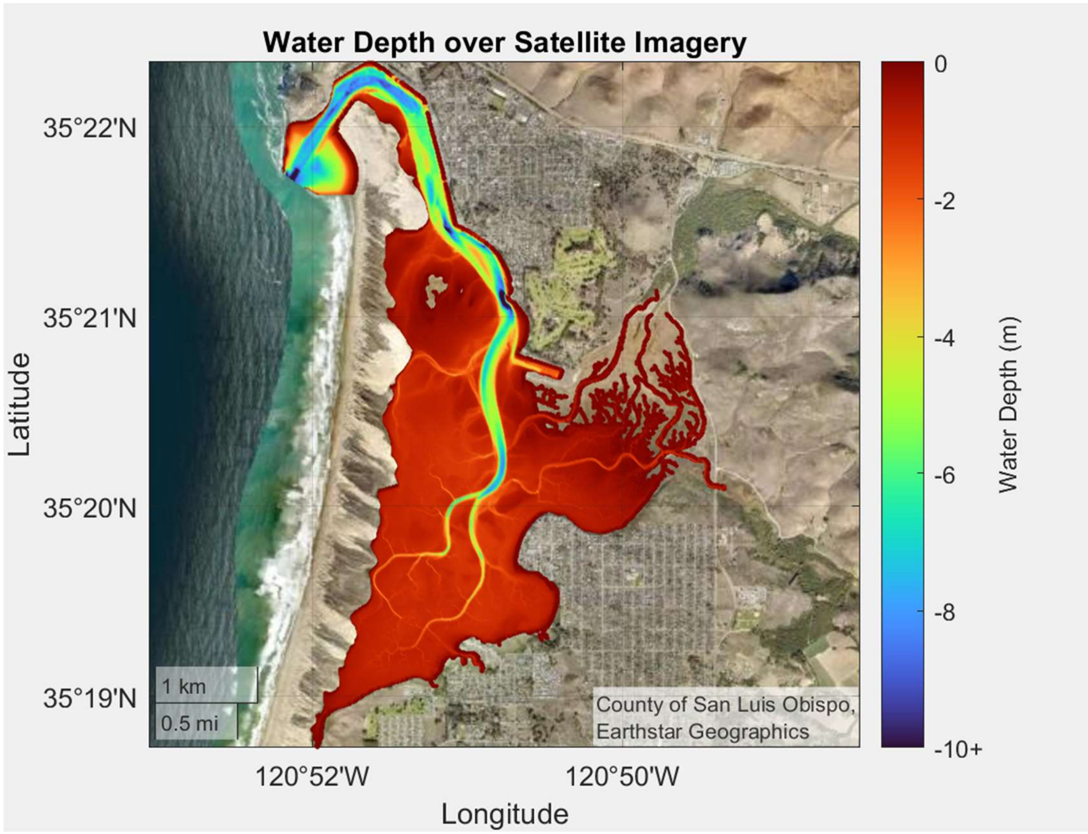

Figure 37: Overall Water Depth in Morro Bay from MatFlood at a Water Level of 1.212 m NAVD88

To calculate the volume of water in a general sense, the surface area of a water body is multiplied by the depth of the water. On a pixeled scale, the array of individual surface areas is multiplied by the array of individual flood depths corresponding to the same geographical location. The result is an array of individual volume measurements. The entire volume contained inside Morro Bay at the specified flood water level can then be calculated by summing the array of individual volume measurements.

Afte this process, MatFlood was equipped to estimate the surface area and a volume of water for all water levels in Morro Bay. Below -1.35 m NAVD88, I relaxed the principle of hydraulic connectivity to allow unconnected regions to contain water. It is important to note that this issue will not affect the tidal prism calculation when accounting for hydraulic connectivity as the issue occurs well below the MLLW line as determined by Tetra Tech in 2019, i.e., -0.045 m NAVD88 (Tetra Tech, 2020).

3.4 Tidal Prism Calculation

I used MatFlood to estimate the surface area of water and volume of water for all water levels to generate surface area of water vs water level and volume of water vs water level curves. The tidal prism is then the difference between the volumes of water at MHW and MLW as defined in **Section 2.1.3**. Additionally, I utilized a spatially variating flood water level in MatFlood to approximate the tidal prism.

3.4.1 Uncertainty

I utilized the estimated precision error and the observed bias between the monthly tidal datums from the Stilltek and Cal Poly Coast Guard gauges to estimate the total uncertainty in the tidal datums (Magnusson, n.d.). The total uncertainty (TU) is the total uncertainty in the monthly mean high or mean low tidal datum (mm), and can be defined as follows (**Eq. 3**):

$$TU = \sqrt{E^2 + b^2} \qquad \textbf{(3)}$$

where E is the 95 % confidence interval for precision error (mm), and b is the bias at the mean high or mean low tidal datum (mm). I explored the effects of the estimated total uncertainty in monthly tidal datums on the tidal prism volume.

3.4.2 2022 Tidal Prism

I used average monthly mean tidal datums from NOAA Port San Luis to determine the 2022 tidal prism in MatFlood. Then, after processing the 30-minute data from the Stilltek gauge in 2022 into monthly mean tidal datums, I estimated the tidal prism volume.

3.4.3 2023 Tidal Prism

First, I used average monthly mean tidal datums from NOAA Port San Luis to determine the 2023 tidal prism in MatFlood. Then, after processing the 30-minute data from the Stilltek gauge in 2023 into monthly mean tidal datums, I estimated the tidal prism volume. Then, after processing the 5-minute data from the Cal Poly Coast Guard gauge in 2023, I estimated the tidal prism volume.

3.4.4 2023 Tidal Prism with Spatially Varying Monthly Tidal Datums

I explored the effects that spatially varying tide levels have on the tidal prism following the observation that high water may differ by up to 0.5 ft (0.152 m) between the Coast Guard North T-Pier and Baywood Los Osos (Tetra Tech, 1999). In MatFlood, I first utilized the 2022 annual MHW and MLW from the Stilltek gauge to determine the tidal prism assuming a uniform water level across both locations. I then added 0.5 ft (0.152 m) to the 2022 annual MHW from the Stilltek gauge for only the Baywood Los Osos Location, while leaving MLW the same, to estimate the tidal prism using spatially varying monthly tidal datums. I calculated the percentage difference to observe changes within the tidal prism due to spatial variability of water levels in Morro Bay.

Next, I utilized the experimental data collected during 2023 from the four Cal Poly gauges to explore spatial variability of monthly mean tidal datums in Morro Bay using MatFlood. With available data and accuracy of measurements conducted for this project, I analyzed the tidal prism using spatially varying monthly tidal datums from each of the four Cal Poly Gauges in Morro Bay. I compared the estimated tidal prism approximated using spatially varying monthly tidal datums from the four Cal Poly gauges to the estimated tidal prism approximated using only one gauge near the mouth of the estuary, or the Cal Poly Coast Guard gauge.

3.4.5 Estimated Future Tidal Prism

To account for SLR in the tidal prism estimate, I utilized the various RCP scenarios for San Francico (explained in **Section 2.2**; **Table 1**) (Griggs et al., 2017). The SLR scenarios are relative to the MSL in the year 2000 (“Y2K”), or the average MSL from 1991-2009. To determine the future MHW and MLW in Morro Bay based on the MHW and MLW measured in 2022, the different SLR scenarios for the years 2050 and 2100 must be corrected to account for SLR that has occurred since Y2K. The future MHW, in meters relative to NAVD88, can be estimated as follows (**Eq. 4**):

$$MHW(t, SLR_i) = SLR_i - (MSL_{2022} - MSL_{Y2K}) + MHW_{2022} \tag{4}$$

where t represents the year of projection based on the SLR scenario (2050 or 2100), SLR_i represents the various SLR scenarios for San Francisco from Griggs et al. (2017) relative to the Y2K MSL (m). MSL_{2022} and MSL_{Y2K} are the approximate MSL for 2022 and 1991-2009 (“Y2K”) (m NAVD88), and MHW_{2022} is the mean high water in 2022 (m NAVD88). This definition can also be used to estimate the future MLW. I estimated the MSL_{2022} and MSL_{Y2K} as 0.848 m and 0.827 m NAVD88, respectively, by averaging the monthly MSL data from NOAA Port San Luis (*NOAA Port San Luis Data Inventory Page*, n.d.). I utilized the annual mean tidal datums from the Stilltek gauge for MHW and MLW in 2022 for the projection of mean tidal datums into the future.

I used the 2019/2022 bathymetry merge to predict the future tidal prism, assuming no change in bathymetry. If sedimentation continues at the rate estimated by the USGS (Freeman & Chase M, 2016), the estimated future tidal prism for this study will likely overestimate the actual future tidal prism.

3.5 Tidal Prism Variability

Two main factors are responsible for the tidal prism volume varying: variations in sea levels and changes in bathymetry. It was desired to explore variations between the two to gain insight into changes in the tidal prism.

3.5.1 MSL Hydrograph

To observe the seasonal variability in water levels, I analyzed monthly MSL and monthly mean tidal range (MTR) data from the NOAA Port San Luis Tide Station (*NOAA Port San Luis Data Inventory Page*, n.d.).

I determined the difference between each monthly tide statistic and the associated annual tide statistic, or the anomaly. Finally, I calculated the average monthly anomaly from 1972 to 2021, along with the 10^{th} and 90^{th} percentiles.

3.5.2 Bathymetry Changes

To observe the change in elevation and volume of sediment in Morro Bay, I differenced and summed the 2019 and 2022 bathymetry elevations below the MHW line. I utilized the 2022 annual MHW from Stilltek, or 1.421 m NAVD88. Additionally, I evaluated changes in elevation within the annual tidal range as estimated from the Stilltek gauge in 2022.

To observe more specific changes in bathymetry in Morro Bay, I plotted the hypsometric curve (surface area of water vs. water level) and the volume of water vs. water level plot for Morro Bay. In 2019, Tetra Tech determined surface areas and volumes at various contours between -40 and 5 ft MLLW (-12.192 and 1.524 m), and that MLLW was -0.045 m NAVD88 in Morro Bay (Tetra Tech, 2020). To provide comparability between results, I calculated the 2022 surface areas and volumes of water at the same contour intervals as done by Tetra Tech in 2019, but relative to the fixed datum of NAVD88.

3.6 Potential Eelgrass Habitat Area Calculation

For the purpose of this study, the viable eelgrass habitat can be identified using the vertical growth range. In 2021, Tetra Tech estimated the vertical growth range in Morro Bay to be +1.5 to -6 ft MLLW (+0.457 to -1.829 m) based on historical eelgrass distribution from 2007 to 2019 (Tetra Tech, 2021). I corrected this range to +0.412 m to – 1.784 m NAVD88 based on the estimation of MLLW to be -0.045 m NAVD88 made by Tetra Tech in 2019 (Tetra Tech, 2020). As sea levels rise, MLLW will likely rise, and therefore, viable habitat area will potentially shift.

I applied the principle of hydraulic connectivity used in MatFlood to identify the areas within Morro Bay that lie within the viable growth band at current and future expected water levels. I culled elevation points outside the viable range from the elevation dataset, and the habitat area can be estimated by summing the individual surface area pixels remaining.

3.6.1 Predicted Viable Eelgrass Habitat Area Estimated vs. Actual Eelgrass Extent for 2019

Based on the vertical growth range determined by Tetra Tech in 2021, I used MATLAB code identify all locations in Morro Bay that are considered viable eelgrass habitat for the year 2019 (Tetra Tech, 2021). I conducted this analysis using the 2019 bathymetry from NOAA.

I compared the predicted viable eelgrass habitat area to the actual eelgrass area for 2019. Cal Poly and the MBNEP processed shapefiles for the actual eelgrass area from drone footage in Morro Bay from 2019. I loaded this into MATLAB and adjusted the coordinates to UTM Zone 10S. I calculated and summed the area of each shape using the "polyarea" tool in MATLAB to estimate the actual eelgrass area in 2019.

3.6.2 Viable Area in 2022

Based on the vertical growth range determined by Tetra Tech in 2021, I used MATLAB to identify all locations in Morro Bay that are considered viable eelgrass habitat for the year 2022 (Tetra Tech, 2021). I conducted this analysis using the merged 2019/2022 NOAA bathymetry I created in GIS.

3.6.3 Future Predicted Viable Area

To account for SLR in the potential viable eelgrass habitat area estimate, I estimated the future upper and lower growth bounds for the different SLR scenarios for San Francisco (**Table 1**) (Griggs et al., 2017). The future upper and lower growth limitation bounds, in meters relative to NAVD88, can be estimated as follows (**Eq. 5**):

$$H(t, SLR_i) = SLR_i - (MSL_{2022} - MSL_{Y2K}) + H \tag{5}$$

where t represents the year of the SLR scenario (2050 or 2100) and H represents the elevation of the upper or lower eelgrass growth bound as determined by Tetra Tech in 2021 (m NAVD88) (Tetra Tech, 2021). More information on the SLR and MSL variables can be found in **Section 3.2.5**.

I used the 2019/2022 bathymetry merge to predict the future potential eelgrass habitat area, assuming no change in bathymetry. With geomorphological changes, the future eelgrass habitat will likely be different than predicted in this study, potentially influencing the future tidal prism.

Chapter 4: RESULTS & DISCUSSION

The results of this thesis are discussed below. Using the geodetic survey results, I determined monthly mean tidal elevations in various locations around Morro Bay using multiple data sources. Additionally, I approximated the 2022 and 2023 monthly tidal prism, as well as the future expected tidal prism in the years 2050 and 2100. Lastly, I estimated the 2019 and 2022 viable eelgrass habitat area and estimated the future potential viable habitat area in the years 2050 and 2100.

4.1 Tidal Datums

I evaluated data from multiple water level gauges to determine the tidal datums for Morro Bay using the methodology in **Section 3.2**. I tied the gauges into NAVD88 using survey data, determined monthly and annual mean tidal datums, and compared results to each other and to the NOAA gauge in Port San Luis.

4.1.1 Survey Results

The geodetic survey results for the water level gauges are summarized (**Table 5**; see **Section 3.1.5** for methods). Different methods of surveying resulted in varying results: for example, the leveling surveys for the Cal Poly Coast Guard gauge range from 3.112 to 3.312 m NAVD88. The Total Station measurement at the Stilltek gauge in 2022 was estimated to be 21 mm lower than the Total Station measurement taken at the Stilltek gauge in 2023.

I used the surveys that I considered to be the most accurate leveling values to determine the elevation of the instrument, in meters relative to NAVD88, for each of the water level instruments. In **Table 5**, the surveys I considered to be most accurate are indicated as "Used" in the "Surveying Method" column and are listed first and highlighted orange under the “Instrument” column for each gauge. Based on reported instrument accuracy, the Total Station is considered to be the most accurate and used whenever possible (SOM Survey Instruments, n.d.). Aggregating the differences between the accepted “Used” leveling values and other leveling surveys for each gauge yields an overall RMSE of 202.6 mm.

Possible reasons for errors include instrumental uncertainty, surveying errors and, to a lesser extent, vertical dock motion (heave). Total station measurements are indicated to have a typical uncertainty of +/- 3 mm, as compared to +/- 8 mm for GPS based systems (SOM Survey Instruments, n.d.). The accuracy of the Trimble S7, with a prism (as used) is 1.0 mm (*Trimble S7*, n.d.). The Trimble R8 GNSS receiver has a maximum vertical precision of 8 mm (*Trimble R8’s*, n.d.). With GNSS receivers, longer monitoring periods allow connection with more satellites, and allows a better estimate of elevation (Moyer, 2021). Various surveying errors, such as incorrect tripod setup, can lead to uncertainty in the elevation estimate. Over time, docks can heave, or expand and contract, as the dock settles into place, causing changes in the elevation of the dock and therefore the water level gauge. Similarly, benchmarks may have subsided since last being tied into a geodetic datum, producing inaccuracy. More measurements are needed to understand the deviation between surveying methodologies, and to evaluate vertical land motion at the instrument locations.

*Table 5: Surveying Results for Morro Bay Tide Gauges. Survey performed by Bioresource and Agricultural Engineering (BRAE) 447, Advanced Surveying, from April 19th-May 26th of 2022 and from May 9th-11th of 2023. See Methods **Section 3.1.5** for more details. The leveling measurements that I determined to be the most accurate/reliable and utilized to survey in the gauges are indicated as "(Used)" in the "Surveying Method" Column, are listed first in the "Instrument" column for each gauge and are highlighted orange.*

Location	Instrument	Surveying Method	Elevation to Survey Point (m NAVD88)	Location to Instrument	Offset to Instrument Probe Zero Point (m)	Elevation to Zero Point (m NAVD88)
Coast Guard North T Pier	**Cal Poly**	Total Station (Used)	3.282	Top of Plastic Casing	-0.065	3.217
		Leveling	3.12	To Wooden cantilever	-0.008	3.112
		Leveling	3.24	To Wooden cantilever	-0.008	3.232
		Leveling	3.32	Top of Plastic Casing	-0.065	3.255
		Static (15 min)	3.264	Top of Plastic Casing	-0.065	3.199
		Static (30 min)	3.283	Top of Plastic Casing	-0.065	3.218
		Static (30 min)	3.377	Top of Plastic Casing	-0.065	3.312
	Tide Staff	Total Station (2022) (Used)	2.967	Top of Tide Staff	-3.6576	-0.6900
		Leveling	3.65	Top of Tide Staff	-3.6576	-0.0076
	Stilltek	Total Station (Used)	3.408	Top of Plastic Casing	-0.1778	3.230
		Total Station (2022)	3.387	Top of Plastic Casing	-0.1778	3.209
		Leveling	3.89	Top of Metal Bracket	-0.611	3.279

		Static (30 min)	3.85	Top of Metal Bracket	-0.611	3.239
Bayfront Marina	**Cal Poly**	Static (15 min) (Used)	2.747	To the Wooden Cantilever	-0.01	2.737
		Leveling	2.74	To the Wooden Cantilever	-0.01	2.73
Morro Bay State Park Marina	**Cal Poly**	Total Station (Used)	3.420	To Instrument Probe	0	3.420
	Tide Staff	Total Station (Used)	3.420	Measured from Guage P4A sensor probe to top of 10' staff	-3.581	-0.161
Private Pier in Los Osos	**Cal Poly**	Static (15 min) (Used)	2.731	Top of Plastic Casing	-0.065	2.666
		Leveling	2.73	Top of Plastic Casing	-0.065	2.665

4.1.2 Mean Tidal Datums in 2022

I estimated verified monthly MHW and MLW from the NOAA Port San Luis Station to be slightly lower than the estimated monthly MHW and MLW from the Stilltek gauge in 2022, by an annual average of 0.022 m for both MHW and MLW (**Table 6** and **Table 7)**. I estimated the annual mean tidal ranges at the Port San Luis and the Morro Bay Coast Guard Dock to be virtually the same (1.08 m) and to be slightly less than the 19-year average at Port San Luis of 1.09 m (1983-2001 epoch) (*Datums - NOAA Tides & Currents*, 2023). During 2022, the monthly MHW and MLW at the NOAA Port San Luis gauge varied by up to 0.182 and 0.232 m respectively. Similarly, the MHW and MLW at the Stilltek gauge varied by up to 0.192 and 0.212 m respectively. Variability in tides due to the time of year can yield differences in the magnitude of the tidal prism volume. Compared to the tidal datums estimated by Tetra Tech in August 2019, I estimated the 2022 August MHW and MLW from Stilltek to be 0.072 and 0.120 m higher, respectively (Tetra Tech, 2020).

The small differences between MLW and MHW obtained from the NOAA Port San Luis gauge and the Stilltek gauge could result from measurement and datum uncertainty. However, this could also occur from slightly higher mean water levels within the bay due to locational differences. Additionally, the instrumentation between the two locations varies. The NOAA Port San Luis gauge utilizes a stilling well, and may use a different algorithm than the Stlltek gauge to calculate the distance measurement using the speed of sound based on measured atmospheric air temperatures (*NOAA Port San Luis Data Inventory Page*, n.d.).

Table 6: Monthly and Annual MHW in 2022. Water levels are given in meters relative to NAVD88.

Month	NOAA Port San Luis	Stilltek	Difference (m)
January	1.411	1.429	-0.018
February	1.345	1.370	-0.025
March	1.356	1.369	-0.013
April	1.309	1.325	-0.016
May	1.324	1.344	-0.020
June	1.411	1.425	-0.014
July	1.411	1.432	-0.021
August	1.448	1.467	-0.019
September	1.491	1.517	-0.026
October	1.444	1.466	-0.022
November	1.397	1.427	-0.030
December	1.441	1.475	-0.034
Annual	**1.399**	**1.421**	**-0.022**

Table 7: Monthly and Annual MLW in 2022. Water levels are given in meters relative to NAVD88.

Month	NOAA Port San Luis	Stilltek	Difference (m)
January	0.302	0.336	-0.034
February	0.284	0.295	-0.011
March	0.241	0.284	-0.043
April	0.200	0.232	-0.032
May	0.235	0.278	-0.043
June	0.362	0.360	0.002
July	0.357	0.371	-0.014
August	0.384	0.395	-0.011
September	0.432	0.444	-0.012
October	0.368	0.398	-0.030
November	0.313	0.325	-0.012
December	0.354	0.374	-0.020
Annual	**0.319**	**0.341**	**-0.022**

4.1.3 Mean Tidal Datums in 2023

I estimated the verified monthly MHW and MLW from the NOAA Port San Luis Station to be lower than the estimated MHW and MLW from the Stilltek gauge in 2023, by an average of 0.024 m and 0.007 m, respectively (**Table 8** and **Table 9)**. The MHW and MLW from the Stilltek gauge were typically higher than the Cal Poly gauge, on average by 0.003 and 0.027 m, respectively. Compared to the tidal datums estimated by Tetra Tech in August 2019, I estimated that the 2023 August MHW and MLW from the Stilltek gauge and the Cal Poly gauge increased by 0.170 and 0.155 m, and 0.168 and 0.132 m, respectively (Tetra Tech, 2020). I discussed reasons for variation between the NOAA and Stilltek gauges in **Section 4.1.2**. The Stilltek gauge and the Cal Poly gauge could differ based on surveying errors and the calculated speed of sound used to correct the distance measurement and is explored more below in **Section 4.1.5 and 4.1.6**.

Table 8: Mean High Water in 2023. Dashes indicate months in which no/limited data for a particular data source was available. Water levels are given in meters relative to NAVD88.

Month	NOAA Port San Luis	Stilltek (Coast Guard North T-Pier)	Cal Poly (Coast Guard North T-Pier)	Difference (m) (NOAA-Stilltek)	Difference (m) (NOAA-CalPoly)	Difference (m) (Stilltek-CalPoly)
January	1.438	-	-	-	-	-
February	1.368	-	-	-	-	-
March	1.364	-	1.369[2]	-	-0.005	-
April	1.307	-	1.322[3]	-	-0.015	-
May	1.407	1.433[1]	1.429[4]	-0.026	-0.022	0.004
June	1.407	1.436	1.431	-0.029	-0.024	0.005
July	1.476	1.497	1.496	-0.021	-0.020	0.001
August	1.546	1.565	1.563	-0.019	-0.017	0.002

1) Missing High Water Values from May 1st-9th, 2023 were infilled with values from the Cal Poly Coast Guard gauge
2) Missing High Water Values from March 11th-24th, 2023 were infilled with values from the NOAA Port San Luis gauge
3) Missing High Water Values from April 29th-30th, 2023 were infilled with values from the NOAA Port San Luis gauge
4) Missing High Water Values from May 1st were infilled with values from the NOAA Port San Luis gauge

Table 9: Mean Low Water for 2023. Dashes indicate months in which no/limited data for a particular data source was available. Water levels are given in meters relative to NAVD88.

Month	NOAA Port San Luis	Stilltek (Coast Guard North T-Pier)	Cal Poly (Coast Guard North T-Pier)	Difference (m) (NOAA-Stilltek)	Difference (m) (NOAA-CalPoly)	Difference (m) (Stilltek-CalPoly)
January	0.372	-	-	-	-	-
February	0.290	-	-	-	-	-
March	0.275	-	0.280[2]	-	-0.005	-
April	0.259	-	0.245[3]	-	0.014	-
May	0.367	0.369[1]	0.348[4]	-0.002	0.019	0.021
June	0.365	0.383	0.353	-0.018	0.012	0.030
July	0.407	0.414	0.380	-0.007	0.027	0.034
August	0.429	0.430	0.407	-0.001	0.022	0.023

1) Missing Low Water Values from May 1st-9th,2023 were infilled with values from the Cal Poly Coast Guard gauge
2) Missing Low Water Values from March 11th-24th, 2023 were infilled with values from the NOAA Port San Luis gauge
3) Missing Low Water Values from April 29th-30th, 2023 were infilled with values from the NOAA Port San Luis gauge
4) Missing Low Water Values from May 1st were infilled with values from the NOAA Port San Luis gauge

Additionally, I analyzed the other Cal Poly gauges around Morro Bay using the methodology described in **Section 3.1.3** to explore spatially varying tidal elevations (**Table 10** and **Table 11**). MHW at the Bayfront Marina and the Morro Bay State Park were estimated to be higher than at the Coast Guard, with a maximum difference in the monthly tidal datums of 0.043 and 0.050 m respectively. MLW at the Bayfront Marina and the Morro Bay State Park are higher than at the Coast Guard Pier, with a maximum difference of 0.029 and 0.018 m respectively. The "Number of Points from Gauge" column indicates the number of high or low tides from the original gauge. Typically, in a month, there are 62 high and 62 low tides. I infilled missing data with nearby gauges to reduce bias in the monthly tidal elevation estimate.

Table 10: Mean High Waters in Morro Bay from the Cal Poly Gauges. Dashes indicate months in which no/limited data for a particular data source was available. Water levels are given in meters relative to NAVD88.

Month	Coast Guard North T-Pier	Number of Points from Gauge	Bayfront Marina	Number of Points from Gauge	Morro Bay State Park Marina	Number of Points from Gauge	Los Osos Private Pier	Number of Points from Gauge
March	1.369[1]	37	1.369[4]	41	-	-	-	-
April	1.322[2]	55	1.365[5]	58	1.372[7]	45	1.337[10]	40
May	1.429[3]	59	1.458[6]	43	1.474[8]	48	-	-
June	1.431	58	-	-	1.472[9]	43	-	-
July	1.496	59	1.532	59	-	-	-	-
August	1.563	60	1.599	60	-	-	-	-

1) Missing High Water Values from March 11th-24th, 2023 were infilled with values from the NOAA Port San Luis gauge to allow for N = 61
2) Missing High Water Values from April 29th-30th, 2023 were infilled with values from NOAA Port San Luis to allow N = 59
3) Missing High Water Values from May 1st were infilled with values from NOAA Port San Luis to allow N = 61
4) Missing High Water Values from March 1st-10th, 13th and 23rd, 2023 were infilled with values from Cal Poly Coast Guard and NOAA Port San Luis to allow N = 61
5) One Missing High Water Value from April 12th, 2023 was infilled with the value from the Cal Poly Coast Guard gauge to allow N=59
6) Missing High Water Values from May 9th -11th and 24th – 31st, 2023 were infilled with values from Cal Poly Coast Guard to allow N = 61
7) Missing High Water Values from April 1st - 4th and 18th – 20th ,2023 were infilled using values from the Cal Poly Coast Guard gauge to allow N = 59
8) Missing High Water Values from May 15th – 18th and 21st – 24th, 2023 were infilled with values from the Cal Poly Coast Guard gauge to allow N = 61
9) Missing High Water Values from June 22nd – 30th, 2023 were infilled with values from the Cal Poly Coast Guard gauge to allow N = 58
10) Missing High Water Values from April 28th– 30th, 2023 were infilled with values from the Cal Poly Coast Guard gauge and the NOAA Port San Luis gauge to allow N = 59

Table 11: Mean Low Water in Morro Bay from the Cal Poly Gauges. Dashes indicate months in which no/limited data for a particular data source was available. Water levels are given in meters relative to NAVD88.

Month	Coast Guard North T-Pier	Number of Points from Gauge	Bayfront Marina	Number of Points from Gauge	Morro Bay State Park Marina	Number of Points from Gauge
March	0.280[1]	37	0.326[4]	43	-	-
April	0.245[2]	54	0.274[5]	58	0.253[7]	45
May	0.348[3]	58	0.372[6]	42	0.366[8]	48
June	0.353	58	-	-	0.365[9]	42
July	0.380	58	0.402	58	-	-
August	0.407	59	0.437	59	-	-

1) Missing Low Water Values from March 11th-24th, 2023 were infilled with values from the NOAA Port San Luis gauge to allow for N = 61
2) Missing Low Water Values from April 29th-30th, 2023 were infilled with values from NOAA Port San Luis to allow N = 59
3) Missing Low Water Values from May 1st were infilled with values from NOAA Port San Luis to allow N = 59
4) Missing Low Water Values from March 1st-10th and 20th, 2023 were infilled with values from Cal Poly Coast Guard and NOAA Port San Luis to allow N = 61
5) Missing Low Water Values from April 20th, 2023 were infilled with values from the Cal Poly Coast Guard gauge to allow N = 59
6) Missing Low Water Values from May 24th -31st, 2023 were infilled with values from the Cal Poly Coast Guard gauge to allow N = 59
7) Missing Low Water Values from April 1st – 4th and 18th – 20th, 2023 were infilled with values from the Cal Poly Coast Guard gauge to allow N = 59
8) Missing Low Water Values from May 15th – 18th and 22nd – 23rd, 2023 were infilled with values from the Cal Poly Coast Guard gauge to allow N = 59
9) Missing Low Water Values from June 22nd – 30th, 2023 were infilled with values from the Cal Poly Coast Guard gauge to allow N = 58

4.1.4 RMSE and Precision

I compared data from available tide gauges to tide staffs at the Coast Guard North T-Pier and the Morro Bay State Park Marina (**Table 12**). Additionally, I compared tidal datums from the Stilltek and the Cal Poly gauge at the Coast Guard North T-Pier. These gauges were deployed at the same location and would provide the same water level measurements in the absence of errors and processing differences. I estimated the RMSE between the Coast Guard Tide Staff and the Cal Poly Gauge at the Coast Guard North T-Pier for 2023 as 22.3 mm. This is slightly higher than the value determined by Dunn

(2023) (RMSE of 15.5 mm). Due to the lack of leveling on the Cal Poly gauge, Dunn (2023) assumed that the sensor probes were at equal elevations, potentially removing surveying errors and improving the RMSE. I estimated the RMSE between the Stilltek gauge and the Cal Poly Coast Guard gauge for 2023 as 18.9 mm. The Tide Staff to Cal Poly gauge RMSE at the Coast Guard North T-Pier is likely larger than the Stilltek to Cal Poly gauge comparison due to measurement uncertainty within reading the tide staff in the field.

Table 12: RMSE Values for Various Gauges in Morro Bay

Location	**Comparison**	**RMSE (mm)**	**Number of Points**
Coast Guard North T-Pier	Staff-Stilltek (Dunn 2023)	17	>100
	Staff-CalPolyGauge (Dunn 2023)	15.5	>100
	Staff-CalPolyGauge	22.3	18
	Stilltek-CalPolyGauge	18.9	5436
Morro Bay State Park Marina	Staff-CalPolyGauge	142.0	4

The 95% confidence interval for precision within the monthly mean tidal datums can be estimated using **Equation 2**, under the assumption that the variance between individual Stilltek and Cal-Poly Coast Guard gauge measurements is dominated by random processes. I utilized the RMSE, ~20 mm, for a conservative estimate on the order of magnitude for σ (sigma), or standard deviation (**Table 12**). In a typical month, there are 62 high and 62 low waters, hence there are 61 degrees of freedom (*T Score Table Degrees of Freedom*, 2018). The 95 % confidence interval in the monthly mean is 5.08 mm, which can be interpreted as the uncertainty in the monthly mean tidal datum caused by random variation, or precision errors.

4.1.5 Bias

The difference in water levels at the adjacent Stilltek and Cal Poly Coast Guard gauges is a function of tidal stage (**Figure 38**Error! Reference source not found.). At high waters, the average difference is only 3.0 mm, while at low waters, the average difference is 29.92 mm, indicating an observed bias that primarily occurs at low tidal stages. At high and low water, the spread of values is similar, around 40-60 mm. A closer look at the 5-minute data from May 12th-13th (**Figure 39** and **Figure 40**Error! Reference source not found.) depicts differences of up to 36 mm at low water.

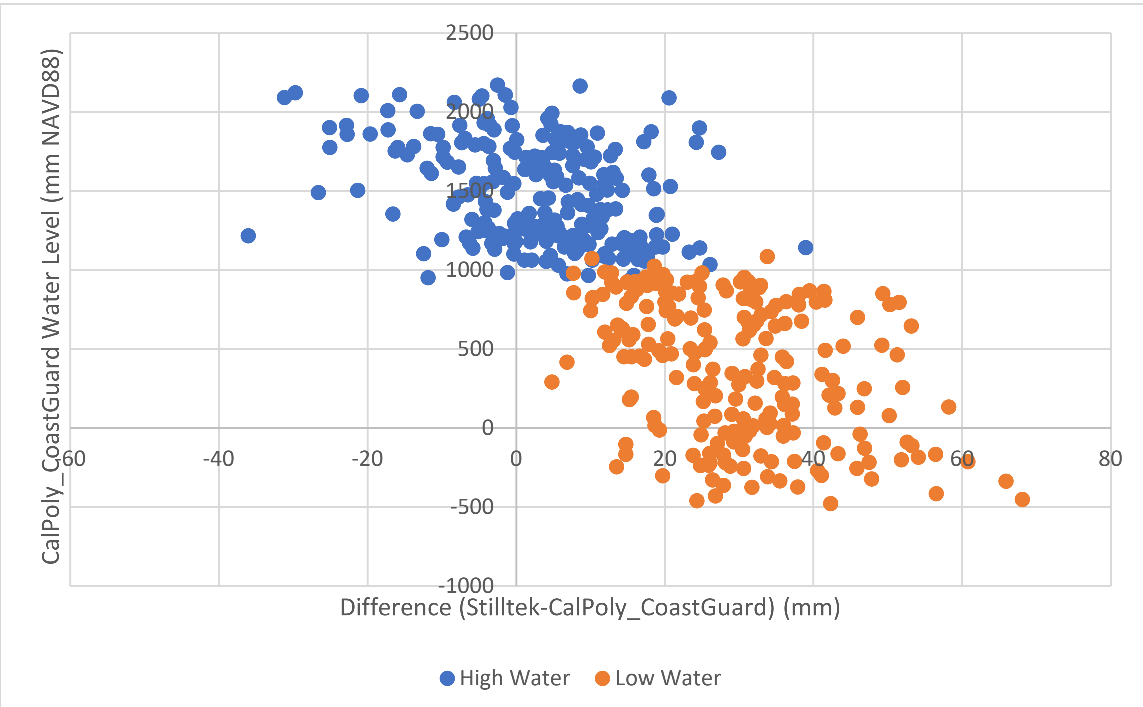

Figure 38: Difference plot between the Stilltek and the Cal Poly Coast Guard gauge for Identified High and Low Waters. "CPCG" refers to the Cal Poly Coast Guard gauge.

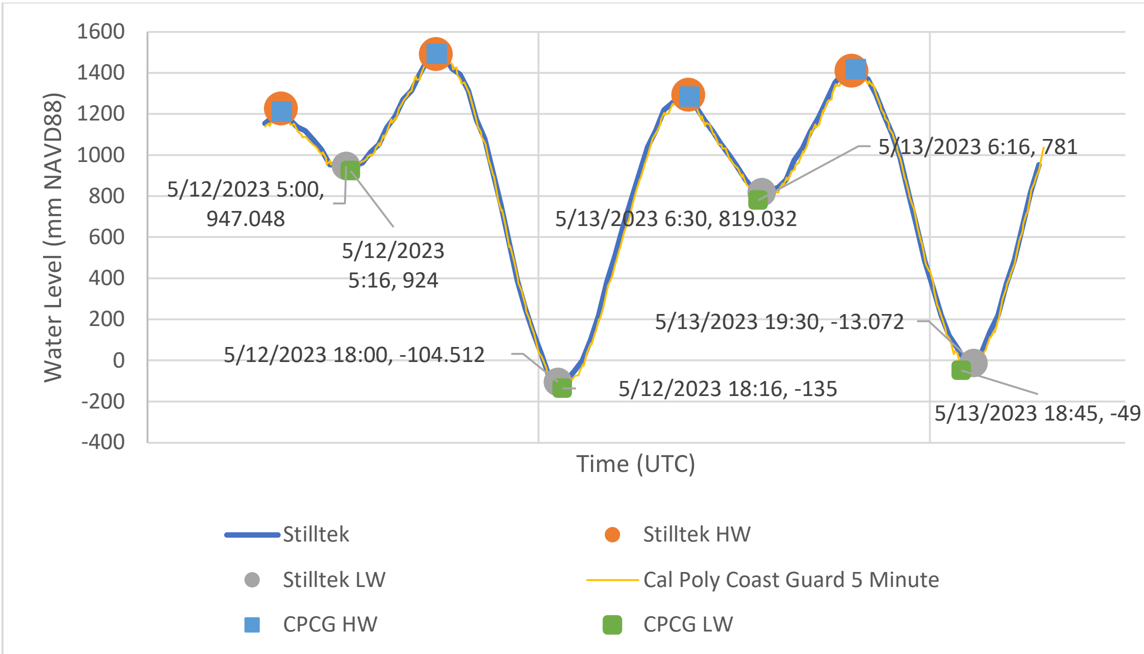

Figure 39: Stilltek and Cal Poly Coast Guard Tidal Elevations with Identified High and Low Waters for May 12th-13th. "HW" refers to high water and "LW" refers to low water. "CPCG" refers to the Cal Poly Coast Guard gauge.

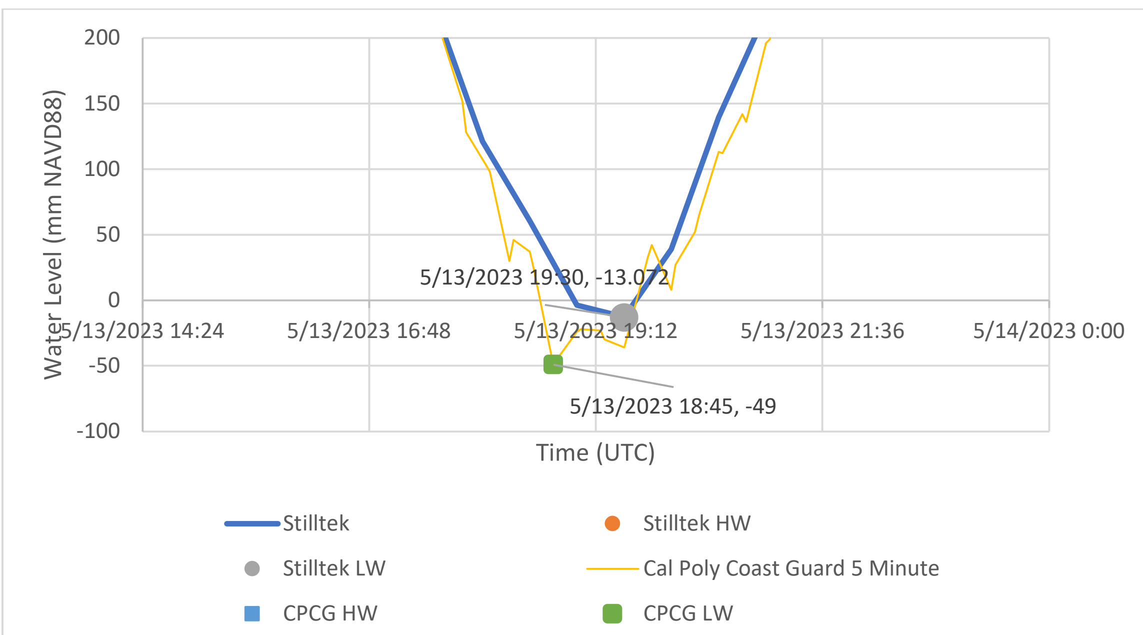

Figure 40: A zoomed in version of Figure 39 for the second low water on 5/23/2023 estimated from the Stilltek and Cal Poly Coast Guard gauges. Here, the difference in elevation of the identified low water is 36 mm. "HW" refers to high water and "LW" refers to low water. "CPCG" refers to the Cal Poly Coast Guard gauge.

There are some possible explanations for variations between the two gauges. Leveling surveys conducted and the measured offsets between the instrument probe and the survey point could differ in approximated elevations. Additionally, averaging water level measurements can lead to variability within measurements, and the prediction of high and low water. For example, the Stilltek estimates a 1-minute median every 30 minutes while the Cal Poly Coast Guard gauge utilizes 5-minute averages (**Figure 40**). Differences in averaging periods can affect water level data by smoothening out (truncating) time scale variations in water levels as seen in **Figure 40**. The coarser time resolution within the Stilltek measurements results in the reductions of high-water estimates and increases in low water estimates. Another possible explanation is differences in the estimation of the speed of sound due to differences in the estimation of air temperature, which I explore below.

4.1.6 Temperature Comparison

Comparing the air temperature from the Cal Poly Coast Guard gauge to the Stilltek gauge yields an RMSE and mean difference of 1.40 degrees C and 1.33 degrees C, respectively. Comparing the air temperature from the Cal Poly Coast Guard gauge to the NOAA OX1MB MET Station at the Coast Guard North T-Pier yields an RMSE and mean difference of 1.46 degrees C and 0.67 degrees C, respectively (**Table 13**). Results show that the Stilltek temperature measurement follows the diurnal variations in the Cal Poly Coast Guard air temperature measurement but is commonly offset lower by 1.33 degrees Celsius (**Figure 41).** The nighttime temperatures between the Cal Poly Coast guard gauge and the NOAA OX1MB MET station match well, but the daytime temperatures for the Cal Poly Coast Guard gauge temperature are higher (**Figure 42**). Thus, the shaded Cal

Poly external Temperature and Humidity sensor probe still registers higher air temperatures during daytime hours than the NOAA OX1MB MET station. It is unknown whether the daytime differences reflect real air temperature differences caused by factors such as different elevations and exposure to wind, or whether the superior shielding of the NOAA OX1MB MET station reduces the heating effect of reflections or radiation from the dock.

Table 13: RMSE and Mean Difference for Air Temperature Data in Morro Bay

Comparison	RMSE (°C)	Mean Difference (°C)	Number of Points
Stilltek-CalPoly_CG	1.40	1.33	5477
OX1MB MET-CalPoly_CG	1.46	0.67	4351

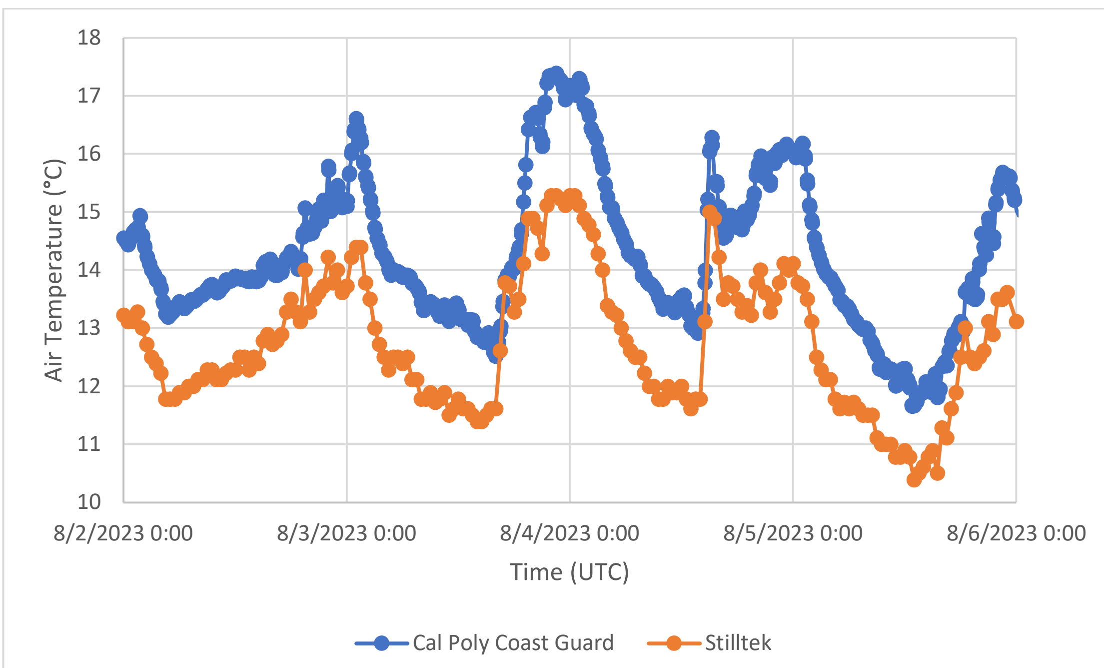

Figure 41: Stilltek vs Cal Poly Coast Guard Air Temperature

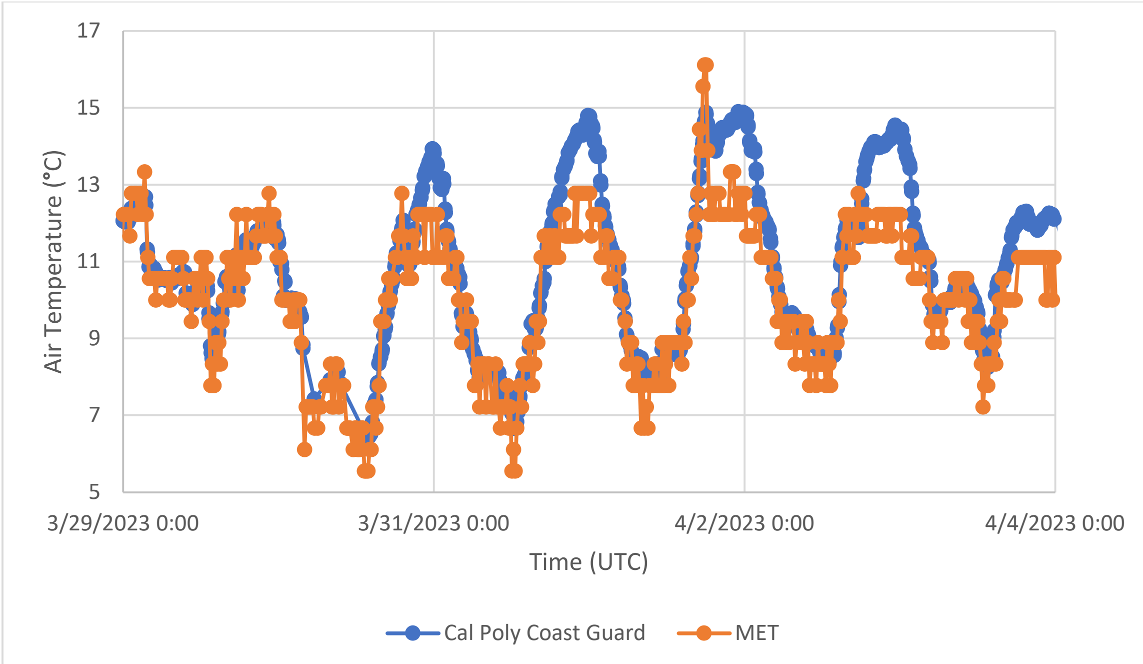

Figure 42: Cal Poly Coast Guard Gauge vs NOAA OX1MB MET Air Temperature

The persistent offset in air temperatures used in the processing of water level data for the Stilltek and the Cal Poly Coast Guard gauge leads to small differences in the estimated speed of sound, and hence might lead to a stage-dependent difference in the water levels estimated by the two gauges. Differences would be greatest at a low tide and higher temperatures, as found by exploring the effect of the observed temperature differences on the corrected distance measurement (**Table 14**). I explored the effects using typical values of high and low water, and the minimum and maximum temperatures over the project period. At high temperatures and low water, up to 9 mm of the difference is due to different speed of sound estimates. The actual impact of the bias between the Stilltek and Cal Poly Coast Guard gauge under these conditions is likely similar but is unknown because the exact algorithm for the Stilltek speed of sound estimation is not known. I explored more explanations for differences between the gauges in **Section 4.1.5**.

Table 14: Comparison of corrected distance measurements for typical values of high and low water at maximum and minimum air temeratures. The effect of the observed offset of 1.33 °C in air temperature between the Stilltek and Cal Poly Coast Guard gauge was explored.

Distance to Water (mm)	Air Temperature (°C)	Relative Humidity (%)	Corrected Distance (mm)	Difference (mm)
1000	10.56	84	977.5	2.5
1000	11.89	84	980.0	
1000	23.89	84	1002.5	2.6
1000	25.22	84	1005.1	
3500	10.56	84	3421.5	8.6
3500	11.89	84	3430.1	
3500	23.89	84	3508.9	9.0
3500	25.22	84	3517.9	

4.2 Tidal Prism Estimate

I estimated the tidal prism in Morro Bay using the methodology described in **Section 3.4.** I verified the volume estimate obtained using MatFlood, and determined the uncertainty in monthly mean tidal datums and the tidal prism. Additionally, I determined the monthly tidal prism in 2022 and 2023 and projected the estimate into the years 2050 and 2100 using accepted SLR scenarios (Griggs et al., 2017).

4.2.1 MatFlood Volume Estimate Verification

I verified the volume estimate obtained using MatFlood (see **Section 3.4.1** for methodology) by comparing against published values determined by Tetra Tech in 2019 (**Table 15**). The tidal prism estimates from MatFlood exhibited negligible differences, less than 1%, from GIS based estimates of Tetra Tech.

Table 15: Comparing Tetra Tech Tidal Prism Estimates to MatFlood Tidal Prism

Bathymetry Year	Tidal Datum Year	MLW (m NAVD88)	MHW (m NAVD88)	Tidal Prism from Tetra Tech 2019 (Acre-Feet)	Tidal Prism from Tetra Tech 2019 (m^3)	Tidal Prism from MatFlood (Acre-Feet)	Tidal Prism from MatFlood (m^3)	% Difference
2019	1998	0.260	1.418	6805.6	8.39E+06	6812.0	8.40E+06	0.094
2019	2019	0.274	1.395	6589.4	8.13E+06	6595.5	8.14E+06	0.092

4.2.2 Uncertainty

There was an observed precision error and bias within the water levels as estimated from the Stilltek gauge and the Cal Poly Coast Guard gauge as discussed in **Sections 4.1.4 and 4.1.5**. Using the 95% confidence interval and the observed bias, I estimated the magnitude of total uncertainty in the monthly mean tidal datums using **Equation 3** (**Table 16**).

Table 16: Total Uncertainty for Monthly Mean Tidal Datums

Source	MHW Uncertainty (mm)	MLW Uncertainty (mm)
95 % Precision	5.08	5.08
Bias	3.00	29.92
Total	**5.89**	**30.35**

The total uncertainty in monthly tidal datums yielded up to a 2.90 percent difference, or 185 acre-feet (2.28E+05 m^3), in the estimated tidal prism volume (**Table 17**). I added and subtracted the total uncertainty in high and low water estimates from the tidal datums as determined by Tetra Tech in August 2019 (**Table 16**). The "Uncertainty Combination" column in **Table 16** indicates if the total uncertainty in monthly tidal datums was added or subtracted to MHW and MLW, respectively. For example, "+/+" indicates that I added the total uncertainty to both MHW and MLW, whereas "+/-" indicates that I added the total uncertainty to MHW but subtracted the total uncertainty from MLW. Based on the approximate 3% difference in the tidal prism estimate attributable to total measurement uncertainty, a change of at least 5-6% in the tidal prism, indicating a signal-to-noise ratio of two, is required to conclude that a real shift in tidal prism has occurred. Other sources of bias and precision errors in the bathymetry, surveying, and averaging likely add additional uncertainty to the tidal prism estimate.

Table 17: The total uncertainty effect on the tidal prism. The tidal prism volumes with uncertainty considered are compared to the baseline tidal prism, or original tidal prism determined by Tetra Tech in 2019 (shaded in orange below).

Uncertainty Combination (MHW/MLW)	MHW (m NAVD88)	MLW (m NAVD88)	Tidal Prism (Acre-Feet)	Tidal Prism (m^3)	% Difference (To Baseline)
Baseline (No Uncertainty)	1.395	0.274	6506.2	8.03E+06	-
+/+	1.405	0.305	6439.8	7.94E+06	1.03
-/-	1.387	0.244	6566.9	8.10E+06	-0.93
+/-	1.405	0.244	6686.3	8.25E+06	-2.73
-/+	1.387	0.305	6320.4	7.80E+06	2.90

4.2.3 2022 Tidal Prism

I utilized the monthly and annual MHW and MLW from NOAA Port San Luis and the Morro Bay Stilltek gauge, tabulated in **Section 4.1.2,** to calculate the monthly tidal prism values in MatFlood (**Table 18**). The associated surface areas and volumes at MHW and MLW are found in **Appendix B**. Seasonal variability in sea level yields monthly differences in the tidal prism for the NOAA Port San Luis gauge and the Stilltek gauge of up to 367.2 and 468 acre-feet (4.53E+05 and 5.77E+05 m^3), respectively. The difference in monthly tidal prism estimates using data from two locations ranges from –2.36% to + 1.27%, for an annual average percentage difference of -0.83%. The small maximum difference of estimates between gauges, 152 acre-feet (1.87E+05 m^3) in November of 2022, may result from the different locations of the gauges or different gauge types as discussed in **Section 4.1.5**. Compared to the tidal prism estimate by Tetra Tech in August of 2019, I approximated the 2022 August tidal prism from Stilltek to be smaller by 2.05 percent (Tetra Tech, 2020). Compared to the tidal datums estimated by Tetra Tech in August 2019, I estimated the 2022 August MHW and MLW from Stilltek to be higher by 0.072 and 0.12 m respectively (Tetra Tech, 2020). Despite tidal elevations getting larger, I predicted that the tidal prism became be smaller. This is likely a bathymetric effect, explored more in **Section 4.3.2**.

Table 18: Tidal prism volume estimates in 2022 from the MHW and MLW estimated from the NOAA Port San Luis and Stilltek gauges.

Month	**NOAA Port San Luis (Acre-Feet)**	**NOAA Port San Luis (m^3)**	**Stilltek (Acre-Feet)**	**Stilltek (m^3)**	**% Difference**
January	6492.1	8.01E+06	6467.4	7.98E+06	0.38
February	6124.9	7.55E+06	6251.4	7.71E+06	-2.04
March	6370.2	7.86E+06	6289.6	7.76E+06	1.27
April	6208.3	7.66E+06	6194.9	7.64E+06	0.22
May	6179.4	7.62E+06	6141.6	7.58E+06	0.61
June	6229.2	7.68E+06	6335.0	7.81E+06	-1.68
July	6251.6	7.71E+06	6330.4	7.81E+06	-1.25
August	6378.4	7.87E+06	6455.7	7.96E+06	-1.20
September	6445.2	7.95E+06	6563.0	8.10E+06	-1.81
October	6424.3	7.92E+06	6436.8	7.94E+06	-0.19
November	6351.1	7.83E+06	6502.7	8.02E+06	-2.36
December	6467.1	7.98E+06	6609.0	8.15E+06	-2.17
Annual	6337.2	7.82E+06	6390.3	7.88E+06	-0.83

4.2.4 2023 Tidal Prism

For January through August of 2023, I repeated the analysis conducted in **Section 4.2.3**, using the monthly tidal datums from the NOAA Port San Luis gauge, the Stilltek gauge, and the Cal Poly gauges, tabulated in **Section 4.1.3,** to calculate the tidal prism values

(**Table 19**). The associated surface areas and volumes at MHW and can be found in **Appendix B**. Seasonal variability in sea level yields monthly differences in the tidal prism for the NOAA Port San Luis gauge, the Stilltek gauge and the Cal Poly Coast Guard gauge of up to 863.1, 632.8 and 923.5 acre-feet (1.06E+06, 7.81E+05 and 8.25E+06 m^3), respectively. The difference in monthly tidal prism estimates between the NOAA Port San Luis gauge and the Stilltek gauge varies by -1.42% to -2.64%. The difference in monthly tidal prism estimates between the NOAA Port San Luis gauge and the Cal Poly Coast Guard gauge varies by -0.21% to -3.97%. The difference in monthly tidal prism estimates between the Stilltek gauge and the Cal Poly Coast Guard gauge varies by –1.05% to -2.32%. Differences of estimates between gauges may result from the different locations of the gauges, different gauge types, different processing methods and different duty cycles as discussed in **Sections 4.1.4** and **4.2.3**. Compared to the tidal prism estimate by Tetra Tech in August of 2019, I estimated the tidal prism in August of 2023 from the Stilltek gauge and the Cal Poly gauge to be larger by 5.06 and 6.77 percent, respectively (Tetra Tech, 2020). Compared to the tidal datums estimated by Tetra Tech in August 2019, I approximated the MHW and MLW in August of 2023 from the Stilltek gauge and the Cal Poly gauge to be larger by 0.170 and 0.155 m, and 0.168 and 0.132 m, respectively (Tetra Tech, 2020).

Table 19: The tidal prism in 2023 from the MHW and MLW estimated from the NOAA Port San Luis, Stilltek, and Cal Poly Coast Guard gauges.

Month	NOAA Port San Luis (Acre-Feet)	NOAA Port San Luis (m^3)	Stilltek (Acre-Feet)	Stilltek (m^3)	Cal Poly Coast Guard (Acre-Feet)	Cal Poly Coast Guard (m^3)	% Difference (NOAA-Stilltek)	% Difference (NOAA-Cal Poly)	% Difference (Stilltek-Cal Poly)
January	6365.7	7.85E+06	-	-	-	-	-	-	-
February	6253.9	7.71E+06	-	-	-	-	-	-	-
March	6288.9	7.76E+06	-	-	6302.1	7.77E+06	-	-0.21	-
April	5972.4	7.37E+06	-	-	6127.6	7.56E+06	-	-2.57	-
May	6179.7	7.62E+06	6345.6	7.83E+06	6413.0	7.91E+06	-2.64	-3.71	-1.05
June	6188.7	7.63E+06	6300.3	7.77E+06	6400.9	7.90E+06	-1.79	-3.37	-1.58
July	6461.2	7.97E+06	6568.6	8.10E+06	6722.7	8.29E+06	-1.65	-3.97	-2.32
August	6835.5	8.43E+06	6933.1	8.55E+06	7051.1	8.70E+06	-1.42	-3.11	-1.69

4.2.5 Tidal Prism with Spatially Varying Tidal Datums

I explored the effect of spatially varying water levels on the tidal prism in Morro Bay using historically observed spatial differences. Additionally, I used the four Cal Poly gauges to estimate the effects that spatially varying tidal datums have on the tidal prism volume for 2023. I considered the order of magnitude of uncertainty in the monthly mean tidal datums when determining if real changes had occurred in the tidal prism volume.

I utilized the historically observed spatial difference in tidal elevations from Tetra Tech in 1998 to explore the magnitude of effects on the tidal prism volume (Tetra Tech, 1999). Tetra Tech observed that tides were 0.5 ft (0.152 m) higher in the back of the bay than near the mouth. I utilized the methodology described in **Section 3.4.4** to estimate the tidal prism with spatially varying monthly tidal datums. The tidal prism using spatially varying tidal datums exhibited a 9.60 percent increase when compared to the uniform tidal prism (**Table 20**). Thus, comparing the tidal prism utilizing one gauge location near the mouth of the estuary to the tidal prism using spatially varying tidal datums based on two locations reveals potentially non-negligible contributions to the tidal prism volume estimate.

Table 20: Comparing the estimated tidal prism utilizing one gauge location near the mouth of the estuary ("Uniform") vs the tidal prism estimated utilizng spatially varying tidal datums ("Spatially Varying"). The tidal datums utilized were from Tetra Tech in 1998 with the observed spatial variation of high water of up to +0.5 ft (0.152 m) in Baywood Los Osos.

<table>
<tr><th></th><th>Location</th><th>MHW
(m NAVD88)</th><th>MLW
(m NAVD88)</th><th>Tidal Prism (Acre-Feet)</th><th>Tidal Prism (m^3)</th></tr>
<tr><td>Uniform Prism</td><td>Coast Guard
North T-Pier</td><td>1.421</td><td>0.3414</td><td>6389.9</td><td>7.88E+6</td></tr>
<tr><td rowspan="2">Spatially Varying Prism</td><td>Coast Guard
North T-Pier</td><td>1.421</td><td rowspan="2">0.3414</td><td rowspan="2">7034.0</td><td rowspan="2">8.68E+6</td></tr>
<tr><td>Baywood</td><td>1.574</td></tr>
<tr><td>Percent Difference</td><td colspan="3"></td><td colspan="2">9.60</td></tr>
</table>

I determined the tidal prism in 2023 using spatially varying monthly tidal datums from the various Cal Poly gauges. I found that the monthly tidal prism utilizing spatially varying tidal datums could be up to 2.88 percent larger when compared to the monthly tidal prism as calculated from only the Cal Poly Coast Guard gauge in 2023 (**Table 21)**. I estimated the tidal prism using spatially varying monthly tidal datums using the MHW and MLW data from the Cal Poly gauges in Morro Bay (**Table 10** and **Table 11** in **Section 4.1.6**). The surface areas and volumes can be found in **Appendix B**.

Table 21: Comparison between the 2023 tidal prism as calculated using only the Cal Poly Coast Guard Gauge ("Uniform") to the tidal prism estimated from spatially varying monthly tidal datums from the four Cal Poly Gauges in Morro Bay ("Spatially Varying").

Month	Uniform Tidal Prism (Acre- Feet)	Uniform Tidal Prism (m^3)	Spatially Varying Tidal Prism (Acre-Feet)	Spatially Varying Tidal Prism (m^3)	% Difference
March	6302.1	7.77E+06	6133.2	7.57E+06	2.72
April	6127.6	7.56E+06	6234.4	7.69E+06	-1.73
May	6413.0	7.91E+06	6564.2	8.10E+06	-2.33
June	6400.9	7.90E+06	6588.0	8.13E+06	-2.88
July	6722.6	8.29E+06	6852.9	8.45E+06	-1.92
August	7051.1	8.70E+06	7156.8	8.83E+06	-1.49

The uncertainty in the tidal prism due to uncertainty in monthly mean tidal datums, as determined in **Section 4.2.2,** was up to 2.90 percent. Thus, the effect of spatially varying tides on the tidal prism within Morro Bay lies outside the range of uncertainty. However, undiagnosed, or underestimated errors in the tidal datum measurements are possible and the certainty for the geodetic survey results could be improved upon. Additionally, long-term tidal surveys at additional locations (for at least a year) are recommended to better observe spatial varying tidal elevations.

4.2.6 Estimated Future Tidal Prism with SLR

I projected annual mean tidal datums from the Stilltek gauge during 2022 in Morro Bay to the years 2050 and 2100 using the SLR scenarios from Griggs and **Equation 4** (**Table 22**) (Griggs et al., 2017). The overall projected trend in tidal prism indicates that the tidal prism will most likely increase by up to 39.4 percent by 2100 from 2022 levels (**Table 22**). The tidal prism by 2100 is predicted to range between 7325 and 9525 acre-feet

(9.04E+06 and 1.17E+07 m^3) based on the range of SLR scenarios (**Figure 43**). It is important to disclose that this estimate does not consider local land subsidence, sediment input from local watersheds and the ocean, and sand placement or dredging activities. Future changes in morphology due to these activities would alter the future tidal prism (Ghosh et al., 2006).

Table 22: Estimated Future Tidal Prism. The percentage difference is in comparison to the annual tidal prism estimate from the Stilltek gauge in 2022 (6390.3 acre-feet or 7.88E+06 m^3).

SLR Scenario	SLR (m above Y2K MSL)	Tidal Prism Volume (Acre-Feet)	Tidal Prism Volume (m^3)	% Difference
2050	0.274	6912.4	8.53E+06	7.9
2100 RCP-2.6	0.488	7325.7	9.04E+06	13.6
2100 RCP-4.5	0.579	7486.9	9.23E+06	15.8
2100 RCP-8.5	0.792	7834.5	9.66E+06	20.3
2100 H++	3.048	9525.5	1.17E+07	39.4

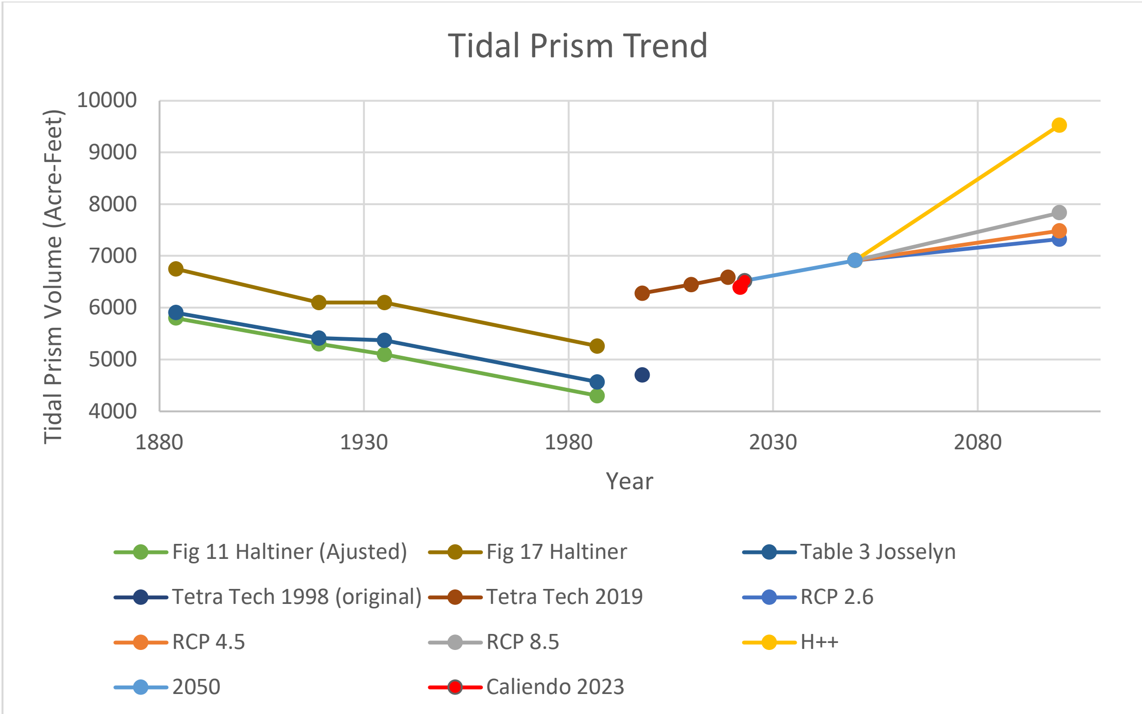

Figure 43: The Projected Tidal Prism. The historically estimated tidal prism values (1884-2019) are included and were explained in ***Section 2.4****.*

4.3 Tidal Prism Variability

Factors affecting the tidal prism are discussed in this section. Changes in bathymetry and varying sea levels can contribute to differences in the tidal prism estimate and are explored.

4.3.1 MSL Hydrograph

Changing high and low tide water levels influences the tidal prism, or volume of water exchanged during a tidal cycle. Tidal datums shift both from astronomical forcing, but also because of changes in MSL on seasonal, interannual, and decadal time scales.

The MSL varies in a region over time as seen with the trend in monthly and annual MSL trends for NOAA Port San Luis (**Figure 44** and **Figure 45**). NOAA states that the MSL trend in Port San Luis is rising at a rate of +0.96 +/- 0.35 mm per year based on historical water level data dating back to 1945 (*NOAA Port San Luis Data Inventory Page*, n.d.). From 1972 to 2021, monthly MSL varied from 0.667 m to 1.071 m NAVD88 while the annual MSL varied from 0.758 m to 0.928 m NAVD88. During El-Nino events, the MSL is the highest observed, as seen in 1983 and 2015.

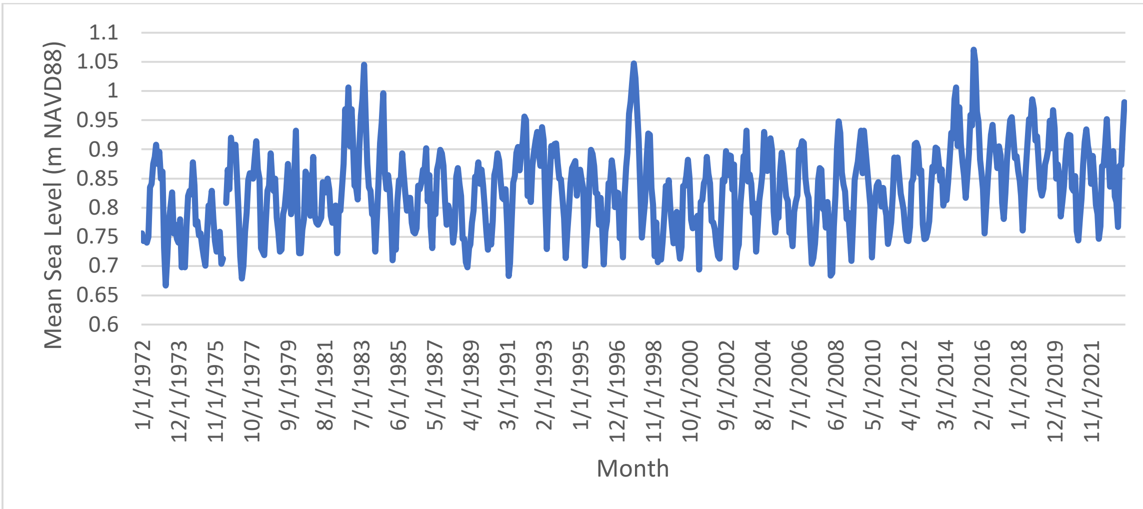

Figure 44: Monthly MSL Hydrograph for NOAA Port San Luis from 1972 to 2023

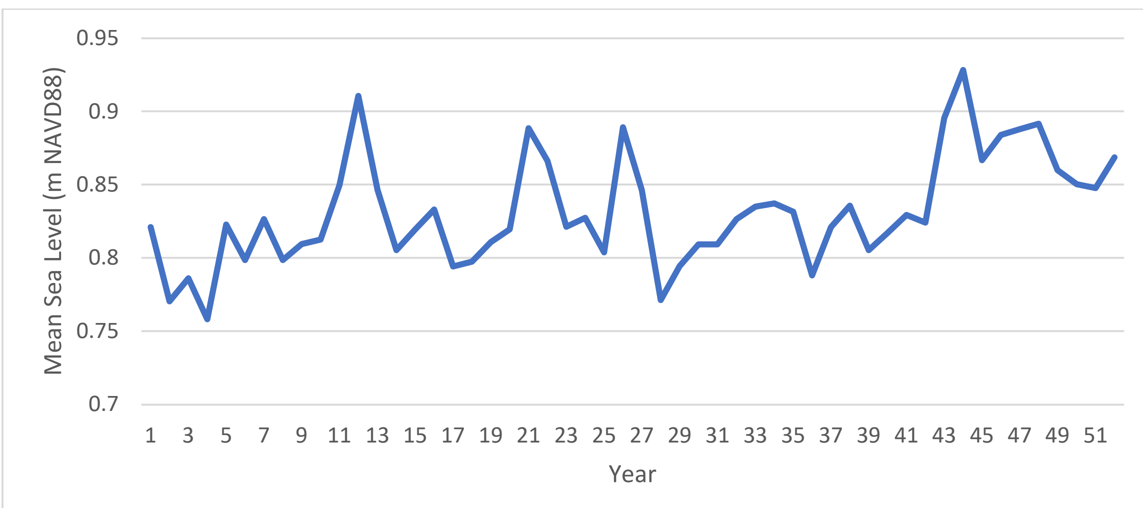

Figure 45: Annual MSL Hydrograph for NOAA Port San Luis from 1972 to 2023

I calculated the monthly MSL anomaly, or the amount that the monthly MSL differs from that year's annual MSL for that month. Average monthly MSL at Port San Luis can typically vary by up to 0.069 m from its monthly climatology based on 51 years of data

(**Figure 46**). Error! Reference source not found.It can be observed that typically, water levels in April are lower, and water levels in September are higher (**Figure 46**). This is due to the typical seasonal cooling and heating of the ocean surface off the Coast of California. Upwelling due to equatorward winds occurs around April, causing cold sea surface temperatures (SST). Around September is when winds relax, resulting in higher sea levels (Legaard & Thomas, 2006). This indicates that one month of tidal monitoring will not be reflective of annual sea level conditions. This was an assumption previously made in estimates of the tidal prism in Morro Bay.

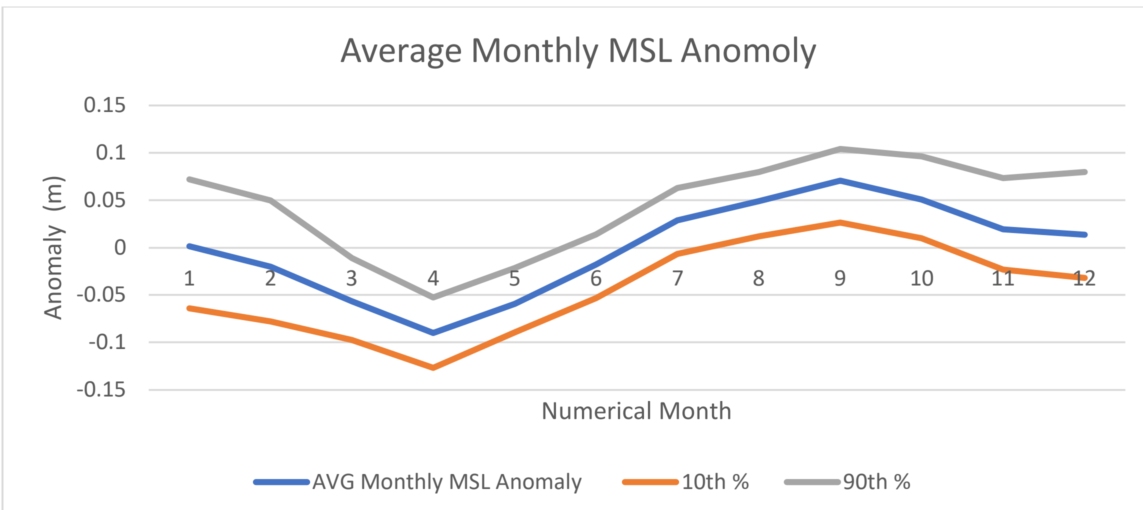

Figure 46: Monthly MSL Anomaly for NOAA Port San Luis from 1972 to 2023. The 10th and 90th percentiles are Displayed on the plot.

The MTR at NOAA Port San Luis varies seasonally over the 18.61 year nodal cycle, and appears to have slightly decreased between 1971 and 2021 (***Figure 47***Error! Reference source not found. and **Figure 48**Error! Reference source not found.). The monthly MTR spanned from 0.961 m to 1.189 m NAVD88 (***Figure 47***Error! Reference source not found.) while the annual mean tidal range spanned from 1.068 m to 1.139 m NAVD88 (**Figure 48**Error! Reference source not found.).

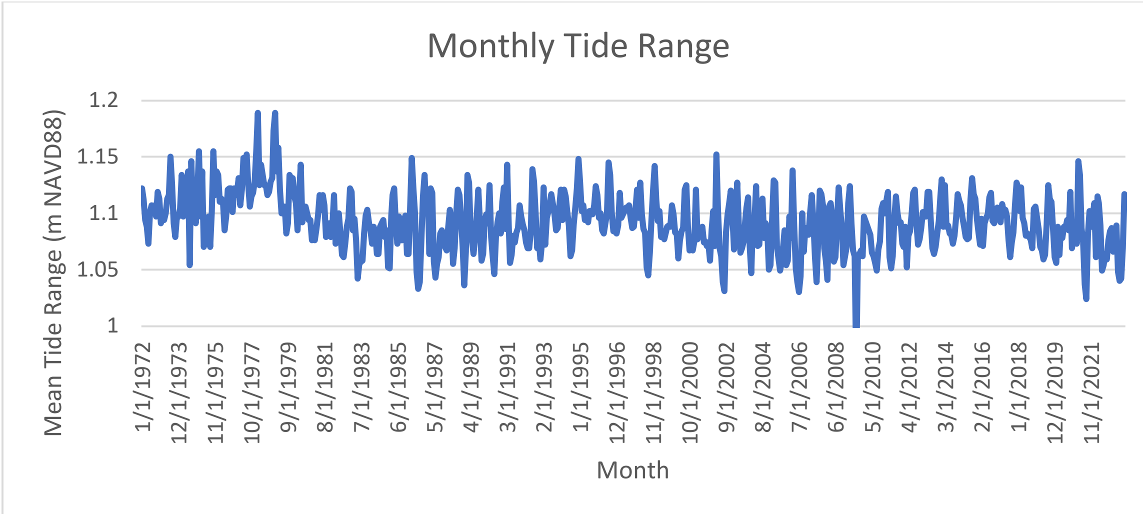

Figure 47: Monthly MTR Hydrograph for NOAA Port San Luis from 1972 to 2023

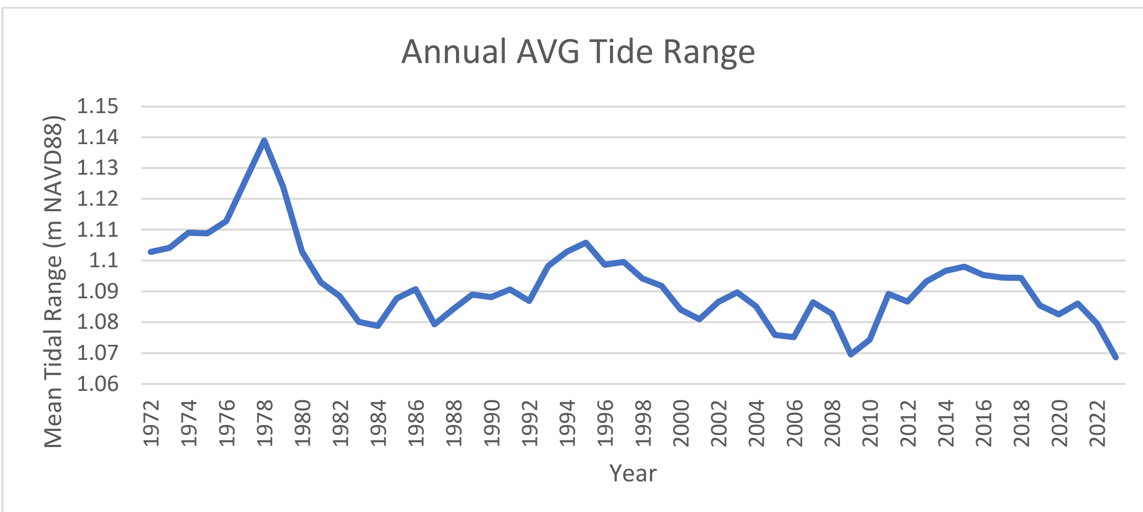

Figure 48: Annual MTR Hydrograph for NOAA Port San Luis from 1972 to 2023

I calculated the monthly MTR anomaly, or the amount that the monthly MTR differs from that year's annual MTR for that month. The average monthly MTR can vary by up to 0.040 m from the annual average (**Figure 49**Error! Reference source not found.). The monthly anomaly is greatest during March and August.

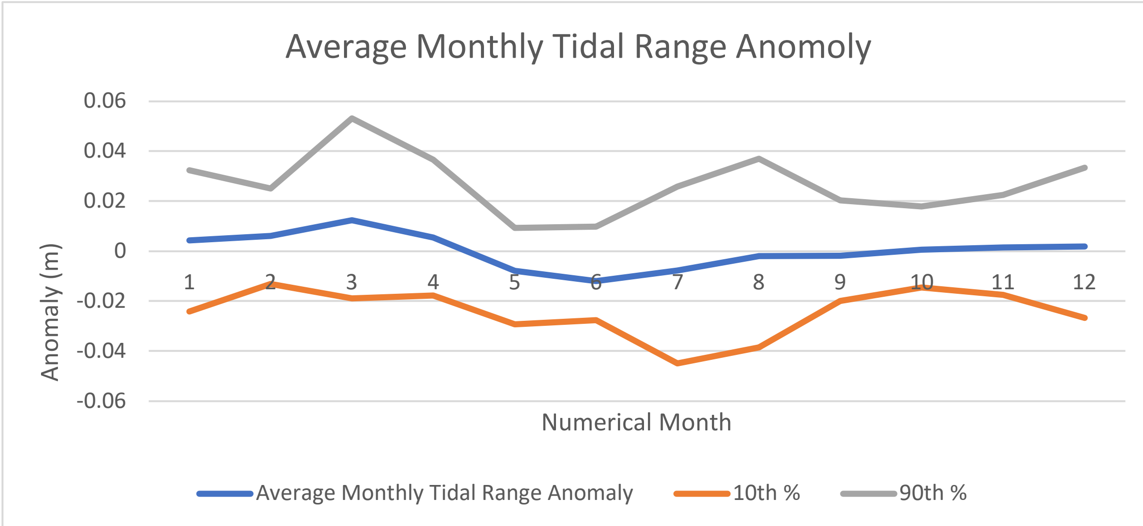

Figure 49: Monthly MTR Anomaly for NOAA Port San Luis from 1972 to 2023. The 10th and 90th percentiles are Displayed on the plot.

Monthly and yearly variations in MSL and MTR indicate that the time of year, the reference year for the calculation, the duration of tidal monitoring and the tidal epoch can influence the magnitude of the tidal datums and therefore the tidal prism.

4.3.2 Bathymetry Changes

Changes in bathymetry and/or the digital elevation model lead to an altered tidal prism volume. I evaluated elevation changes between 2019 and 2022. Additionally, I evaluated surface area and volume of water changes at various contour levels.

The elevation from 2019 to 2022 decreased by an average of 0.039 m below the annual 2022 MHW from Stilltek, or 1.421 m NAVD88 (**Figure 50**). I calculated the change in sediment volume to be -265.2 acre-ft (-3.27E+05 m^3), meaning erosion occurred. However, the average elevation change is within the range of uncertainty specified by NOAA for this DEM so the significance of this change is unclear.

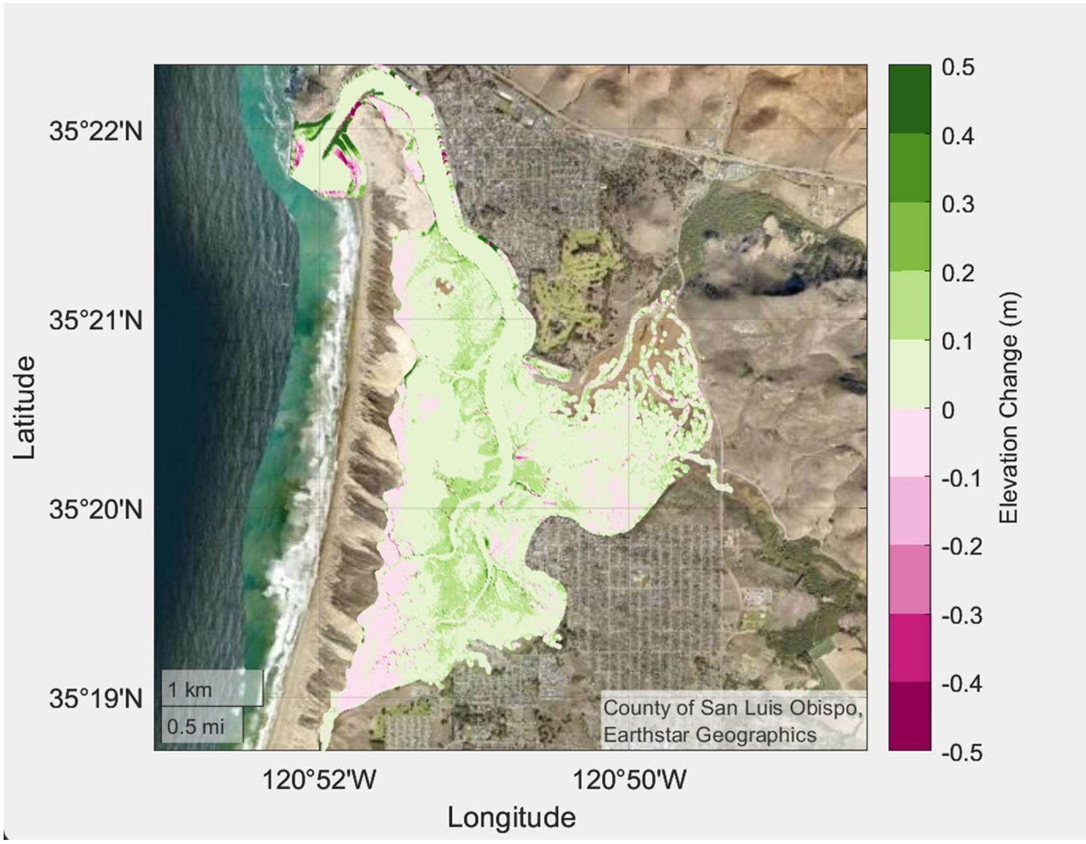

Figure 50: Change in Elevation Between 2019 and 2022

The average change in elevation from 2019 to 2022 decreased by 0.034 m for all levels between annual 2022 MHW and MLW from Stilltek, or 1.421 and 0.341 m NAVD88 respectively (**Figure 51**). I calculated the change in sediment volume within the tidal range to be -73.5 acre-feet (-9.06E+04 m^3). Thus, changes within the tidal range will have implications on the tidal prism volume. However, the average elevation change in Morro Bay is within the range of uncertainty specified by NOAA for this DEM so the significance of this change is unclear.

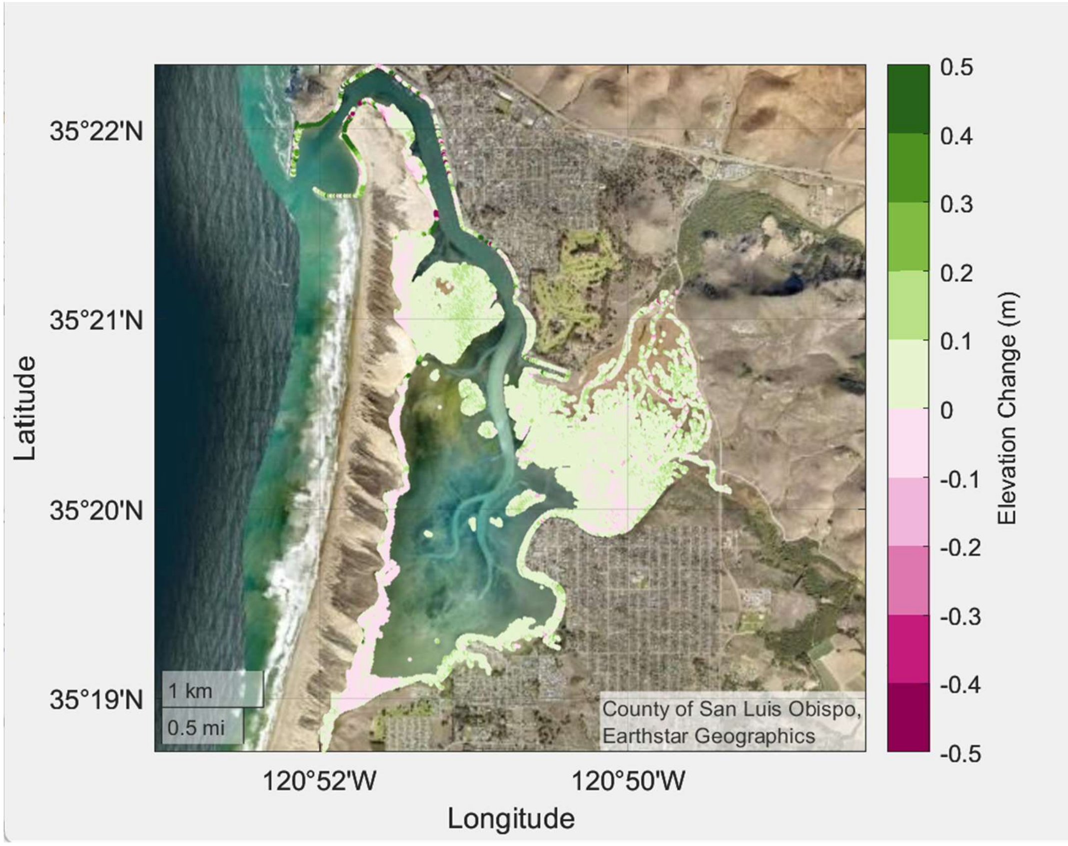

Figure 51: Changes in Elevation Between 2019 and 2022 within the Tidal Range

I determined the changes between 2019 and 2022 in surface area to depth and volume to depth relationships for various contour lines. The largest changes in surface area to depth relationships between 2019 and 2022 occurred between -6.051 and -3.003 m NAVD88 and 0.045 and 0.960 m NAVD88 (**Table 23** and **Figure 52**Error! Reference source not found.). Changes in surface area within the tidal range (**Figure 53**Error! Reference source not found.) will have implications on the volume, and therefore the tidal prism. In **Figure 52**Error! Reference source not found. and **Figure 53**Error! Reference source not found., a steep slope indicates a region where small rises in water levels will have little impact on the surface area of water, such as regions above and below the mudflats. A flatter slope indicates areas where small rises in water levels will greatly increase the surface area, such as the mudflats. Because the hypsometric curve is non-linear, any rises in sea levels would cause a change in the relationship between the surface area of water at a given tidal stage as tidal datums shift.

Table 23: Percent Changes in Surface Area of Water Between 2019 and 2022

Water Level (m NAVD88)	2019 (Acres)	2019 (m^2)	2022 (Acres)	2022 (m^2)	% Change
1.569	2100	8.50E+06	2108.0	8.53E+06	0.38
1.264	2020	8.17E+06	2021.7	8.18E+06	0.09
0.960	1897	7.68E+06	1915.1	7.75E+06	0.97
0.655	1620	6.56E+06	1663.5	6.73E+06	2.68
0.350	1289	5.22E+06	1356.6	5.49E+06	5.25
0.045	746	3.02E+06	761.4	3.08E+06	2.07
-0.259	457	1.85E+06	456.9	1.85E+06	-0.03
-0.564	399	1.61E+06	401.5	1.62E+06	0.62
-0.869	366	1.48E+06	369.0	1.49E+06	0.83
-1.174	345	1.40E+06	346.5	1.40E+06	0.42
-1.479	331	1.34E+06	331.8	1.34E+06	0.25
-3.003	253	1.02E+06	257.4	1.04E+06	1.76
-4.527	137	5.54E+05	142.3	5.76E+05	3.87
-6.051	57	2.31E+05	60.0	2.43E+05	5.29
-9.099	3	1.21E+04	2.7	1.09E+04	-10.38
-12.167	0	0.00E+00	0.4	1.62E+03	-

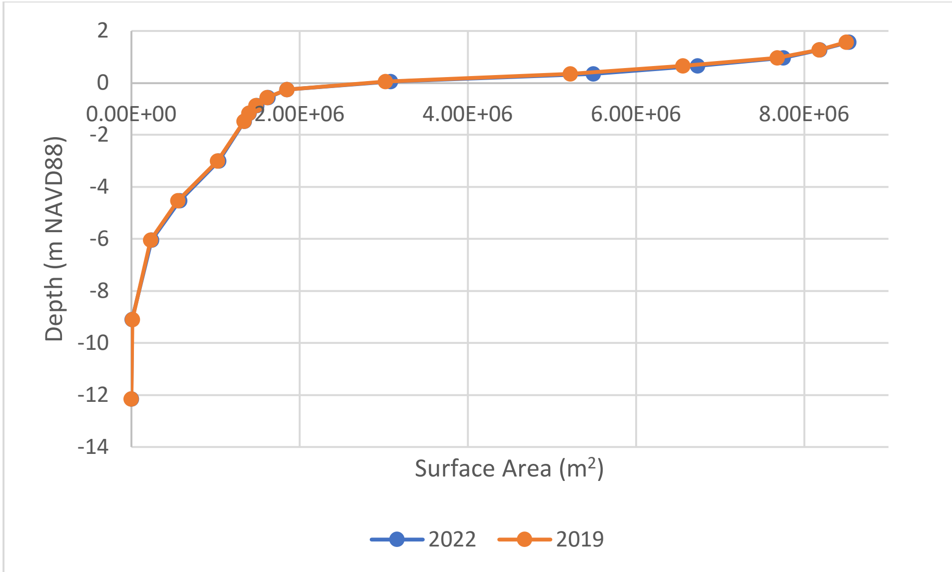

Figure 52: Changes in Surface Area of Water as a Function of water level for 2019 and 2022 at all Water Levels in Morro Bay

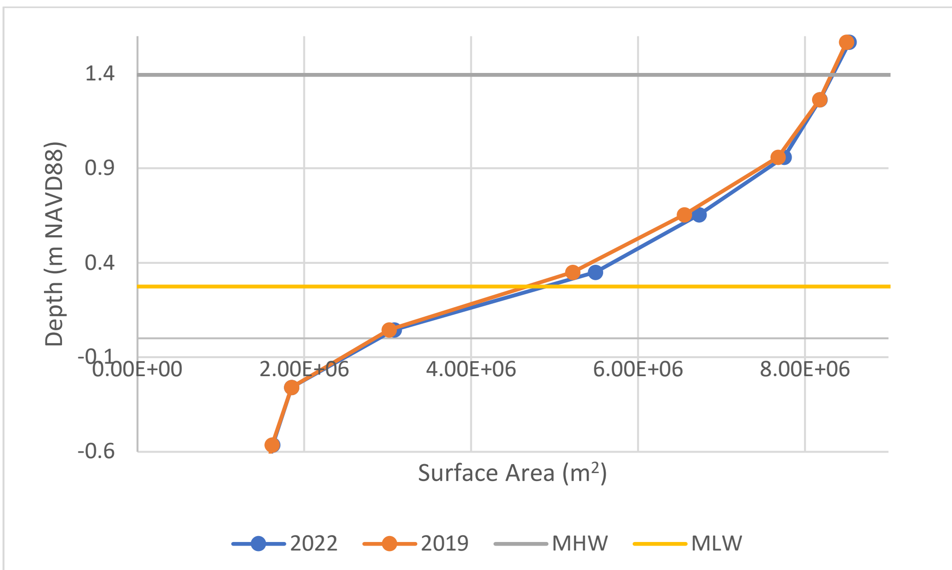

Figure 53: Zoomed in view of Figure 50, depicting changes in surface area of water for 2019 and 2022 from 0.6 to 1.6 m, relative to NAVD88.

The volume to water level relationship is a nonlinear change in volume of water that slowly decreases as water level increases. (**Figure 54**Error! Reference source not found.). The largest changes in volume between 2019 and 2022 occurred between 0.350 and 1.264 m NAVD88 and -6.051 and -1.174 m NAVD88 (**Table 24Error! Reference source**

not found.). Changes in volume of water within the tidal range seen in **Figure 55**Error! Reference source not found. will have implications on the volume of water, and therefore the tidal prism. In **Figure 54**Error! Reference source not found. and **Figure 55**Error! Reference source not found., a steep slope indicates a region where rises in water levels will not greatly affect the volume. Regions where a steep slope occurs are where the surface area of water is low, or in regions below the intertidal canals and mudflats. A flat slope indicates regions where rises in water levels would greatly increase the volume of water in the bay. Regions where this could occur include areas where the surface area of water is large, or in the tidal mudflats. Because the curve is non-linear, any rises in sea levels would cause a change in the relationship between the volume of water at a given tidal stage as tidal datums shift.

Table 24: Percent Changes in Volume of Water in Morro Bay Between 2019 and 2022

Water Level (m NAVD88)	2019 (Acre-Feet)	2019 (m^3)	2022 (Acre-Feet)	2022 (m^3)	% Change
1.569	13421	1.66E+07	13671.9	1.69E+07	1.87
1.264	11368	1.40E+07	11615.5	1.43E+07	2.18
0.960	9398	1.16E+07	9635.7	1.19E+07	2.53
0.655	7631	9.41E+06	7829.5	9.66E+06	2.6
0.350	6160	7.60E+06	6312.3	7.79E+06	2.47
0.045	5146	6.35E+06	5233.0	6.45E+06	1.69
-0.259	4580	5.65E+06	4659.8	5.75E+06	1.74
-0.564	4157	5.13E+06	4234.5	5.22E+06	1.86
-0.869	3775	4.66E+06	3850.2	4.75E+06	1.99
-1.174	3421	4.22E+06	3493.4	4.31E+06	2.12
-1.479	3083	3.80E+06	3154.6	3.89E+06	2.32
-3.003	1609	1.98E+06	1668.7	2.06E+06	3.71
-4.527	640	7.89E+05	675	8.33E+05	5.47
-6.051	170	2.10E+05	184.3	2.27E+05	8.39
-9.099	13	1.60E+04	13.7	1.69E+04	5.62
-12.147	1	1.23E+03	1.1	1.36E+03	9.21

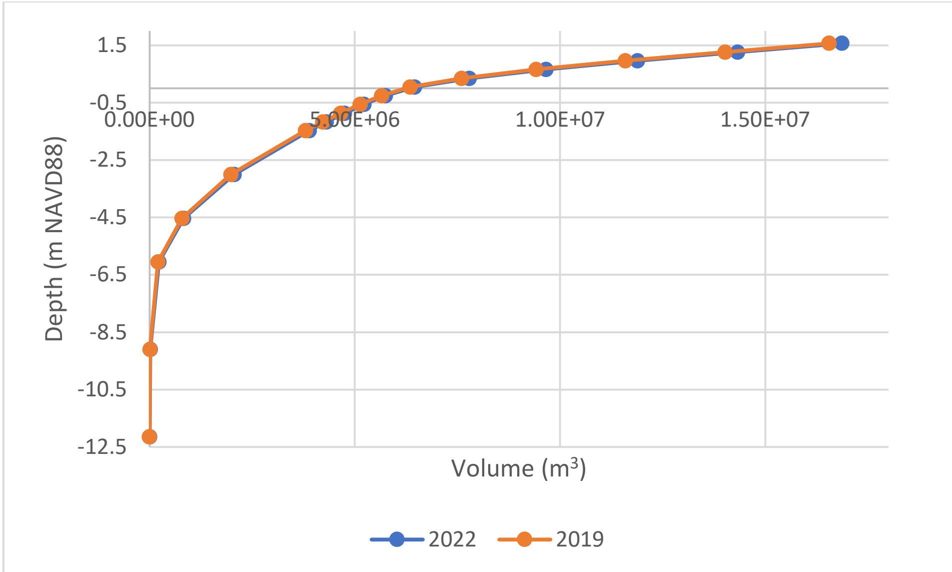

Figure 54: Changes in Volume of Water from 2019 to 2022 at all Water Levels in Morro Bay

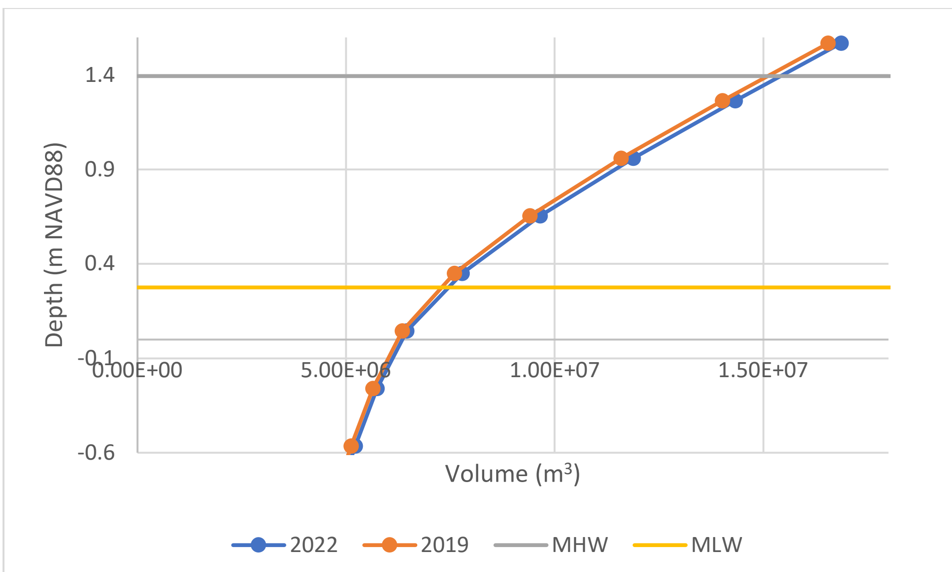

Figure 55: Zoomed in version of Figure 52 depicting changes in volume of water from 2019 to 2022 from -0.6 to 1.6 m, relative to NAVD88.

4.4 Viable Eelgrass Habitat Area

I approximated the viable eelgrass habitat area in Morro Bay for 2019 and 2022 and compared it to actual coverage using the methodology in **Section 3.6**. I projected viable eelgrass habitat area estimates into the years 2050 and 2100 using SLR scenarios, under the assumption that bathymetry from 2022 will not drastically change.

4.4.1 Predicted Viable Eelgrass Area for 2019 and 2022

I estimated the viable eelgrass habitat area in 2019 to be 1138.7 acres (4.60E+06 m^2) and the actual observed eelgrass extent to be 37 acres (1.50E+05 m^2) (see **Section 3.6.1** for methodology) (**Figure 56**). The MBNEP also estimated the actual observed eelgrass area in 2019 as 37 acres (1.49E+05 m^2) using the same shapefiles (Bay, 2021). I estimated the viable area for 2022 as 1107.5 acres (4.48E+06 m^2) using the merged 2019/2022 bathymetry (**Figure 57**). Spatially dependent environmental factors, such as salinity levels, limit eelgrass in the upper reaches of the Chorro delta, resulting in a likely overprediction of viable habitat area (Bay, 2021).

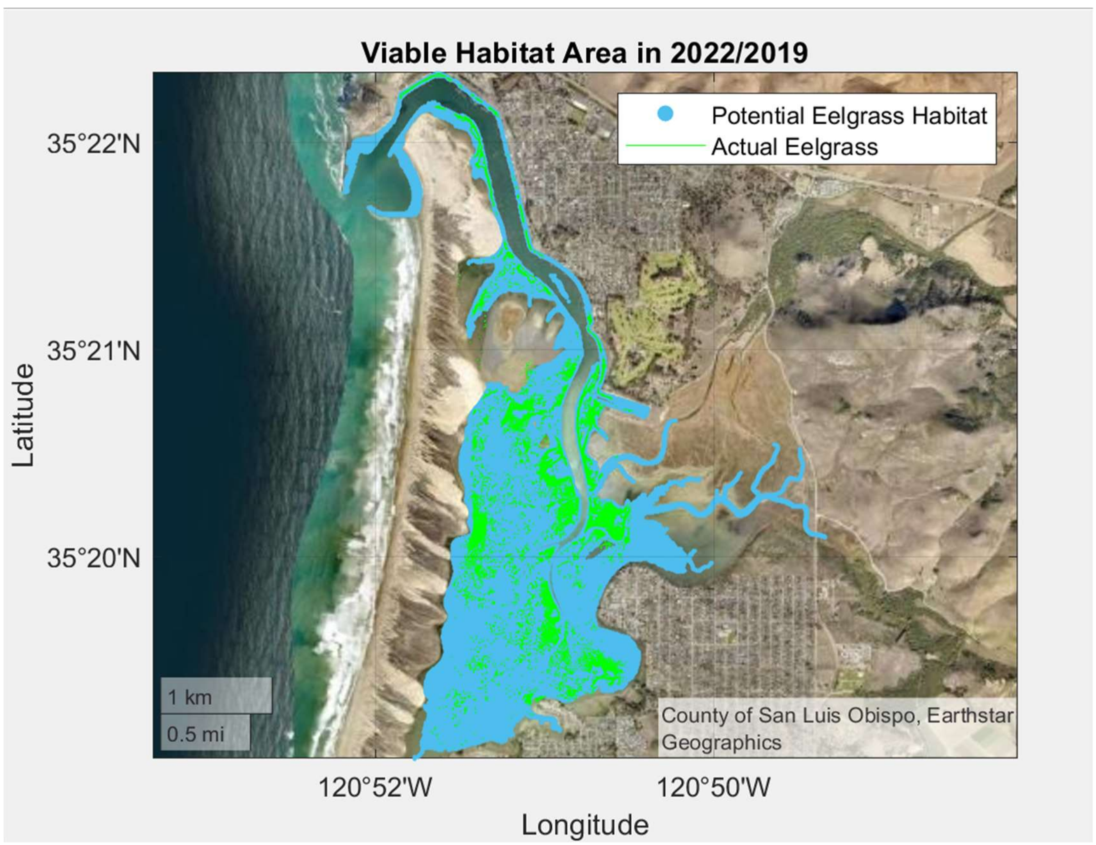

Figure 56: Viable Eelgrass Habitat Area vs Actual Eelgrass Extent for 2019 in Morro Bay

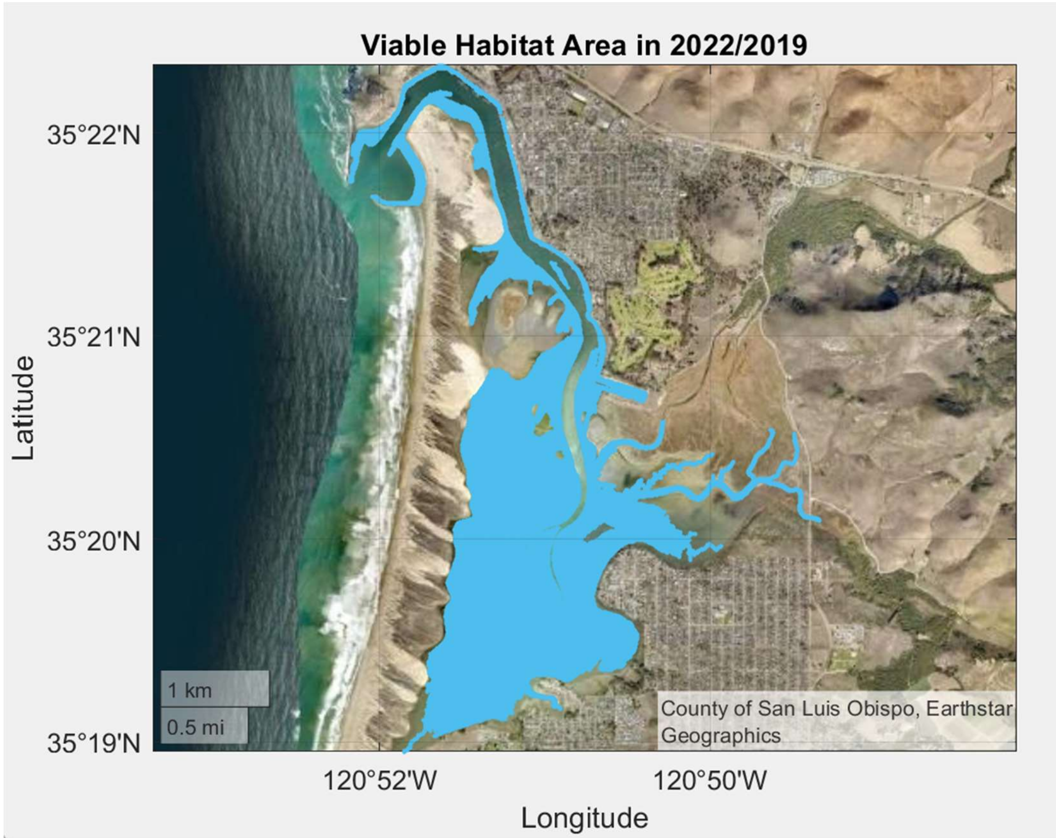

Figure 57: Viable Eelgrass Habitat Area for 2022 in Morro Bay

4.4.2 Future Viable Habitat Area

I approximated the future potential viable eelgrass habitat area using the merged 2019/2022 bathymetry and the adjusted viable growth range using **Equation 5** (**Table 25**). **Figure 58** depicts the various viable eelgrass areas for the different SLR scenarios. Rising water levels over time can shift eelgrass habitat zonation based on the limiting growth range relative to sea level. For RCP scenarios 2.6 through 8.5, I precited that viable eelgrass habitat area will increase. However, with scenario H++, I predicted the potential viable eelgrass habitat area to significantly decrease to just 610.5 acres (2.47E+06 m^2), or by 59% from the 2022 estimate. The available depth range for eelgrass will no longer be supported inside Morro Bay as the light compensation point, or the water depth at which the eelgrass cannot receive sufficient sunlight for growth, is exceeded. The band of habitat that remains (seen for SLR scenario H++ in **Figure 58**) is an example of the phenomenon known as the coastal squeeze, or when retreating habitats are limited in their migration by seaside slopes and manmade infrastructure (Pontee et al., 2022). This study assumed no change in bathymetry, but with measured sedimentation in Morro Bay, the severity of the collapse under scenario H++ will likely not be as severe (Freeman & Chase M, 2016). It is important to reiterate that this estimate does not consider local land subsidence, sediment input from local watersheds and the ocean, and sand placement or dredging activities. Future changes in morphology due to these activities can alter the future potential eelgrass habitat area and thus the tidal prism (Panda et al., 2013).

Table 25: The Future Potential Viable Eelgrass Habitat Area at Various SLR Scenarios determined by Griggs (Griggs et al., 2017)

SLR Scenario	SLR (m above Y2K MSL)	Potential Viable Eelgrass Habitat Area (Acres)	Potential Viable Eelgrass Habitat Area (m^2)
2050	0.274	1366.1	5.53E+06
2100 RCP-2.6	0.488	1540.1	6.23E+06
2100 RCP-4.5	0.579	1586.4	6.42E+06
2100 RCP-8.5	0.792	1650.3	6.68E+06
2100 H++	3.048	610.5	2.47E+06

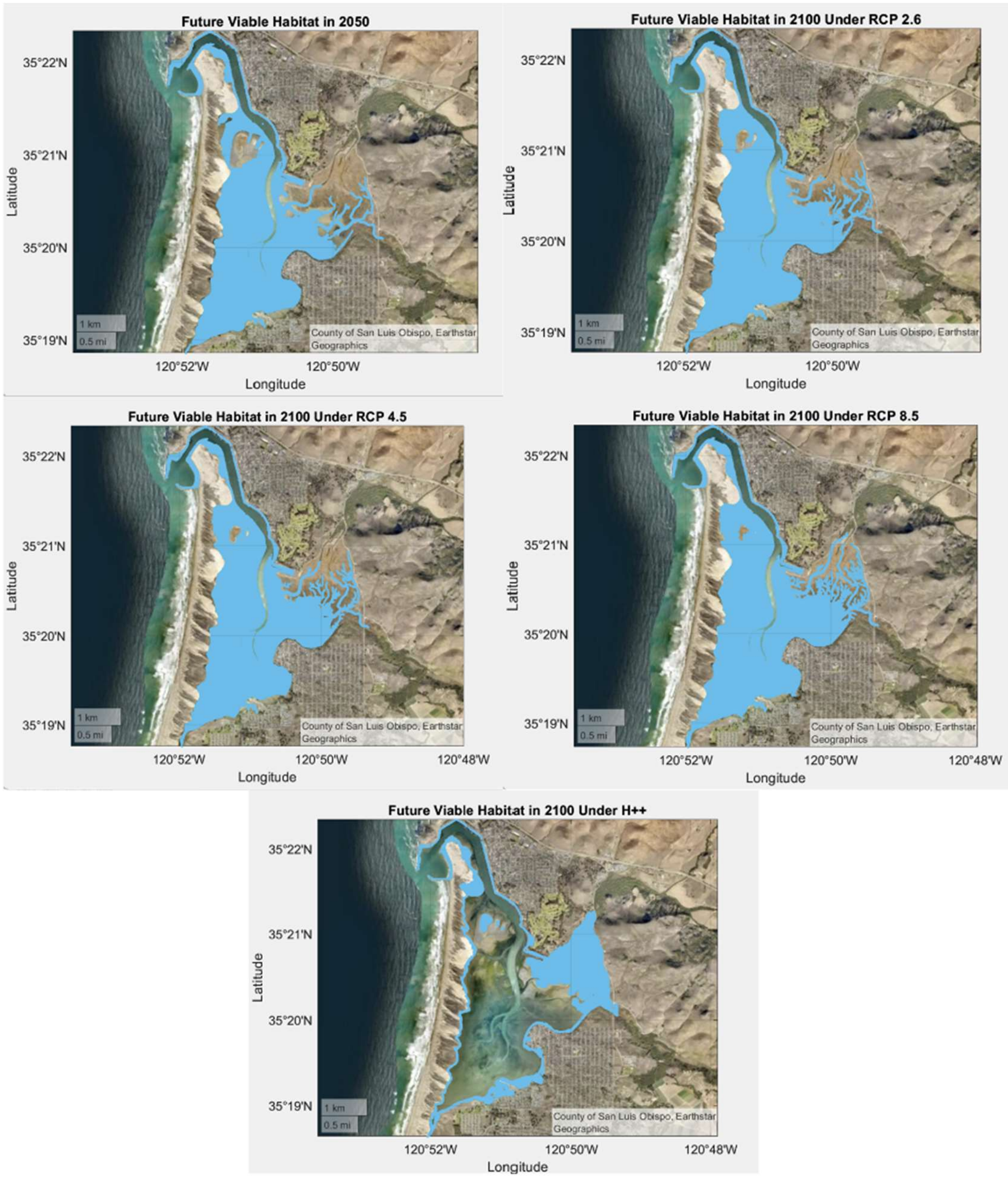

Figure 58: Potential Viable Eelgrass Habitat Area for the SLR Scenarios (Griggs et al., 2017)

4.4.3 Viable Habitat Sea Level Rise Threshold

I determined that the maximum potential viable eelgrass habitat area, or 1938.2 acres (7.84E+06 m^2), occurs with 1.5 m of SLR above 2000 levels (**Figure 59**Error! Reference source not found.). With additional SLR above this level, the potential viable eelgrass habitat area is predicted to decline (**Figure 60**). These results suggest that potential eelgrass habitat area will not be under any threat in the near future, and with most SLR scenarios. However, it is difficult to predict if the changing conditions inside Morro Bay as sea levels rise will be suitable for eelgrass growth in the future. Loss of habitat can result in changes in geomorphology, thus potentially further altering the available habitat and tidal prism (Ghosh et al., 2006).

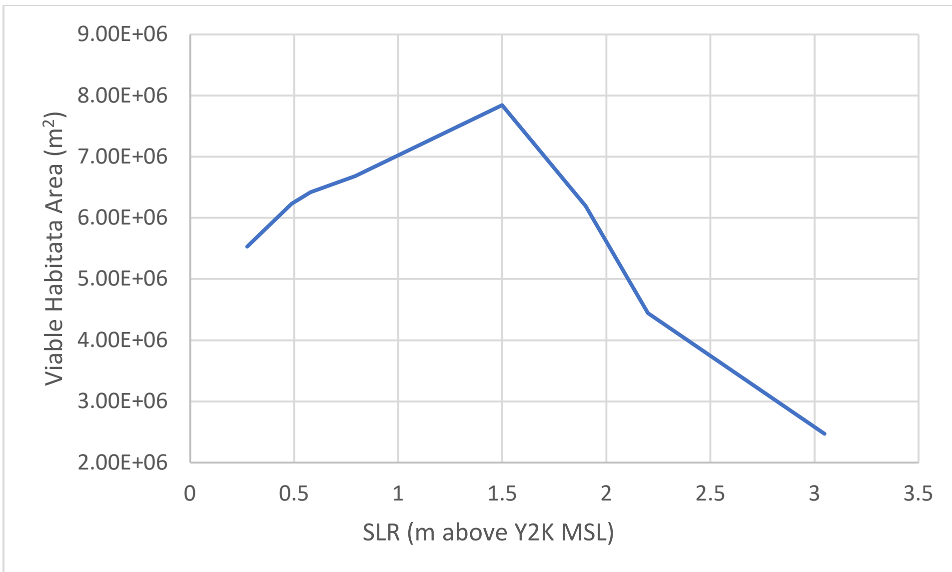

Figure 59: Potential Viable Eelgrass Habitat Area vs SLR above Y2K Levels for the Various SLR Scenarios (Griggs et al., 2017)

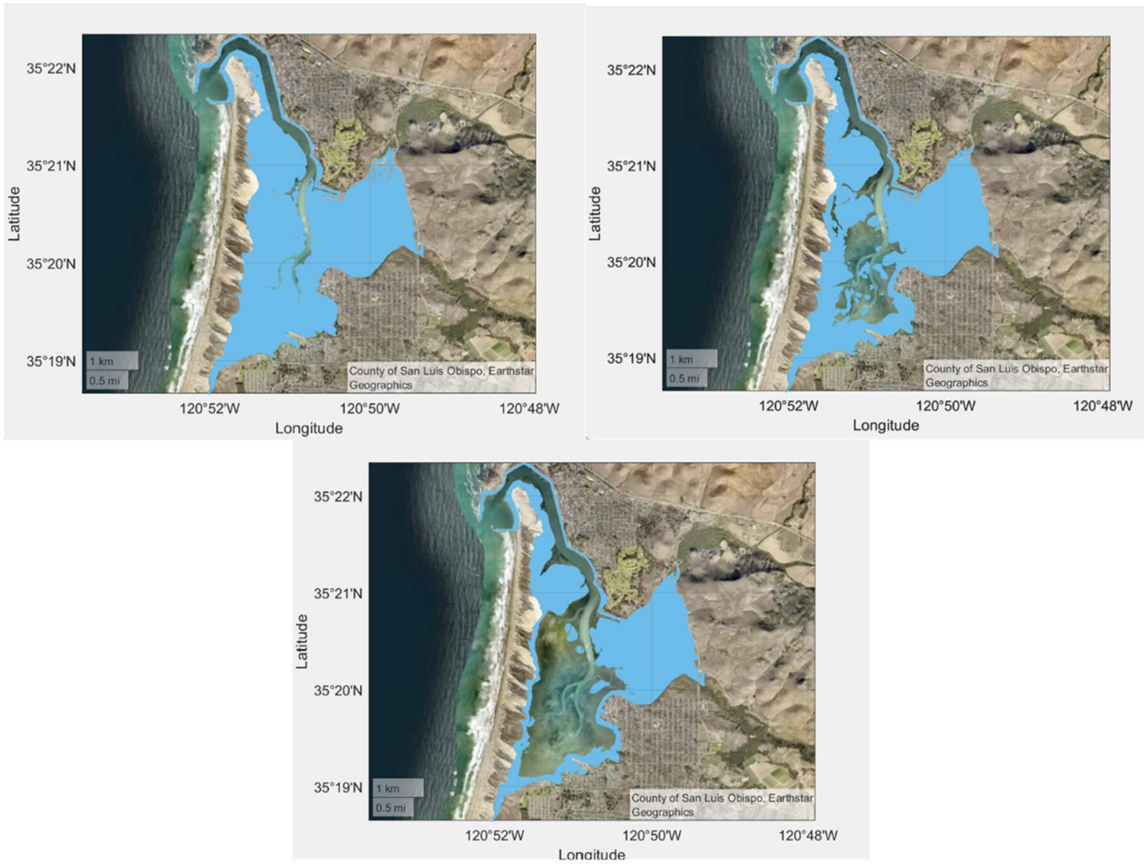

Figure 60: Viable Habitat Area under 1.5, 1.9 and 2.2 m of SLR from Y2K levels (from left to right).

Chapter 5: CONCLUSION & RECOMMENDATIONS

In addition to adding to the available tidal data in Morro Bay, I estimated the tidal prism, and viable eelgrass habitat area, and projected these estimates into the future to account for SLR. In doing so, these metrics can be used to guide future efforts to restore habitat and respond to rising sea levels in Morro Bay.

5.1 Contributions to the Field

The Cal Poly ultrasonic tidal gauges developed by Dunn compared well with the tide staff and Stilltek gauge, with low error at the Coast Guard North T-Pier. However, the Cal Poly gauge exhibited an average 29.9 mm difference at low waters as compared to commercial Stilltek gauge, partially due to different temperature readings used to calculate the speed of sound and correct the ultrasonic distance measurement. Different instrumentation provided up to ~4 percent variations in the tidal prism estimate. Comparisons to a nearby NOAA OX1MB MET station reveals that the Cal Poly gauge air temperature readings may be more accurate than the Stilltek commercial gauge, and therefore may reflect more accurate water level measurements.

Uncertainty within the monthly tidal datums can provide up to ~3 percent uncertainty within the monthly tidal prism estimate. Therefore, a ~6% change is needed to conclude real differences if a signal-to-noise ratio of 2x is desired. Compared to the tidal prism in August 2019, the August 2022 tidal prism from the Stilltek gauge decreased by ~2 percent. Compared to the tidal prism in August 2019, the August 2023 tidal prism from the Stilltek gauge and the Cal Poly Coast Guard gauge increased by ~5 and ~7 percent, respectively. I estimated that the tidal prism estimated from spatially varying monthly tidal datums was up to ~3 percent different than the tidal prism estimated from just the Cal Poly Coast Guard gauge in 2023. However, I estimated that with historically observed 0.5 ft (0.152 m) higher mean high tide elevations in the back of Morro Bay, that the tidal prism estimated from spatially varying water levels was up to ~10 percent different than the tidal prism estimated from just one gauge at the mouth of the estuary (assuming a uniform water level). Overall, assuming no change in bathymetry, the tidal prism is predicted to be trending upwards with sea level rise, with an estimated maximum increase of ~40 percent by 2100 from 2022 levels under the most extreme SLR scenario (H++).

Utilizing the viable growth range of eelgrass in Morro Bay determined by Tetra Tech in 2021, I predicted the 2022 viable eelgrass habitat area to be 1108 acres (4.48E+06 m^2). Potential viable eelgrass habitat area will initially increase as sea levels rise. Once sea levels rise 1.5 m above 2000 levels, potential viable eelgrass area is predicted to have reached a maximum of 1938 acres (7.82E+06 m^2). Under SLR scenario H++, potential viable habitat area is predicted to decrease by up to 59% by 2100 from 2022, assuming no change in bathymetry.

5.2 Suggested Future Work

There are a few things that future students and researchers can do to build upon this study. Below, I will discuss some of the suggested future work options.

Pressure transducer or radar gauge tide data could be compared to the Stilltek and Cal Poly Guage data. Doing so might allow a better estimate of mean tidal datums in Morro Bay by eliminating uncertainty due to variations in measured air temperatures used to correct the distance measurements with the ultrasonic tidal instruments. Surveying should also be repeatedly conducted on the tidal instruments. More surveys conducted on each of the gauges would reduce uncertainty associated with tying the gauges into the fixed datum of NAVD88. A better analysis regarding spatially varying water levels in Morro

Bay could then be conducted with a better estimate of gauge elevations. A more accurate representation of water levels would lead to a more accurate estimation of the tidal prism. More bathymetric measurements can be made to better estimate local SLR and sedimentation trends. A better estimate of local trends can help to project the tidal prism and eelgrass habitat area into the future. With predicted rates of SLR from NOAA of +0.96 mm/year (*Tide Predictions - NOAA Tides & Currents*, n.d.), and a maximum MSL anomaly of -0.125 m in Port San Luis, it could take more than a century at present rates for projections to exceed natural sea level variability. However, sea-level rise is predicted to be accelerating, reducing this time scale. Based on the sedimentation rate of +2.0 mm/year estimated by the USGS (Freeman & Chase M, 2016), and the uncertainty of bathymetric surveys, it may also take at least two decades before the role of sedimentation on tidal prism can be ascertained. Better estimates of sedimentation rates in Morro Bay could provide more insight on rates of change within the bathymetry and tidal prism. A new LiDAR scan could be conducted to obtain current conditions in Morro Bay following the 2023 winter storms but may not be necessary given the slow rate of sedimentation discussed above. If conducted, this scan should aim to include more of the Chorro and Los Osos Creeks delta. Additionally, repeated surveying along the shoreline could be analyzed to observe the local effects of Vertical Land Motion in Morro Bay. Doing so can provide a better estimate for local SLR and sedimentation patterns, and therefore potentially improve upon future tidal prism and future potential viable eelgrass estimates. In general, I have a few recommendations for anyone else who attempts to calculate the tidal prism in the future. Always refer to fixed datums, and not MLLW, as it can vary over time. This also allows people in the future to compare estimates with ought having to make datum conversions, reducing potential error. Often, limited data for MLLW was available to correct to NAVD88. Additionally, it is important to be clear about methods and results, so that results between different periods are comparable and reproducible.

REFERENCES/WORKS CITED/BIBLIOGRAPHY

About Tidal Datums. (n.d.). Retrieved September 29, 2023, from https://tidesandcurrents.noaa.gov/datum_options.html

Authority, D. (1996). *An Integrated Management Planning Framework for Conservation and Wise Use C H I L I K A An Integrated Management Planning Framework for Conservation and Wise Use*. http://south-asia.wetlands.org/

Basic Concepts in Physical Oceanography: Tides. (n.d.). Retrieved September 29, 2023, from https://www.oc.nps.edu/nom/day1/partc.html#:~:text=The%20moon%27s%20orbit%2C%20and%20hence%20the%20tidal%20bulges%2C,tide%2C%20and%20gives%20rise%20to%20the%20diurnal%20tides.

Bay, M. (2021). *Morro Bay National Estuary Program Morro Bay Eelgrass Report 2020*. http://www.mbnep.org/library,

Birds and Morro Bay. (n.d.). Retrieved September 29, 2023, from https://www.mbnep.org/2016/01/22/birds-and-morro-bay/

Central Coast California Map. (n.d.). Retrieved November 8, 2023, from https://motivasi.my.id/

Central Coast Regional Water Quality Control Board. (2002). *Morro Bay Total Maximum Daily Load for Sediment (including Chorro Creek, Los Osos Creek and the Morro Bay Estuary) State of California Central Coast Regional Water Quality Control Board Prepared on*.

Chestnut, J. (1999). *Eelgrass Habitat in Morro Bay*.

Cramer, O. (n.d.). *The variation of the specific heat ratio and the speed of sound in air with temperature, pressure, humidity, and CO2 concentration*.

Datums - NOAA Tides & Currents. (2023). https://tidesandcurrents.noaa.gov/datums.html?datum=MLLW&units=1&epoch=0&id=9412110&name=Port+San+Luis&state=CA

Dunn. (2023). *Development of a Low-Cost Acoustic Gauge for Simultaneous Tide and Wave Measurement*.

Enriquez, A., Wahl, T., Talke, S., Orton, P., Booth, J., & Santamaria-Aguilar, S. (2023). *MatFlood: An efficient algorithm for mapping flood extent and depth*.

Freeman, & Chase M. (2016). *Effects of Climate Change on Tidal Marshes along a Latitudinal Gradient in California*.

Gerdes, G., Primbs, E., Browning, B., Edon, C., Aplin, J., Lidberg, J., & Speth, J. (1974). *The Natural Resources of Morro Bay*.

Ghosh, A. K., Pattnaik, A. K., & Ballatore, T. J. (2006). Chilika Lagoon: Restoring ecological balance and livelihoods through re-salinization. *Lakes and Reservoirs: Science, Policy and Management for Sustainable Use*, *11*(4), 239–255. https://doi.org/10.1111/j.1440-1770.2006.00306.x

Gravitational Forces . (n.d.). Retrieved December 5, 2023, from https://virtuallearningacademy.net/VLA/LessonDisplay/Lesson2593/SCI180U02Gravitational_Forces.html

Griggs, G., Cayan, D., Tebaldi, C., Fricker, H. A., Árvai, J., Deconto, R., Kopp, R. E., Whiteman, L., & Moser, S. (2017). *Rising Seas in California - An Update on Sea Level Rise Science*.

Griggs, G., & Lester, C. (2017). *Coastal protection on the edge: The challenge of preserving California's legacy*. https://theconversation.com/coastal-protection-on-the-edge-the-challenge-of-preserving-californias-legacy-76927#:~:text=Some%2075%20percent%20of%20the%20state%E2%80%99s%20jobs%20are,of%20that%20is%20provided%20by%20tourism%20and%20recreation.

Haltiner. (1998). *#96F Sedimentation Processes Morro Bay, 1988*.

iGuage Data Link. (n.d.). Retrieved November 12, 2023, from https://stilltek.com/cgi-bin/qrySBD.php?site=iGage77&num=900&format=html

Jacob, J., & Cravo, A. (2019). *Recent evolution of the tidal prisms at the inlets of the western sector of the Ria Formosa, south coast of Portugal*.

Josselyn, Martindale, & Callaway. (1989). *Biological Resources of Morro Bay as Impacted by Watershed Development in Los Osos and Chorro Creek Watersheds*.

Kvale, E. (2006). *The origin of neap–spring tidal cycles*.

Legaard, K. R., & Thomas, A. C. (2006). Spatial patterns in seasonal and interannual variability of chlorophyll and sea surface temperature in the California Current. *Journal of Geophysical Research: Oceans*, *111*(6). https://doi.org/10.1029/2005JC003282

Magnusson, B. (n.d.). *The bias component in Uncertainty Measurment*. Retrieved November 13, 2023, from https://www.eurachem.org/images/stories/workshops/2012_05_MUMVTRC/pdf/2_4_magnusson_bias.pdf

Marani, M., Belluco, E., D'Alpaos, A., Defina, A., Lanzoni, S., & Rinaldo, A. (2003). *On the drainage density of tidal networks*. https://doi.org/https://doi.org/10.1029/2001WR001051

Moyer, B. (2021). *Improving Accuracy In Satellite Navigation Systems*. https://semiengineering.com/improving-accuracy-in-satellite-navigation-systems/

Munsch, S., Beaty, F., Beheshti, K., Chesney, B., Endris, C., Gerwing, T., Hessing-Lewis, M., O'Leary, J., Rehshitnyk, L., Sanderson, B., & Walter, R. K. (2023). *Northeast Pacific eelgrass dynamics: interannual expansion distances and meadow area variation over time*.

Munsch, S. H., Walter, R. K., Sanderson, B. L., Reshitnyk, L., O'Leary, J. K., Kiffney, P. M., Hessing-Lewis, M., Gerwing, T. G., Endris, C. A., Chesney, W. B., Beheshti, K. M., & Beaty, F. L. (2023). Decades of eelgrass meadow dynamics across the northeast Pacific support seascape-scale conservation. *ICES Journal of Marine Science*. https://doi.org/10.1093/icesjms/fsad162

NOAA. (n.d.). *National Geodetic Survey Data Explorer*. Retrieved November 12, 2023, from https://www.ngs.noaa.gov/NGSDataExplorer/

NOAA Data Access Viewer. (n.d.). Retrieved November 11, 2023, from https://coast.noaa. gov/dataviewer/#/lidar/search/-13457732.510972984,4205259. 548137256,-13449400.874889899,4216419.354266891

NOAA Port San Luis Data Inventory Page. (n.d.). Retrieved October 25, 2023, from https://tidesandcurrents.noaa.gov/inventory.html?id=9412110

NOAA Tides & Currents. (n.d.). Retrieved April 16, 2023, from https://tidesandcurrents.noaa.gov/datum_options.html#MHHW

Office of Science Quality and Integrity. (2019, March). *Guidance on Use and Documentation of Horizontal and Vertical Datums in USGS Publication Series Information Products*. https://www.usgs.gov/about/organization/science-support/office-science-quality-and-integrity/guidance-use-and

O'Leary, J., Goodman, M., Walter, R., Willits, K., Pondella, D., & Stephens, J. (2021). *Effects of Estuary-Wide Seagrass Loss on Fish Populations*.

Panda, U. S., Mohanty, P. K., & Samal, R. N. (2013). Impact of tidal inlet and its geomorphological changes on lagoon environment: A numerical model study. *Estuarine, Coastal and Shelf Science*, *116*, 29–40. https://doi.org/10.1016/j.ecss.2012.06.011

Pareja-Roman, Orton, P. M., & Talke, S. (2023). *Effect of Estuary Urbanization on Tidal Dynamics and High Tide Flooding in a Coastal Lagoon*. https://doi.org/10.1029/2022JC018777

Parker, B. B., Gutierrez, C. M., Lautenbacher, C. C., Dunnigan, J. H., Administrator, A., & Szabados, M. (2007). *Tidal Analysis and Prediction Center for Operational Oceanographic Products and Services*. http://tidesandcurrents.noaa.gov

Petti, M., Bosa, S., Pascolo, S., & Uliana, E. (2019). Marano and grado lagoon: Narrowing of the lignano inlet. *IOP Conference Series: Materials Science and Engineering*, *603*(3). https://doi.org/10.1088/1757-899X/603/3/032066

Petti, M., Pascolo, S., Bosa, S., & Busetto, N. (2021). *On the Tidal Prism: The Roles of Basin Extension, Bottom Friction and Inlet Cross-Section*.

Pontee, Tempest, Pye, & Blott. (2022). *DEFINING HABITAT LOSSES DUE TO COASTAL SQUEEZE* .

Pugh, D. (1987). *Tides, Surges and Mean Sea-Level*. https://eprints.soton.ac.uk/19157/1/sea-level.pdf

Samal, R. (2011). *The transport of sediments in Chilika lagoon, East Coast of India*.

Sassi, M., Duran-Matute, M., van Kessel, T., & Gerkema, T. (2015). Variability of residual fluxes of suspended sediment in a multiple tidal-inlet system: the Dutch Wadden Sea. *Ocean Dynamics*, *65*(9–10), 1321–1333. https://doi.org/10.1007/s10236-015-0866-2

Schureman, P. (2001). *Manual of Harmonic Analysis and Tides*.

Short, F., Polidoro, B., Livingstone, S., Carpenter, K., Bandeira, S., Bujang, J., Calumpong, H., Carruthers, T., Coles, R., Dennison, W., Erfemeijer, P., Fortes, M., Freeman, A., Jagtap, T. G., Kamal, A., Kendrick, G., Kenworthy, J., Nafie, Y., Nasution, I., … Zeiman, J. (2011). *Extinction risk assessment of the world's seagrass species*.

SOM Survey Instruments. (n.d.). *Total Station vs GPS Surveying*. Retrieved October 30, 2023, from https://somsurveyinstruments.com/total-station-vs-gps-surveying

T Score Table Degrees of Freedom. (2018, April). https://officialbruinsshop.com/t-score-table-degrees-of-freedom/

Tetra Tech. (1999). *MORRO BAY NATIONAL ESTUARY PROGRAM Hydrodynamic Circulation Model Final Report*.

Tetra Tech. (2020). *FINAL Memorandum_Morro Bay Tidal Prism*.

Tetra Tech. (2021). *FINAL MBNEP Eelgrass Analysis Report*.

Tide Predictions - NOAA Tides & Currents. (n.d.). Retrieved March 24, 2023, from https://tidesandcurrents.noaa.gov/noaatidepredictions.html?id=9412110&legacy=1

Tides and Currents Glossary. (n.d.). Retrieved September 29, 2023, from https://tidesandcurrents.noaa.gov/glossary.html#NationalTidalDatumEpoch

Trimble R8's. (n.d.). Retrieved November 16, 2023, from http://stg-geospatial.trimble.com/sites/geospatial.trimble.com/files/2020-10/Datasheet%20-%20Trimble%20R8s%20GNSS%20-%20English%20US%20-%20Screen.pdf

Trimble S7. (n.d.). Retrieved November 16, 2023, from http://dev-geospatial.trimble.com/sites/geospatial.trimble.com/files/2021-02/Datasheet%20-%20Trimble%20S7%20Total%20Station%20-%20English%20US%20-%20Screen_1.pdf

Tyler, R. (2021). *On the Tidal History and Future of the Earth–Moon Orbital System*.

US ARMY COE. (1974). *EIR's on Maintenance Dredging* .

U.S. Coast and Geodetic Survey. (2001). *Geodetic Glossary*.

Walter, R. K., O'Leary, J. K., Vitousek, S., Taherkhani, M., Geraghty, C., & Kitajima, A. (2020). Large-scale erosion driven by intertidal eelgrass loss in an estuarine environment. *Estuarine, Coastal and Shelf Science*, *243*, 106910. https://doi.org/10.1016/J.ECSS.2020.106910

What is the Tide? (n.d.). Retrieved September 29, 2023, from https://byjus.com/free-ias-prep/tides/

Wong, G. S. K. (1990). Approximate equations for some acoustical and thermodynamic properties of standard air. In *J. Acoust. Soc. Jpn. (E)* (Vol. 11).

Yasuda, I. (2018). Impact of the astronomical lunar 18.6-yr tidal cycle on El-Niño and Southern Oscillation. *Scientific Reports*, *8*(1). https://doi.org/10.1038/s41598-018-33526-4

APPENDICIES

Appendix A: Gauge Installation and Maintenance Notes

Gauge	Date	Person	Notes
Coast Guard Pier (P3D	3/1/23	Kaden and Luke and August	Collected data from Alexs old sensor (Gauge D) now that I have taken over maintenance.
Los Osos (P4C)	3/1/23	Kaden, Luke and August	Installed the new gauge along the pier with permission and oversight from homeowner. Modified cantilever setup to be tucked away under the railing per request of the homeowner. Leveled on three axes to ensure proper readings. Set at a height where the water level should never exceed 10 m or be less than .5 m.
P3D and P4C	3/10/23	Kaden	Collected data from existing sensors. Checked functionality of Los Osos sensor.
Bayfront (P4B)	3/10/23	Kaden	Installation of gauge. Used the normal cantilever setup on the middle of the pier in locations where no boats dock. Leveled on three axes to ensure proper readings. Set at a height where the water level should never exceed 10 m or be less than .5 m.
P3D, P4C, and P4B	3/23/23	Kaden	Collected data from existing sensors. Checked the functionality of Bayfront.
State Park (P4A)	4/04/23	Kaden	Installation of gauge onto pier pylon. Used a t shape mount with hose clamps to secure at a high tide. Leveled on three axes to ensure proper readings. Set at a height where the water level should never exceed 10 m or be less than .5 m.
All Sensors	4/21/23	Kaden	Routine Data Collection.
State Park (P4A)	5/4/23	Kaden	Battery change at state park and checking to ensure operation. No Los Osos temp ...must use Coast Guard for corrected distances
Coast Guard (P3D)	5/5/23	August	Collected data from the Coast Guard Pier.
Los Osos (P4C)	5/9/23	Kaden	Discovered broken probe while surveying....pulled instrument to fix in the lab. Approximate disruption in the data occurred at 682570653 UNIX GMT time. Assumption made due to the increasing number of outliers that occur after the probe was damaged. Ensured to install in exact same location by leaving mounting structure behind. No Los Osos temp ...must use Coast Guard for corrected distances

Los Osos (P4C)	5/11/23	Kaden	Reinstalled with new Temp/humidity and ultrasonic probe. Exact same location just aligned screw holes.
All Sensors	5/23/23	Kaden	Routine Data Collection No broken probes, missing parts. All sensors were still running upon retrieval.
All sensors	6/22/23	Kaden	Routine Data Collection Bayfront did not collect data...ensured the blue and red light were on when I left last time...I did again and will check soon Los Osos Temp did not collect data...must use Coast Guard data to correct distances
All Sensors	7/23/23	Kaden/Serena	Routine Data Collection Bayfront Collected Data...yay!! Los Osos Temp also collected data State Park location was too low of tide to access...will return tomorrow at high tide
State Park (P4A)	7/24/23	Kaden	Went back to the state park for data collection at high tide. Also took a staff measurement. State Park sensor did not collect data????
All Sensors	9/8/23	Kaden	Routine Data Collection State park did not collect again....stayed and fixed...supposedly
All Sensors	10/23/23	Kaden and Jonathan	Routine data Collection Coast Guard Sd cards are worn out and need to be replaced Bayfront did not collect Also....Bayfront had dead eelgrass accumulated under sensor.....results in higher "low tide" Measured survey offsets to stilltek and state park tide staff
All Sensors	11/30/23	Kaden, Serena, Luke and others	Routine data collection Kaden passed all necessary info to Serena Coast Guard Gauge D did not record - Should be replaced w new iteration (it is 3rd currently) Bayfront Battery port came disconnected……taken back to lab to be fixed and redeployed Los Osos(p4c) removed from the location and is in lab - the instrument probe is malfunctioning

Appendix B: Surface Area and Volume Estimates for Determining the Tidal Prism

NOAA Port San Luis 2022

Tidal Prism in 2022 from NOAA Port San Luis							
Month	**MHW (m NAVD88)**	**Surface Area (Acres)**	**Volume (Acre-Feet)**	**MLW (m NAVD88)**	**Surface Area (Acres)**	**Volume (Acre-Feet)**	**Tidal Prism (Acre-Feet)**
January	1.411	2048.4	12595.6	0.302	1288.6	6103.5	6492.1
February	1.345	2036.6	12153.1	0.284	1256.7	6028.2	6124.9
March	1.356	2038.60	12226.7	0.241	1169.7	5856.5	6370.2
April	1.309	2030.0	11912.7	0.2	1084.2	5704.3	6208.3
May	1.324	2032.90	12012.9	0.235	1157.4	5833.4	6179.4
June	1.411	2048.4	12595.6	0.362	1371.4	6366.5	6229.2
July	1.411	2048.4	12595.6	0.357	1365.3	6344.0	6251.6
August	1.448	2056.2	12844.9	0.384	1396.0	6466.5	6378.4
September	1.491	2068.4	13136.2	0.432	1446.0	6691.0	6445.2
October	1.444	2055.2	12817.9	0.368	1378.1	6393.6	6424.3
November	1.397	2045.8	12501.5	0.313	1306.9	6150.5	6351.1
December	1.441	2054.5	12797.7	0.354	1361.8	6330.5	6467.1
Annual	1.399	2046.1	125145.0	0.31933	1316.2	6177.8	6337.2

Stilltek 2022

Tidal Prism in 2022 from Stilltek							
Month	**MHW (m NAVD88)**	**Surface Area (Acres)**	**Volume (Acre-Feet)**	**MLW (m NAVD88)**	**Surface Area (Acres)**	**Volume (Acre-Feet)**	**Tidal Prism (Acre-Feet)**
January	1.429	2052.0	12719.4	0.336	1340.4	6252.0	6467.4
February	1.371	2041.1	12325.1	0.295	1276.2	6073.7	6251.4
March	1.370	2040.9	12317.4	0.284	1256.6	6027.9	6289.6
April	1.325	2033.1	12019.1	0.233	1152.8	5824.2	6194.9
May	1.344	2036.4	12145.9	0.278	1244.7	6004.3	6141.6
June	1.425	2051.2	12691.2	0.360	1368.5	6356.3	6335.0
July	1.432	2052.6	12737.2	0.371	1381.6	6406.8	6330.4
August	1.467	2061.1	12974.6	0.395	1408.8	6518.9	6455.7
September	1.517	2078.8	13312.1	0.444	1458.0	6749.1	6563.0

October	1.466	2060.8	12967.1	0.398	1411.3	6530.2	6436.8
November	1.428	2051.7	12707.2	0.325	1325.7	6204.4	6502.7
December	1.475	2063.4	13030.9	0.374	1385.2	6421.8	6609.0
Annual	1.421	2050.4	12665.6	0.342	1347.1	6275.3	6390.3

NOAA 2023

Uniform 2023 Tidal Prism from NOAA Port San Luis							
Month	**MHW (m NAVD88)**	**Surface Area (Acres)**	**Volume (Acre-Feet)**	**MLW (m NAVD88)**	**Surface Area (Acres)**	**Volume (Acre-Feet)**	**Tidal Prism (Acre-Feet)**
January	1.438	2053.8	12777.4	0.372	1382.7	6411.7	6365.7
February	1.368	2040.7	12307.1	0.290	1268.2	6253.9	6253.9
March	1.364	2039.9	12280.3	0.275	1239.0	5991.3	6288.9
April	1.307	2029.7	11899.3	0.259	1204.8	5926.9	5972.4
May	1.407	2047.6	12568.7	0.367	1376.9	6389.0	6179.7
June	1.407	2047.6	12568.7	0.365	1374.8	6379.9	6188.7
July	1.476	2063.6	13034.4	0.407	1420.9	6573.1	6461.2
August	1.546	2092.9	13512.3	0.429	1442.8	6676.8	6835.5
Overall	1.414	2048.9	12615.8	0.346	1352.1	6294.9	6320.9

Stilltek 2023

2023 Tidal Prism from Stilltek							
Month	**MHW (m NAVD88)**	**Surface Area (Acres)**	**Volume (Acre-Feet)**	**MLW (m NAVD88)**	**Surface Area (Acres)**	**Volume (Acre-Feet)**	**Tidal Prism (Acre-Feet)**
May	1.433	2052.8	12743.7	0.369	1379.2	6398.1	6345.6
June	1.435674	2053.4	12761.0	0.382905	1394.8	6461.5	6300.3
July	1.496602	2070.4	13174.3	0.413953	1427.8	6605.7	6568.6
August	1.565132	2105.2	13644.4	0.436254	1450.3	6711.3	6933.1

Cal Poly Coast Guard (Gauge D) 2023

Uniform 2023 Tidal Prism from Gauge D

Month	MHW (m NAVD88)	Surface Area (Acres)	Volume (Acre-Feet)	MLW (m NAVD88)	Surface Area (Acres)	Volume (Acre-Feet)	Tidal Prism (Acre-Feet)
March	1.369	2040.8	12313.7	0.28	1248.1	6011.7	6302.1
April	1.322	2032.5	11999.5	0.245	1177.1	5871.9	6127.6
May	1.429	2051.9	12716.7	0.348	1354.4	6303.7	6413.0
June	1.431	2052.2	12726.9	0.353	1360.7	6325.9	6400.9
July	1.496	2070.2	13171	0.38	1391.8	6448.3	6722.7
August	1.563	2103.4	13626.5	0.407	1421.3	6575.4	7051.1

Spatially Varying 2023

2023 Spatially Varying Tidal Prism					
Month	**MHW Surface Area (Acres)**	**MHW Volume (Acre-Feet)**	**MLW Surface Area (Acres)**	**MLW Volume (Acre-Feet)**	**Tidal Prism (Acre-Feet)**
March	2040.9	12313.8	1323.9	6180.6	6133.2
April	2038.2	12192.1	1221.5	5957.6	6234.4
May	2060.7	12956.8	1379.4	6392.6	6564.2
June	2061.0	12957.5	1373.5	6369.6	6588.0
July	2084.7	13389.8	1414.7	6535.9	6852.8
August	2131.9	13853.9	1449.4	6697.0	7156.8